Applications and Industry®

July 1961

Transactions Papers

NUMBER 55

Published Bimonthly by

AMERICAN INSTITUTE OF ELECTRICAL ENGINEERS

Communication and Electronics—July 1961

Communication Division

Instrumentation Division

Science and Electronics Division

(See inside back cover)

Note to Librarians. The six bimonthly issues of "Applications and Industry," March 1961–January 1962, will also be available in a single volume (no. 80) entitled "AIEE Transactions—Part II. Applications and Industry," which includes all technical papers on that subject presented during 1961. Bibliographic references to Applications and Industry and to Part II of the Transactions are therefore equivalent.

Applications and Industry. Published bimonthly by the American Institute of Electrical Engineers, from 20th and Northampton Streets, Easton, Pa. AIEE Headquarters: 33 West 39th Street, New York 18, N. Y. Address changes must be received at AIEE Headquarters by the first of the month to be effective with the succeeding issue. Copies undelivered because of incorrect address cannot be replaced without charge. Editorial and Advertising offices: 33 West 39th Street, New York 18, N. Y. Nonmember subscription $8.00 per year (plus 75 cents extra for foreign postage payable in advance in New York exchange). Member subscriptions: one subscription at $5.00 per year to any one of three divisional publications: Communication and Electronics, Applications and Industry, or Power Apparatus and Systems: additional annual subscriptions $8.00 each. Single copies when available $1.50 each. Second-class mail privileges authorized at Easton, Pa. This publication is authorized to be mailed at the special rates of postage prescribed by Section 132.122.

Printed in United States of America

Number of copies of this issue 5,100

Proposed Method of Loss Measurement for Semiconductor Rectifier Equipments

I. K. DORTORT
MEMBER AIEE

IT HAS long been recognized that the efficiency of a large rectifier unit cannot be accurately determined by input–output power measurements. Errors of measurement may be as great or greater than the losses in high efficiency equipments. These errors are aggravated to an unknown degree by the distortion of current and voltage waveshapes inherent in rectifier operation.

Because of this and other difficulties, the accepted procedure is the "segregated loss" method in which the losses in each major component of the equipment are determined separately by conventional methods; conventional, that is, for all parts except the rectifier itself.

It required many years to achieve reasonable agreement on the method of determining the losses in a mercury-arc rectifier. Almost all of the power loss is caused by a relatively constant forward voltage drop, having only a minor dependence on current. The average value of the "arc drop" multiplied by the average forward current is a reasonably accurate measure of the arc loss over a wide range of current waveshapes. The greatest difficulty was caused by the problem of current and power measurements in single-way rectifier circuits.

The same methods cannot be applied to semiconductor rectifiers, even though single-way circuits are not preponderant. The reason is quite apparent in Fig. 1, which shows a typical curve of instantaneous voltage and current values for a silicon cell. The forward current loss is strongly dependent on the current waveshape because of the high incremental resistance and cannot be measured by average voltage drop except in special cases. Rectifier loss measurements are of necessity made with the d-c terminals short-circuited. In consequence, the cell current form factor will be substantially different from that obtained in normal operation.

It is necessary, then, to apply a correction to the losses measured in a short circuit. Some of the previously proposed methods rely on corrections computed from the forward voltage curve.

It was quite logical to facilitate the mathematical work by approximating the curve of actual values by a straight line with slope R_a, intercepting the voltage ordinate at a "threshold voltage" E_{th}. Most of the proposed methods of loss measurement are based on this concept. However, the graphical approach to R_a and E_{th} is not straightforward.

To start with, semiconductor rectifiers in the class under discussion contain many cells, often in the hundreds. It would not be feasible for the equipment manufacturer to measure and plot the characteristic of each cell, so he uses the cell manufacturer's published curves. This is true even where the same company manufactures both the cells and equipments. The published curve represents the average characteristic of many cells, measured at a specified junction temperature.

The spread between cells, even if they have been matched, is quite wide and their individual characteristics are not necessarily parallel. Let us assume, however, that the curve to be used is fairly representative of the batch of cells in the rectifier and that the average E_{th}'s and R_a's of the cells are equal to the E_{th} and R_a of the average curve.

First, the average voltage drop curve must be corrected to the normal operating junction temperature of the rectifier. It is no simple task to measure or compute the mean junction temperatures of many cells in a rectifier, especially if the current division is unequal and the cooling is not uniform. Still more difficult is the task of correcting the curve. The information necessary to do this accurately is not generally available.

Next comes the problem of matching a straight-line equivalent to the curve. The uncertainty introduced by the human element might be overcome by a rigid formulation of procedure. Right or wrong, this would eliminate uncertainty and controversy. It should be noted, however, that the values of E_{th} and R_a are not constant, being dependent on the load level. This is also illustrated in Fig. 1.

There is still another problem. A large rectifier consists of more than just a conglomeration of rectifier cells. There may be heavy current buses, some carrying alternating currents, some carrying unidirectional currents. There will probably be many bolted joints. Some of the buses may be tapered or nonuniformly loaded. There will probably be cell fuses, balancing reactors, and perhaps control reactors. Their I^2R (current^2 resistance) and stray losses or, more rigorously, the total effective resistance must be added to the incremental resistance of the cells.

By making rather dubious assumptions and incongruously painstaking computations, it is possible to come up with a value of effective resistance somewhat better than an educated guess. In very heavy current rectifiers, the losses in these parts can exceed 25% of the cell loss and deserve a more accurate determination.

Direct measurement of losses or effective resistance of these parts is generally not feasible. It introduces problems of instrumentation and requires replacement of at least half of all the cells in one rectifier section with solid conductors having a small resistance compared to the incremental resistance of the cells. The choice between computation and direct measurement is a tossup, somewhat in favor of computation.

Other methods have been suggested and tried for applying waveshape correction factors designed to avoid these

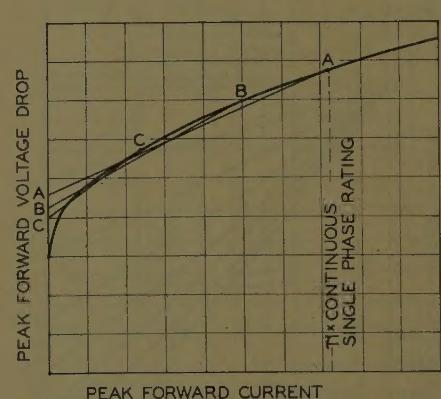

Fig. 1. Typical instantaneous forward voltage characteristic of silicon cells at 100 C junction temperature and straight-line approximations at three loads

A—$E_{th}=0.92$, $R_a=0.00088$
B—$E_{th}=0.85$, $R_a=0.00108$
C—$E_{th}=0.80$, $R_a=0.00146$

Paper 61-23, recommended by the AIEE Semiconductor Rectifier Committee of the Science and Electronics Division and the Industrial Power Rectifier Committee and approved by the AIEE Technical Operations Department for presentation at the AIEE Winter General Meeting, New York, N. Y., January 29–February 3, 1961. Manuscript submitted October 7, 1960; made available for printing November 29, 1960.

I. K. DORTORT is with the I-T-E Circuit Breaker Company, Philadelphia, Pa.

tedious and uncertain computations. These methods involve manipulation of loss values measured in two configurations of the circuit. The variation is produced by replacing at least one series element in every series connection with a solid conductor. If there are no series elements in the rectifier, they must be added. This requires additional connections not provided in the rectifier, and the additional losses must be determined and included in the loss calculations.

In large rectifiers involving hundreds of cells these methods require many hours of labor and introduce errors due to temperature changes in various parts of the rectifier. This is especially true in fuses which are often connected directly to the cell leads and are heated by them.

Note that it is not permissible to use a single, heavy-current jumper to short-circuit a block of parallel cells because to do so would completely change the geometry of the copper (Cu) and the Cu losses.

IEC Proposal

During the 1959 meetings of the Semiconductor Subcommittee 22-2 of the International Electrotechnical Commission (IEC), a Task Force was set up and instructed to come up with an acceptable means of measuring rectifier losses before the end of the Paris sessions, so that the contemplated document of IEC recommendations could be completed and issued for balloting in 1960. The proposals submitted by the several nations were reviewed and a recommendation

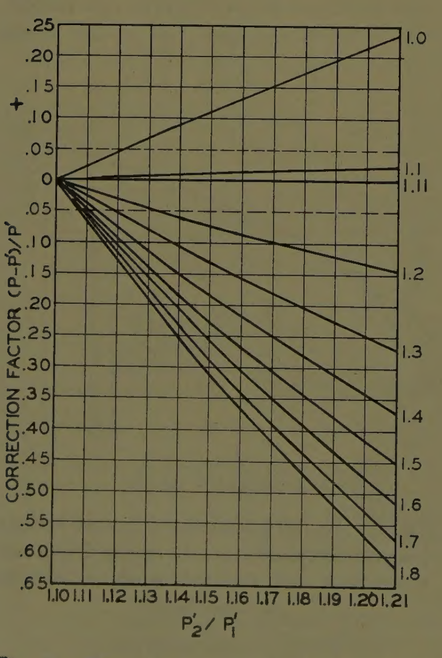

Fig. 2. Correction curves for deviation from sine wave in short circuit

prepared. Towards the end of these deliberations, the United States delegation submitted another proposal, involving two loss measurements without any changes in the configuration of the circuit and without the need for determining E_{th} and R_a. There was not sufficient time for careful study and evaluation, but Dr. J. C. Read, head of the Task Force, was interested. At the last meeting of the Subcommittee, he presented the group's formal recommendation as well as the new proposal. He recommended that the new scheme be studied and developed by correspondence between us, after the close of the Paris meetings, for possible inclusion in the document at a later date. A motion was made and carried to put this plan into effect with the Secretariat in Sweden a cognizant party. Our work culminated in the simple system defined by equation 7 of this paper, and has been included in the latest revision of the IEC Recommendations on Monocrystalline Semiconductor Rectifiers.

Basis of Proposed Method

Within the accuracy of the best straight-line approximation, the forward voltage drop of the cells can be written:

$$v = E_{th} + R_a i \qquad (1)$$

The forward current power loss of a complete rectifier structure, including stray losses, can be expressed in the form:

$$P = A \cdot I_{avg} \cdot E_{th} + I^2_{rms}(bR_a + cR_1 + dR_2 + \dots)$$
$$= A \cdot I_{avg} \cdot E_{th} + B \cdot I^2_{rms} R' \qquad (2)$$

where

E_{th} = threshold voltage of cells
R_a = incremental resistance of cells (straight-line)
I_{avg} = average current of cells
$R_1, R_2, \dots$ = effective resistance of unidirectional current and alternating current carrying conductors and components
R' = total effective resistance, including R_a
A, b, c, d, B are circuit constants
P = power loss of rectifier under a particular mode of operation

Equation 2 is quite obvious and fine as far as it goes, but exceedingly difficult to use for reasons given previously. Furthermore, the circuit constants as well as the R's are influenced by current distribution, temperature variations, etc. Logically, the entire job belongs to an analog computer. In the proposed system the rectifier itself is the analog computer and is exactly tailored to the requirements.

When a rectifier is operated under normal conditions of d-c output voltage and current, the cell currents will usually have a different waveshape than when it is delivering the same average direct current in short circuit. The average value of each cell current must be the same except for possible changes in current distribution. The average value of all the cell currents must be exactly the same. The rms values of the cell currents will generally be quite different. If I_{rms} is the value in short circuit, the value in normal operation can be defined as KI_{rms}. The power loss in normal operation is then written:

$$P = (A \cdot I_{avg} \cdot E_{th}) + K^2(B \cdot I^2_{rms} \cdot R') \qquad (3)$$

If the input power to the rectifier in short circuit is measured at two levels, rated direct current I_d and KI_d, respectively, then

$$P_1 = (A \cdot I_{avg} E_{th}) + (B \cdot I^2_{rms} \cdot R') \qquad (4)$$

$$P_2 = K(A \cdot I_{avg} \cdot E_{th}) + K^2(B \cdot I^2_{rms} \cdot R') \qquad (5)$$

By elimination of the E_{th} and R' terms:

$$P = \frac{K+1}{K} P_2 - KP_1 \qquad (6)$$

From equations 2 and 3 it can be seen that K is the ratio of rms current values in normal and short-circuit operation. It is therefore also the ratio of the form factors of the two waveshapes in these modes of operation and can be so defined.

Assuming rectangular waveshapes without overlap, for normal operation and perfectly sinusoidal waves in short circuit,

$K = 1.1$ for 6-phase double-way and double Y rectifiers
$K = 1.0$ for single-phase full-wave rectifiers, resistive loading
$K = 0.9$ for single-phase full-wave rectifiers, inductive loading

In general, single-phase rectifiers feeding resistive or back electromotive force (emf) loads will, in normal operation, have cell currents approaching sinusoidal rather than flat-topped waves. For these, $K = 1.0$ and, obviously, only one measurement is required.

When measuring the losses in heavy-current rectifiers, the short-circuit bar may account for a significant percentage of the total. This loss will naturally be included in the power loss derived from P_1 and P_2 and must be subtracted. It is most easily determined by measuring the voltage drop V' across the short-circuit bar, and then

$$P = \frac{K+1}{K} P_2 - KP_1 - I_d \cdot V' \qquad (7)$$

In most cases $I_d V'$ can and should be

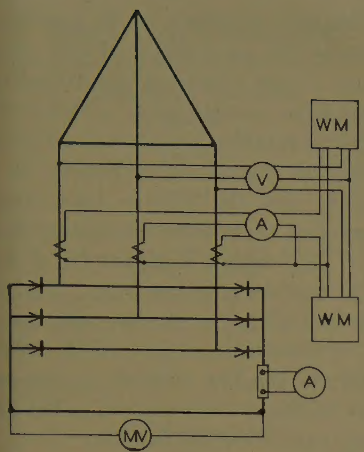

'ig. 3. Test circuit no. 1 direct measurement

nade negligibly small. If the ammeter hunt is not part of the rectifier, its loss hould be subtracted.

CORRECTION FACTORS

The validity of neglecting overlap equires substantiation. It is not enough hat this procedure simplifies things, or ven that it falls in line with existing tandards for rating rectifier transformers nd measuring their losses. Let us ssume a typical 6-phase rectifier with a ommutating impedance of 10%. The ngle of overlap, u, is then 26 degrees and he rms value of cell current in normal peration takes a correction factor for verlap of 0.973.[1] K should theoretically e reduced from 1.1 to 1.07, causing a eduction of approximately 4% in P_2. The net result is a reduction in P of less han 2% in the usual case. Two per cent f a 2% loss is truly negligible and little nough margin for the undetermined ncrease in stray losses produced by the teeper wavefronts of normal operation. No correction for overlap is recommended.

One other error must be considered and valuated. K has been assigned values ased on rectangular cell currents in ormal operation and pure sine-wave urrents in the short-circuit tests. Most ectifiers do draw essentially sinusoidal urrents in short circuit, but not all. Especially in low-voltage high-current ectifiers the waveform may be quite listorted. The most straightforward olution is to determine the true form actor of the cell current in short circuit nd adjust K accordingly. It will be ecalled that K has been defined as the atio of the form factors of the cell curents in normal and in short-circuit peration.

Standardization bodies may prefer to se fixed K factors and apply corrections o the result only in special cases. Therefore, the following procedure is suggested as an alternate. Fig. 2 provides correction factors to be applied to the normally obtained power loss if the form factor of the short-circuit current deviates too much from 1.11 in 6-phase double-way and double-Y rectifiers. There seems to be no need for similar corrections for single-phase rectifiers since deviation from sinusoidal currents is not expected. However, similar curves can be provided if required.

Let F' be the actual form factor, P_1' and P_2' the actual loss measurements, and let P' be computed from them, using the standard K. The equation for the correction factor is then:

$$\frac{P-P'}{P'} = \frac{-K^2(P_2'/P_1'-K)\,[1-(1.11/F')^2]}{(K^2-1)P_2'/P_1'-K^2(K-1)} \qquad (8)$$

A $\pm 5\%$ band of maximum allowable error has been drawn in Fig. 2 as a basis for discussion. Any rectifier falling within this band would have its losses computed directly from equations 6 and 7 without correction. It is believed that most large rectifiers will fall inside this band.

Loss Measurements and Circuits

RECTIFIER TEMPERATURE

The normal rectifier loss falls somewhere between P_1 and P_2, which can differ by no less than 11% or more than 21% of P_1. During the P_2 measurement the loss in the cells will generally be no more than 6% above normal operating loss, even though the output current has been increased 10%. All other losses will be normal or slightly below. Therefore, it is recommended that P_2 be measured at normal rectifier temperature with the rectifier carrying KI_d. The current should then be dropped to I_d and P_1 measured as quickly as possible before the temperature of the Cu buses and heat sinks can change appreciably. It is further suggested that the tests be conducted with the rectifier adjusted to the temperatures that would be obtained in normal operation with an ambient air of 30 C (degrees centigrade) or incoming water at 25 C, depending on the system of cooling employed.

CONDUCTION PERIOD GREATER THAN 180 DEGREES

High-current low-voltage rectifiers, single-way rectifiers, and rectifiers employing control reactors in the cell circuits may have a large part of the total commutating reactance in their unidirectional branches. In such cases, the conduction period in short circuit may be considerably greater than 180 degrees. The successive lobes of the alternating current will not be exact replicas of the cell currents, since those portions beyond 180 degrees will be cancelled either directly or in transformation. Both alternating and cell currents should be checked oscillographically, and form-factor corrections made, if necessary.

COMMUTATING REACTANCE

Reactance in unidirectional circuits is difficult to measure. If large, it becomes an important factor in the regulation, power factor, and ripple output of the rectifier unit. Voltmeter, ammeter, and wattmeter measurements in the following described tests may prove useful in determining the total commutating reactance of the rectifier. When conduction greater than 180 degrees takes place, the conventional methods of determining reactance from the instrument readings will definitely not apply. A satisfactory method is still to be developed.

TEST CIRCUIT 1, FIG. 3

The most desirable way to measure rectifier losses is unquestionably by direct wattmeter measurements at the input terminals of the short-circuited rectifier. For large high-voltage rectifiers, standard wattmeters can often be used without instrument transformers. Industrial rectifiers will almost invariably require current transformers and low-voltage wattmeters. Fig. 3, illustrating a typical circuit, is hardly required, but is included for the sake of completeness. The unusual representation of the a-c

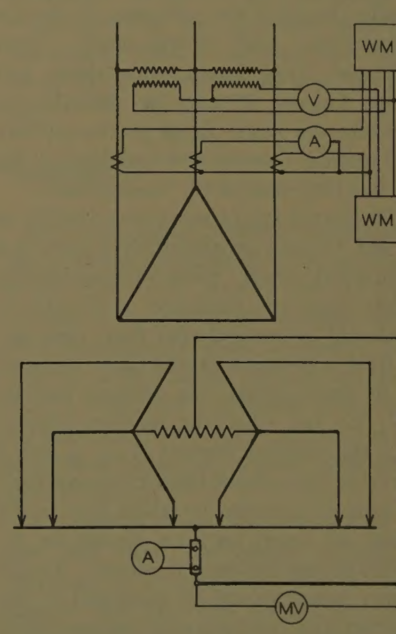

Fig. 4. Test circuit no. 2 primary wattmeter

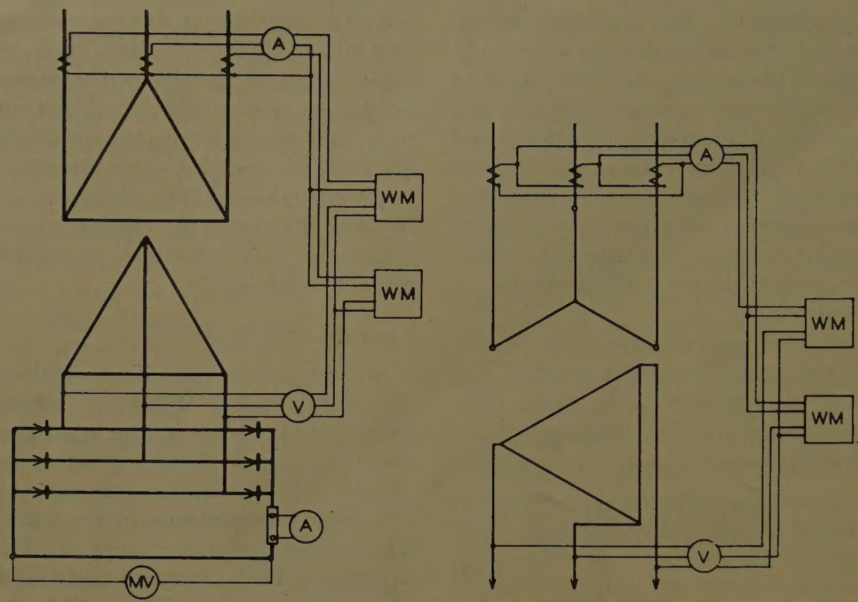

(A) (B)

Fig. 5. Test circuit no. 3 primary-secondary wattmeter

A—Y-connected current transformer
B—Delta-connected current transformer

voltmeter and ammeter connections is used to indicate that all 3-phase currents and voltages are to be measured by any suitable means.

Test Circuit 2, Fig. 4

Single-way rectifiers do not lend themselves to the above method, although instrumentation has been developed for mercury-arc rectifiers and can be adapted for semiconductor rectifiers. Moreover, both single- and double-way rectifiers are being built in current ratings and physical configurations that preclude the insertion of current transformer without significantly changing the geometry of the a-c connections and, consequently, their I^2R and stray losses. For these and other reasons, it may be desirable to measure the power input to the rectifier and rectifier transformer combined at the a-c line terminals of the transformer.

The transformer losses corresponding to P_1 and P_2 must be accurately known and subtracted from these measurements before they are combined to obtain P. It should be remembered that when the rectifier is delivering rated direct current, I_d, in short circuit, the primary current is I_L/K, and when the rectifier delivers KI_d, the primary current is I_L, I_L being the rated line current (neglecting overlap). Because of possible deviation from exact values all input currents should be recorded during loss measurements. Transformer losses should be measured at the currents and temperatures corresponding to the P_1 and P_2 tests, or at values close enough to permit corrections to these conditions with minimum error.

The primary voltage during these tests will be somewhat higher than the impedance voltage of the transformer and will, in many cases, require potential transformers. The power factor may be quite low, and wattmeters of the same class as used for transformer loss measurements are recommended.

Test Circuit 3, Figs. 5(A) and (B)

The preceding test circuit requires much extra labor and time in calibrating the rectifier transformer. With simple double-way rectifiers, it is possible t combine the advantages of test circuit 1 and 2 and eliminate the transforme losses from consideration. This is don by connecting the current coils of the watt meters to current transformers in th primary and the voltage coils directl across the transformer secondary termi nals. This circuit is shown for a delta delta transformer in Fig. 5(A). Fig. 5(B) shows a Y-delta transformer with the cur rent transformers connected in delta t transform the line currents to the sam phase angles and waveshapes as the alter nating currents of the rectifier.

In this test, the rectifier transforme operating at very low induction, wi draw a negligibly small exciting curren It becomes, in fact, a large current trans former.

Test Results

2,800-Kw Rectifier

The first test we had the opportunit to make was carried out on an 8,000 ampere 350-volt single-bridge water cooled rectifier, close-coupled to a delta delta oil-immersed transformer; see Fig 6. The loss measurements were made o the primary side in accordance with tes circuit 2. Although the cell buses ar water-cooled, the bulk of the Cu, con vection-cooled and operating at 75 C, in curs most of the losses. Two sets o measurements were made, the first with the main Cu at 24 C and estimated junc tion temperatures of 54 C; the second test with main Cu at 75 C and estimated junction temperatures of 84 C. Both test results are presented in Table I as a matter of interest.

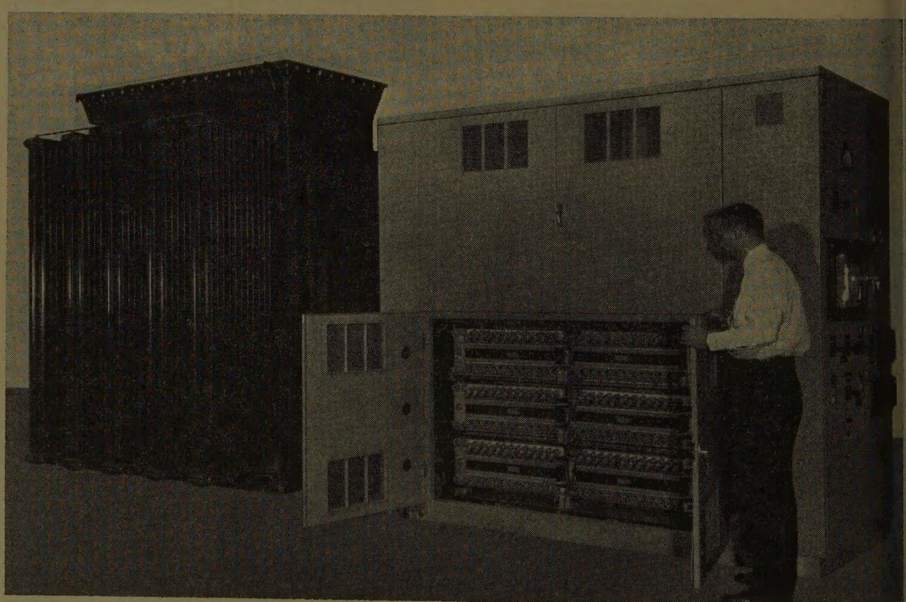

Fig. 6. Rectifier of 2,800 kw on which first test was made

Table I. Loss Measurements*

Transformer Calibration

	Test 1		Test 2	
	Top Oil Temperature, 29 C		Top Oil Temperature, 55 C	
	Loading, I_d		Loading, I_d	
	100%	110%	100%	110%
Cu loss, watts	21,170	25,620	21,870	26,470
Iron loss, watts	100	100	100	100
Total loss	21,270	25,720	21,970	26,570

Loss Measurements

	Test 1		Test 2	
	P_1	P_2	P_1	P_2
Total loss, watts	67,060	79,130	69,900	81,600
Measurements, P_1, P_2	45,790	53,410	47,930	55,030
Rectifier Loss, P, watts	51,750		52,250	

Estimated Rectifier Losses

	Test 1	Test 2
	Estimated Junction Temperature, 54 C; Estimated Average Cu Temperature, 24 C	Estimated Junction Temperature, 84 C; Estimated Average Cu Temperature, 75 C
Cell losses, watts	44,500	42,800
Ampere-trap fuses, watts	1,565	1,820
Cu losses	3,915	4,370
Estimated total loss	49,980	48,990
Error, watts	+1,770	+3,260
Error, %	+3.5	+6.7

* 8,000-ampere 350-volt water-cooled rectifier, bridge-connected; close-coupled to delta-delta oil-immersed self-cooled transformer; circuit 2, primary wattmeter.

Regrettably, our lack of experience, planning, and time detracted from the accuracy of calibration of the transformer. Losses were measured with currents and temperatures different from the values obtained during the rectifier loss tests. Corrections were computed within the limits of accuracy imposed by existing techniques. Small errors in transformer losses can be cumulative and produce a larger error in the final result. It is one of the weaknesses of the primary loss measurements method.

This may or may not be the explanation of the $6^1/_2$% "error." Actually it should be remembered that this error is the difference between a loss computed from measurements by a method we are trying to prove and an estimated loss based on simplifying assumptions. Even so, $6^1/_2$% of a 2% loss is not intolerable.

Measurements were made at two estimated junction temperatures to see how

Table II. Loss Measurements*

Estimated Rectifier Losses

Estimated junction temperature, C	87
Estimated cell losses, watts	4,950
Amp-trap fuses, watts	30
Cu losses at 50 C average, watts	50
Shunt, watts	80
Total loss, watts	5,110

Circuit 1: Direct Measurements

	P_1	P_2
P_1–P_2	4,800	5,440
Rectifier loss, P	5,110	
Error	0	

Circuit 2: Primary Wattmeter

	P_1	P_2
Total watts	7,200	8,200
Transformer loss	2,280	2,710
P_1–P_2	4,920	5,490
Rectifier loss, P	5,070	
Error, watts	−40	
Error, %	−0.8	

Circuit 3: Primary-Secondary Wattmeter

	P_1	P_2
P_1–P_2	4,840	5,370
Rectifier loss, P	4,910	
Error, watts	−200	
Error, %	−3.9	

* 2,000-Ampere 100-volt forced-air-cooled rectifier, bridge-connected; integrally assembled with delta-delta class B transformer.

well E_{th} and R' could be determined, working backward from the measured losses. By solving equations 4 and 5 and substituting $\sqrt{3}\ I_{avg}$ for KI_{rms}, the following is obtained:

$$E_{th}=\frac{K^2P_1-P_2}{K(K-1)AI_{avg}} \qquad (9)$$

$$R'=\frac{KP_2-K^2P_1}{(K-1)B(\sqrt{3}I_{avg})^2} \qquad (10)$$

Substituting suitable values for I_{avg}, A, and B, and from Table I for P_1 and P_2, we arrived at the following results:

	E_{th}, Volts	R', Ohms
54 C Junction, 24 C Cu	0.57	0.0023
84 C Junction, 75 C Cu	0.84	0.0031

Both E_{th} and R' have changed in opposite direction to that expected from increasing temperatures. It is obvious that the loss measurements were not sufficiently accurate to permit this reverse procedure, since we are dealing here with the small difference of two large, nearly equal quantities.

200-Kw Rectifier

We were able to test all three test circuits on a 2,000-ampere 100-volt forced-air-cooled rectifier employing a delta-delta class B transformer; see Fig. 7. The rectifier was bridge-connected. The results are shown in Table II.

We take no credit for the exact coincidence of estimated and measured losses

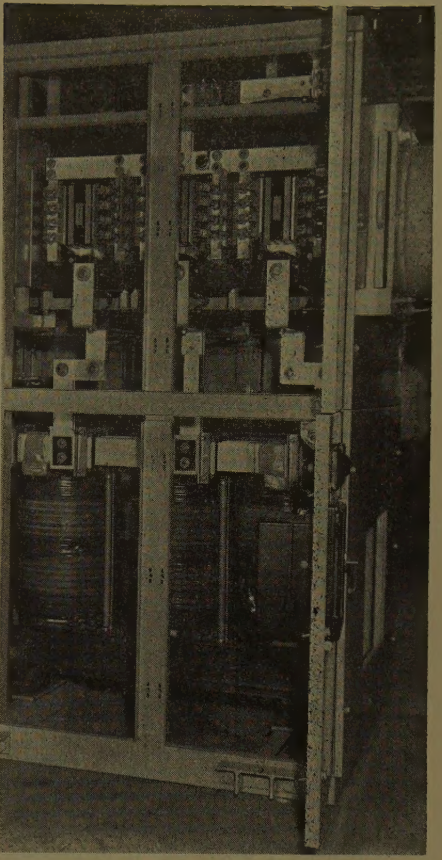

Fig. 7. Rectifier of 200 kw which was tested in all three circuits

in test circuit 1. Had it not occurred, it would still seem reasonable to use the direct measurement as the basis for comparison. $P_2/P_1=1.13$ and P is interpolated between them; any error cannot be much greater than the error of measurement.

It is significant that despite the low secondary voltage of approximately 2.2 volts available for the wattmeters in test circuits 1 and 3, the maximum spread for all three measurements was less than 4%.

Conclusions

By interpolation between two measurements which are generally 15% and never more than 21% apart, the proposed method of measurements achieves results with minimum reliance on human judgment or unreasonably difficult computations. The results obtained in our tests are gratifying, and it is hoped that others have been able to achieve similar or greater success.

The testing of all three circuits on one unit has been particularly rewarding. However, it is recognized that a 2,000-ampere unit does not present the problems encountered in heavy current rectifiers. Nor do the results obtained sup-

port entirely our order of preference of the three test circuits: (1) Circuit 1: direct measurements. (2) Circuits 3A and 3B: primary current, secondary voltage. (3) Circuit 2: primary measurements.

Accurate calibration of a rectifier transformer is difficult and should be avoided if possible. On the other hand, single-way rectifiers do not lend themselves to testing in circuits 1 and 3, and 12-phase rectifiers require special consideration.

A carefully calibrated test transformer would be highly desirable and would save much time. However, it would not be feasible to build one that would cover a wide range of rectifiers, nor would it solve the problem of ultracompact assemblies.

The simplest solution seems to be the combined measurement of transformer Cu losses and rectifier losses without segregating them. Existing and tentative standards would require changing and a considerable saving in testing time would be gained.

If the standards are to be relaxed, a study must first be made of the changes in the procedures for determining the transformer temperature rise as well as the correction of transformer losses to a standard temperature. It might be pointed out that the standard temperature of 75 C for Cu losses seems to be an anachronism for class *B* and class *H* transformers.

Let us test the combined loss method on the measurements made on the 2,800-kw rectifier. Substituting the total P_1 and P_2 measurements of Table I directly in equation 6, combined rectifier and transformer losses of 78,900 and 77,300 watts for the high and low temperatur tests are obtained, respectively. Subtracting the transformer Cu losses (a 110% I_d), the respective rectifier losses are then 52,330 and 51,580 watts, almos the identical values derived in Table I.

If the combined method is adopted circuit 1 then becomes the preferre method, providing the greatest over-al accuracy and requiring the least total tests ing time for combined rectifier and trans former Cu loss measurements and hea runs. The difficulties of separate trans former Cu loss measurements and calibra tion are eliminated.

Reference

1. Mercury Arc Power Rectifiers (book O. K. Marti, H. Winograd. McGraw-Hill Boo Company, Inc., New York, N. Y., 1930.

Discussion

L. F. Borg (Allmänna Svenska Elektriska Aktiebolaget [ASEA] Ludvika, Sweden): As secretary of the IEC Committee on Monocrystalline Rectifiers and Rectifier Equipments, I would like to express great satisfaction with the test method which Mr. Dortort has described in his excellent paper. A fundamental principle in the IEC recommendations, which will be sent out for criticism, is that most measurements on large rectifier installations should be made on the separate units and normally as no-load and short-circuit measurements. It was early felt that a method for short-circuit loss measurements on the rectifier assembly was badly needed and several more or less complicated methods have been discussed. The method described in the paper was proposed in order to make the measurements independent of any previous measurements on the data of the rectifier cells, which was an inherent weakness of the other methods discussed. So far as can be seen now, Mr. Dortort's method is simple, practical, and sufficiently accurate for the purpose.

Mr. Dortort's comments on the importance of overlap are essential and I would like information on one further item in that connection. It seems that with bridge connections the short-circuit conductor to be applied might have an inductance large enough to cause a circulation current component not appearing in the a-c circuit. That is particularly likely in such installations where the plus and minus terminals are situated as far apart as possible to minimize the risk of short circuits. If that is the case I think it might be valuable to introduce a method to correct for the errors caused by that phenomenon. Mr. Dortort's observations on this point would be appreciated.

H. Winograd (Allis-Chalmers Manufacturing Company, Milwaukee, Wis.): Mr. Dortort has rendered a valuable service by presenting this excellent paper at a time when the American standards for semiconductor rectifier equipments are in preparation. The measurement of losses in semiconductor rectifiers has been under discussion for several years, in connection with international and American standardization work. Mr. Dortort had a leading part in developing the proposed method.

While the paper deals with measurements for rated rectifier current, the same method could undoubtedly be applied for other currents, such as 75% or 50% of rated current.

In drafting the standards for loss measurement, consideration should be given to possible deviations from the required test conditions. It might be difficult or impossible to obtain the required operating temperature, particularly for air-cooled assemblies. Permissible deviations from the required temperature, or some reasonable correction factors, should be specified.

In some cases it may be difficult to obtain measurements at specific current values required for the application of equation 6 of the paper because of limitations in the current-regulating equipment or variations of the supply voltage. It would be desirable to include alternative equations for measurements made at two current values related by a ratio other than *K*.

For rectifiers in which the conducting period of the cells during the test is considerably greater than 180 degrees, it was suggested in the paper that form-factor corrections be made from an oscillographic check of the a-c and cell currents. An oscillographic test should be avoided, if at all possible, because of the added complications. Perhaps the power factor determined from the loss-measurement data, or the length of the conducting period measured with an oscilloscope connected across a unidirectional branch, could be used for applying predetermined correction factors, even if they could be considered only approximate. This subject requires further study.

No mention is made in the paper of the losses caused by the reverse voltage of the cells in rectifier operation. In the proposed international standards, the reverse losses in the cells are assumed to be negligible. The losses in voltage-dividing resistors an surge-suppression devices are to be deter mined by calculation. Guides for calculat ing these losses should be included in th standards.

J. C. Read (Associated Electrical Industri Ltd., Rugby, England): I think the pape timely and valuable; it shows how compli cated this problem can be, which at firs seems so simple. Nevertheless, in spite c the fact that I had a small part in puttin this proposal to the IEC, I now believe still requires further consideration. It wi probably be clearest if we divide the subjec into sections, as follows:

1. The suggestion that the standard should call for the transformer Cu loss an rectifier loss to be measured togethe without segregation, seems to me open t several objections. It would not affect th errors discussed under sections 6 and below; the cost and time needed to brin the transformer winding up to 75 C woul be objectionable; and, above all, it woul be inconvenient where the transformer an rectifier are built in different factories, an quite unsuitable in the not infrequent cas where they are built by different maker or in different countries. I think it i indispensable to have a method for deter mining the segregated loss in the rectifie This, it would seem, can only be done b testing the rectifier with a suitable trans former. The transformer used can either b a test plant transformer or the rectifier's own transformer, whichever is convenient.

2. As a rough allowance for the harmoni stray loss in the rectifier it has been pro posed that the rectifier losses determined b the test shall (as for the transformer) b those that would exist with rectangular cur rent waveforms giving the same averag value of d-c output current.

For polyphase rectifiers, this is the sam as assuming that the real current waveform in service will increase the rectifier Cu loss over that which occurs with sinusoidal cur rents, by about 6% of the combined rectifie Cu loss plus resistive component of cell loss This allowance will be too large in som

cases and too small in others. However, I think that, like the corresponding allowance made in determining the transformer Cu loss, it is fully justified on the grounds that (*a*) it greatly simplifies the treatment; (*b*) any error will be small compared with the total loss; and (*c*) above all, it does at least enable tests on different rectifiers to be compared on a uniform basis.

However, for single-phase rectifiers the current waveform in service, which in this case depends on the nature of the d-c load to be supplied, may not be accurately known at the time of the test and an arbitrary assumption must therefore be made. To assume rectangular current waveforms, as is attractive on the grounds of simplicity, would be to assume rms currents actually lower than those likely in service and would thus be equivalent to making a large negative allowance for harmonic stray loss, which would not be desirable. However, in many important cases, including that of traction, the current in service will not be unduly far from sinusoidal. For these reasons I believe that for the purposes of standards it will be best to base the efficiency determination on the current in service being sinusoidal. This means that in the single-phase case nothing would be allowed for harmonic stray loss. I think this is permissible, because in practice there are scarcely any cases where the exact value of the efficiency is very important for single-phase rectifiers, but the main need is rather for accurate comparative figures.

3. For the foregoing reasons the common practice of basing transformer rating and losses on the rms values of rectangular currents giving the specified direct current is undesirable in the single-phase case but these should be calculated on the basis of sine-wave currents.

4. There was great anxiety to obtain a method of loss measurement that would take account of the shape of the forward-voltage-drop characteristic that is shown typically in Fig. 1 of the paper. This led to the suggestion that the short-circuit power input be measured at two different values, resulting in equation 7. I was at first much attracted by this elegant solution, but after further experience with it I now think better accuracy can be obtained in a simpler way. The difficulty with equation 7 is that the loss is calculated from the difference between two comparatively large quantities, both of which have to be measured at low power factor and, therefore, with rather low accuracy. For this reason, with normal standards of testing the result can easily be in error to the extent of 6% or more when the methods of equation 7 are used.

Table III. Values of Rectifier Loss

	Cu Loss 0.1 × Cell Loss	Cu Loss 1.0 × Cell Loss
Input power P_1 at I_d, say..........	100	100
Input power P_2 at 1.1 I_d..........	1.1×45.45+ 1.21×54.55 =115.9	1.1×25+ 1.21×75 =118.2
Loss P given by equation 7 of paper..........	111.2	115.7
Alternatively: Loss P given by a single measurement at 1.08 I_d..	112.7	114.5

Assume for simplicity that U_{th} equals 0.5 of the total cell drop at peak current. Now in our experience, with large rectifiers the loss in the connections, fuses, etc., in the rectifier cubicle is nearly always between extreme limits of about 10% and 100% of the total cell loss. Then, in the absence of instrumental errors, we obtain the extreme values of the rectifier loss shown in Table III. From this table it is obvious that a single short-circuit test at 1.08 I_d, which is slightly simpler to do, would give actually greater accuracy than equation 7.

5. I think that for the purpose of a standard specification it is best to take the losses in the rectifier cubicle as those measured at the temperature normally prevailing in the maker's works, since this gives an inexpensive test and a good comparison between alternative rectifiers. Correction to another temperature would be questionable if calculated and costly if done experimentally.

6. In nearly all cases the input to the rectifier cubicle cannot be metered directly, but must be metered with the aid of a main stepdown transformer. With double-way-connected rectifiers, this presents no undue difficulty. Either (*a*) the power input to the short-circuited rectifier and transformer is measured on the primary side, and then the loss in the transformer and interconnecting leads is measured by short-circuiting at the input terminals to the rectifier cubicle and measuring the input at the same primary current; or (*b*) for a 3-phase bridge connection the input to the short-circuited rectifier is measured directly as in Fig. 5. Either way there are no substantial inherent errors.

However, many semiconductor rectifiers are connected single-way (e.g., 6-phase double-Y or equivalent), and with the constantly increasing voltage rating of the cells available the use of single-way connections is increasing. Here we must meter on the primary side of the transformer, as in Fig. 4, and then measure the losses in transformer and leads as in (*a*) above (except that only particular terminals are short-circuited in this latter test, in accordance with the well-known rules[1]). However, in this case the presence of reactance in the secondary circuit can produce substantial and inherent errors, particularly with low-voltage rectifiers.

The assumption made so far has been that the current waveform in the short-circuit test will be as shown in Fig. 8. With reasonably high total reactance the slight distorting effect of U_{th} is negligible and these waveforms are sufficiently closely approached, provided that the secondary reactance is negligible. However, with single-way rectifiers there will usually be appreciable secondary reactance, partly between the two opposite secondary phases 180 degrees apart, partly in the interconnecting leads, and partly in the internal connections in the rectifier cubicle. In the extreme case where the secondary reactance is the determining feature, the current waveforms (with a perfect rectifier) become as shown in Fig. 9. Practical cases usually lie between the two extremes represented by Figs. 8 and 9, but consideration of Fig. 9 will show the magnitude of the errors that may exist. These are due to two causes.

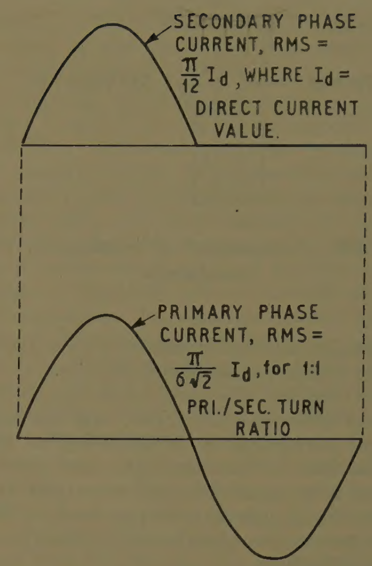

Fig. 8. Rectifier current waveform in short-circuit test when secondary reactance is absent

If we regard the primary and secondary currents in Fig. 8 as unity, then in Fig. 9, for the same current I_d, they become $2/\pi$ and $\sqrt{6}/\pi$ respectively. The presence of secondary reactance may therefore make the resistive component of the cell loss and the Cu loss in the rectifier cubicle appear to be only about 60% of what they should be.

The presence of secondary reactance will also have reduced the losses in the transformer and interconnecting leads. For a 6-phase double-Y or equivalent connection, these losses are allowed for by deducting the measured input watts at the same primary current with three of the a-c input terminals to the rectifier cubicle 120 degrees apart short-circuited (and also deducting the small loss in the interphase transformer, if any). In the case of Fig. 8, this is correct, but in Fig. 9 it is not correct because in this test, the secondary Cu loss is only two thirds of that which existed in the secondary when the rectifier was present in the short-circuit test. This will make the rectifier loss appear greater than it really was.

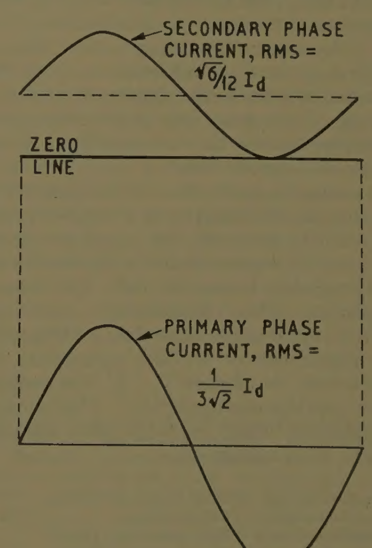

Fig. 9. Rectifier current waveform in short-circuit test when secondary reactance is determining feature

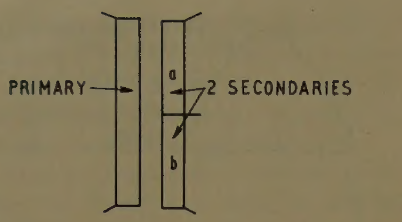

Fig. 10. Arrangement of windings in test transformer

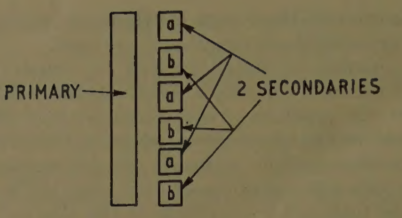

Fig. 11. Winding arrangement in some low-voltage single-way transformers

Similar errors are present in testing single-phase rectifiers of the single-way type.

Mr. Dortort has drawn attention to the first of these possible errors, and has suggested correcting for it according to the actual value of the form factor that existed in the short-circuit test on the rectifier, i.e., as in Fig. 2. Such a measurement of the form factor appears to present serious practical difficulties.

It is thus worth considering what can be done to reduce the effect of secondary reactance. Neither extra primary reactance nor inductance in the d-c short-circuit path help, for in Fig. 9 the primary current is already a sine wave and the direct current is already perfectly smooth. Since it may well be impracticable to reduce the secondary reactance, the most effective means for reducing its effect, i.e., for reducing the secondary current spread, appears to be the introduction of resistance in the secondary circuit, since this, unlike reactance, acts on the whole secondary current and not merely on its a-c component. It is necessary, however, to introduce enough resistance to bring the secondary current fairly close to the half-sine-wave form of Fig. 8, since as long as the current is as in Fig. 9, the bigger the loss in the secondary circuit, the bigger will be the second error discussed above.

It seems to me that for the purpose of standardization the best course in the case of single-way rectifiers will be to set a maximum allowable limit to the departure from 180 degrees of the secondary current spread. Further work appears to be necessary before we can establish what this permissible limit should be. This is very inconvenient, but I cannot at present see any alternative.

7. In some low-voltage heavy-current single-way rectifier equipments, a further substantial error may be present; namely, a change of the stray loss in the transformer according to how this is operating. An example will explain this.

Among our early tests to measure rectifier loss, we tried supplying a double-Y rectifier cubicle from an old stepdown transformer that was available in the works and had originally been built for a synchronous converter. This transformer was connected star/6-phase diametric which, under the conditions of rectifier operation, was equivalent to double-Y. At the voltage used, core loss was negligible. The following transformer input readings were obtained in the short-circuit tests:

Transformer and rectifier (after deducting loss in d-c short-circuiting loop)	22 kw
Transformer only (three secondary terminals short-circuited), at same primary current	27 kw
Hence, apparent loss in rectifier cubicle	−5 kw

Examination showed that this transformer had the center point of the secondary winding brought out half way along the length of the coil, as shown in Fig. 10. The secondary reactance was very high, but the surprising result could not be accounted for by the effects discussed in section 6. The explanation appears to be as follows. When operating with the short-circuited rectifier, the currents (Fig. 9) in the two secondary part-windings in the same stack added up, so far as their a-c components were concerned, to a uniform complete sine wave of current occupying the whole length of the stack. But when only the transformer was short-circuited, across one Y, the secondary current occupied only half the length of the stack and thus half the length of the primary winding. In this latter condition the leakage flux path was quite different, and in the transformer concerned accounted for a great increase of stray loss.

This example cannot be altogether dismissed as a freak case. Many low-voltage single-way transformers have the windings arranged approximately as Fig. 11. This is obviously part way towards the arrangement of Fig. 10. Such transformers are often quite satisfactory for their purposes, and the working loss in them is correctly measured by the existing standard method. However, when used to measure rectifier loss they may give rise to serious error. This error is caused by the wide spread of the secondary current. Consequently the same safeguard as was proposed in section 6 will also guard against this.

8. It is possible that still further points need to be considered. However, so far as we have yet gone, I now believe for the above reasons that for the purposes of standardization, (*a*) the loss in the rectifier cubicle should preferably be taken as the input power to the cubicle measured in a single short-circuit test, at normal factory temperature, at $1.08I_d$ for polyphase or at I_d for single-phase rectifiers; (*b*) in the case of single-way rectifiers the secondary current spread in the test should not depart from 180 degrees by more than a definite amount (to be specified after further investigation); and (*c*) the rating and losses of single-phase rectifier transformers should (unlike polyphase) correspond to sinusoidal currents giving the specified direct current, not rectangular currents.

Reference

1. Recommendations for Mercury Arc Converters. *Publication 84*, International Electrotechnical Commission, Geneva, Switzerland, 1957, clause 342.

I. K. Dortort: It was obvious from the start that the proposed test methods have certain inherent weaknesses which require further study and experience. The three gentlemen who have submitted discussions have pinpointed some of these problems. In particular they have questioned the conditions under which tests are conducted, the marriage of rectifier and transformer, and the validity of tests in which the conducting period is greater than 180 degrees due to inductance in the circuit elements.

Mr. Borg has also brought up the interesting case of extended conduction due to inductance in the d-c circuit. In a 1953 paper,[1] I presented an analysis of a rectifier with all commutating reactance in the a-c circuit but with the d-c short circuit including a large inductance. It was shown that in the ideal case conduction would last 240 degrees. While the paper does not evaluate the effect of finite d-c inductance, our experience leads us to believe that a separate test method to satisfy this condition will not be necessary except for extremely special cases.

In the first place, it appears that the d-c inductance would have to be of the order of magnitude of the leakage inductance of the transformer to produce conducting periods appreciably greater than 180 degrees. Second, losses in the circuit will further decrease conduction beyond 180 degrees. In addition to the extended overlap, the d-c inductance will of course tend to make the cell currents flat-topped, but this error, if appreciable, can be corrected in accordance with Fig. 2 of the paper.

Actually, a high inductance in the short-circuiting bus is more likely to occur in the double-Y rectifier rather than in a bridge-connected rectifier since the d-c terminals are likely to be much further apart, and a further contribution is made by the leakage reactance of the interphase transformer. Moreover, a double-Y connection is more likely to be used for high-current low-voltage rectifiers in which the effect of d-c inductance becomes more pronounced.

More serious, and more prevalent, is the presence of inductance in the unidirectional circuits, i.e., the circuit elements. This is the condition referred to in the present paper. Application of a correction based on form factor from the curve of Fig. 2 seems to be the only practical solution and will give good results for the rectifier itself. However, the extended conduction period reduces the Cu losses in the transformer and makes proper calibration of the transformer more difficult. Dr. Read's suggestion of placing an upper limit on the extended conducting period is well taken. Just what this limit should be is difficult to say at the moment. Considerable study and experience will be required to settle this question. Form-factor correction should be quite satisfactory for the Cu loss in the unidirectional circuits and the secondary of a single-way rectifier transformer. The Cu loss in the primary, as well as in the secondary, of a double-way transformer will be reduced due to cancellation of d-c components. Purely as a guess, a conducting period of 190 degrees is suggested as a starting point for discussion.

Although no investigation has been made, it seems likely that by far the largest number of industrial rectifiers will have conducting periods of less than 190 degrees. The form-factor correction on the rectifier should be adequate, and correction of the transformer copper loss can be estimated fairly well from the primary current readings taken during the tests.

Mr. Winograd questions the use of the oscillograph for determining form factor, nd suggests determination of conducting ngle by means of a cathode-ray oscillograph. t appears to me that measurement of the onducting angle is not sufficient for deternination of the form factor when the angle s appreciably greater than 180 degrees. It vas not the intent to specify a magnetic oscillograph for this work. A plot or picure of the waveform displayed on a cathodeay oscillograph should be sufficiently acurate. I certainly agree that further conideration is required but do not feel that vork on the standards should be delayed. The effect of form factor has been of only econdary importance in the rectifiers tested o far.

Regarding Mr. Winograd's comment conerning P_1 and P_2 measurements at other han I_d and KI_d, it is obvious that loss measrements at three-fourths, one-half, and ne-fourth load can be made easily and vithout too much loss of time by substituting fractional values for I_d but retaining the ame ratio of direct current in the two neasurements. The difficulty of maintaing exact values of direct current presents somewhat more complicated procedure. f, instead of I_d and KI_d, the test is made at I_d and bKI_d, equation 6 of the paper hanges to

$$P=\frac{a(K^2-a)P_2-bK^2(K-b)P_1}{abK(bK-a)}$$

f $a=b$ so that the ratio of the two currents s still K, the above expression is only ightly simplified to

$$P=\frac{(K^2-a)P_2-K^2(K-a)P_1}{a^2K(K-1)}$$

The specification of ambient-air or rawooling-water temperature at the time of the est poses a difficult problem. In a recirulating cooling system, whether air or ater, the temperature of the equipment an be controlled without too much difficulty rovided the raw-cooling-medium temperares are low. If the raw-cooling-medium mperatures are higher than specified, ere would be no recourse but to wait for ore suitable conditions or to find some eans of reducing these temperatures. In rect-cooling systems recirculation can ften be improvised. In any case, I fully gree that tight specifications could be erous and it might be wise at this time to rovide fairly wide latitude in the standards that tests can be made under prevailing nditions except in extreme cases. When tisfactory methods are worked out for aking temperature corrections, the perissible band of ambient temperatures ight be broadened.

While most standardization committees ve agreed that the reverse current losses the cells are to be neglected in computing ficiencies, it is obvious, as pointed out by r. Winograd, that voltage divider resistors, d in some cases surge-suppression devices, ust be taken into account. At no load e rms value of the reverse voltage across a circuit element in a 3-phase bridge-connected rectifier is $0.66E_{do}$. In the double-Y connection the rms value of reverse voltage under the same conditions is $1.33E_{do}$. From these values and the known value of resistance across a circuit element, the loss of a complete bridge rectifier is $8E_{do}^2/3R$ and for a double-Y rectifier it is $32E_{do}^2/3R$. For the sake of simplicity it is suggested that nonlinear surge-suppression resistors be treated as linear elements since in most cases their nonlinearity becomes effective only at excess voltage.

Dr. Read has brought up several points that were bound to cause concern and discussion. While it seems to me that the combined transformer and rectifier loss test is the most advantageous, restriction to this method in the standards would be unwise and unfair. We should not impose higher testing costs by making it mandatory to marry the transformer and rectifier on the test floor. However, the increased cost is not chargeable to the time required to bring the transformer up to temperature. If the rectifier and transformer are not brought together, the transformer must still be subjected to a heat run unless it is a duplicate of a previous design, previously tested. During the rectifier test with a calibrated test transformer, we must still allow enough time to stabilize the temperature of the test transformer in order to make its calibration valid.

With reference to single-phase rectifiers, there can be no serious objection to making $K=1.0$ for all but highly inductive loads. Even then, we would have no serious objection to $K=1.0$ in order to put all tests on a comparable basis, if the standardization committees decide to do so.

The suggestion to substitute a single loss measurement at 1.08 I_d for the two measurements at I_d and KI_d does not seem to be justified by facts. The statement is made that under normal standards of testing the proposed method of testing is subject to at least 3% error because the power loss is the difference of two large quantities, the P_2 and P_1 terms in equation 6. These terms have a ratio of approximately 2 to 1 and errors of measurement can therefore be assumed to be doubled in the result. Dr. Read has offered two examples to show that a single measurement at $1.08I_d$ would be more accurate. If we check P at the two theoretical limits of $E_{th}=100\%$ and $E_{th}=0$, we find that $P=P_1$ and $1.21P_1$ respectively. Had we made a single measurement at 1.08 I_d we would obtain an error of 8% in the first case and of 11% in the second. It is true that these represent extreme theoretical cases, but by now we have seen a variety of rectifiers in which both of these limits have been approached.

After Dr. Read submitted his discussion of this paper, he carried out additional investigations and transmitted the results to me. Using the same copper-loss ratios as in the earlier investigation, he introduced into each case values of E_{th} equal to 25 and 75% of the total cell drop. In three of the four cases the computed error for a single measurement at $K=1.08$ ranged from 0.17 to 2.7%. When E_{th} represented the major portion of the total loss, the error was found to be +4.2%.

It should be noted, however, that equations 6 and 7 of the paper contain the differences of two quantities having a ratio of, roughly, 2 to 1. These quantities in turn contain P_2 and P_1 which differ by approximately 15% and would normally be measured with the same instruments and instrument transformers, all set for the same ranges. Therefore, their errors will not be accumulative. Instrument error will therefore affect the end result to no greater extent than the instrument error of a single measurement at $K=1.08$. The single measurement would introduce an additional error above the instrument errors.

Returning to the question of conducting periods greater than 180 degrees, it is not difficult to account for the negative rectifier loss reported by Dr. Read in a measurement made with a transformer having the winding arrangement illustrated in his Fig. 10. We need not go into the nebulous realm of stray losses to account for this astonishing result. Working only with I^2R, a quick analysis shows that because of the greatly extended conduction period brought about by uncoupled secondaries the secondary copper losses obtained during the short-circuited rectifier test will be 39% less than when the transformer is tested alone in the approved manner. The primary losses are down 60%. It is unlikely that any rectifier transformers designed for industrial use, whether single-phase or 3-phase, would ever embody the construction shown in Fig. 10. The winding arrangement shown in Fig. 11 is more reasonable and the effects of loose coupling would be reduced to about 1/4. Even this winding arrangement is contrary to usual practice.

I wish to thank those who have contributed discussions on the proposed test method, and particularly Dr. Reed. It is necessary to bring to bear on this subject all the technical knowledge and the experience that is being accumulated in various organizations. The need for standards is urgent and cannot wait until a perfect method is developed. Fortunately, the industrial applications in which standards are most needed and to which the bulk of power rectifier production is devoted, can be covered by standards which do not contain all the refinements discussed here. Questions of combined tests and ambient temperatures are not peculiar to rectifiers and can be handled for the time being by reasonably nonrestrictive test codes. Limits must be assigned to avoid application of these standards to rectifiers for which they are not suitable. As the art develops, the standards can be modified to cover rectifiers which must be excluded at this time.

Reference

1. Extended Regulation Curves for 6-Phase Double-Way and Double-Wye Rectifiers, I. K. Dortort. *AIEE Transactions*, pt. I (*Communication and Electronics*), vol. 72, May 1953, pp. 192–202.

Comparison of Steel and Aluminum Subway Cars

L. W. BARDSLEY
MEMBER AIEE

MILD STEEL has been the usual basic structural material for subway-car strength members with aluminum generally utilized for decorative or low-stressed sections.

The characteristics of aluminum alloys, i.e., high strength-to-weight ratio and excellent resistance to corrosion, appear to offer them a place in subway-car construction, where power, brake-shoe wear, and way-maintenance costs reflect car weight, and where corrosion resistance is a vital factor in body life.

The Toronto Transit Commission (TTC), by purchasing at one time a number of otherwise identical steel-shell and aluminum-shell subway cars, established a means whereby practical "in-service" comparisons of steel and aluminum in subway-car construction became possible.

The TTC contracted for 104 steel subway cars for delivery in 1953–54, to operate its Yonge Street line, opened in 1954. These cars were manufactured by Gloucester Railway Carriage and Wagon Company of England. During the course of car construction in 1952–53, the Commission was approached, through the manufacturer, by the Aluminum Development Association (ADA) of Great Britain to consider the construction of a number of these vehicles in aluminum rather than steel.

As a result of discussion with the ADA and the car builder, the Commission revised its order to 100 cars of steel and four of aluminum with the general dimensions as noted in Fig. 1. By this means, since the cars were identical in all respects other than the aluminum application, in-service testing and experience would be able to determine if the operating gains through the use of aluminum would justify the increased initial capital costs.

The advantages of aluminum compared with mild steel (*SAE 1020*) are: a much more favorable strength-to-weight ratio; superior corrosion resistance; and its use in an unpainted condition. From these considerations, operating savings could be expected (1) in areas affected by weight, and (2) in maintenance costs through reduced corrosion of body members.

In any comparison of vehicles where performance is in question, one of the fundamental factors for consideration is the relation of schedule speed and power costs. Also, an examination of any operating line must consider passenger density, headway, cars per train, and schedule speed. Headway and train size are influenced by passenger density and associated with service facilities such as station lengths, station exits, entrances, and so on.

Under a given set of conditions concerning passenger density, headway, and train size, a variety of scheduled speeds, number of trains, and, consequently, cars required for service can be ascertained. However, train speed variations reflect variations in power consumption. For an economic analysis, therefore, the initial capital cost for cars required for a service should be analyzed in respect to annual operating costs of train crews, power consumption, brake-shoe life, and allied factors.

In comparing vehicles such as steel and aluminum subway cars where a weight reduction is obtained by using aluminum, either of two choices may be made:

1. Choice 1 would be to maintain the same operating schedule with the aluminum or lighter subway car because, for any given weight reduction, the lighter car can maintain the schedule of the heavier car at a lower operating cost.

2. Choice 2 would be to utilize the weight reduction to obtain a faster schedule speed for the same power usage. The faster schedule could result in a reduction in the number of trains operating with a consequent saving in train crews and initial capital outlay for rolling stock.

The TTC's aluminum subway cars operate in mixed service with the steel cars and must, therefore, operate on the same schedule. Thus, the comparison of performance must be as in choice 1, that is, determine the savings in operating costs while maintaining the same schedule.

With these factors in mind the Commission decided to establish comparative tests on certain components and operating cost areas where definite savings might be expected as follows: in factors influenced by weight reduction: (1) tractive power costs; (2) journal and drive unit bearing life; (3) wheel and brake-shoe life; (4) permanent way life and maintenance. In factors influenced by corrosion resistance: (1) body maintenance costs.

By assigning values to the saving factors determined and amortizing the initial vehicle costs over a 30-year period, a realistic picture of the financial relationship of the steel and aluminum subway cars can be obtained.

The relatively short in-service life of the vehicles does not permit complete actual analysis. However, the calculated effects together with actual results where possible have been compiled.

Structure and Weight

The steel and aluminum subway cars are basically similar in body appearance

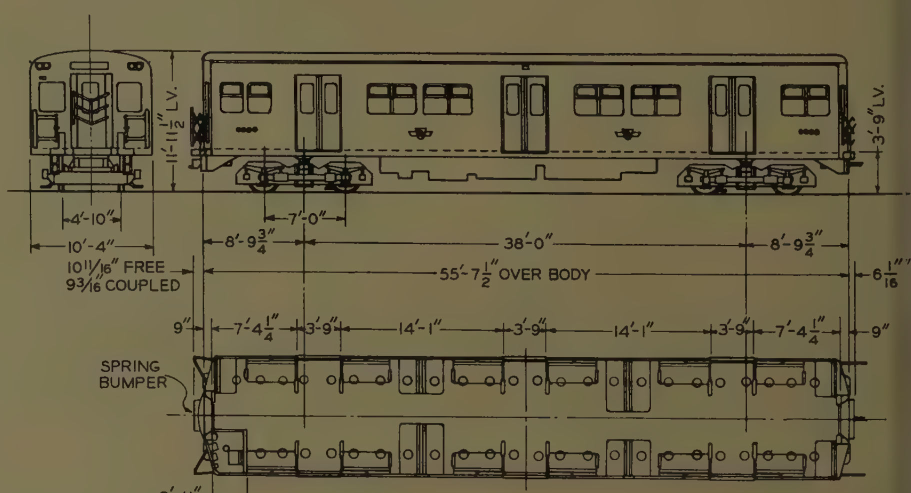

Fig. 1. Toronto Transit Commission subway car plan and elevation

Paper 57-791, recommended by the AIEE Land Transportation Committee and approved by the AIEE Technical Operations Department for presentation at the AIEE Summer General Meeting, Montreal, Que., Canada, June 24–28, 1957. Manuscript submitted March 26, 1957; made available for printing February 21, 1961.

L. W. Bardsley is with the Toronto Transit Commission, Toronto, Ont., Canada.

Fig. 2. Interior body shells

A — Aluminum cars
B—Steel cars

(A)

(B)

Fig. 3. Underframes

A—Sills and body bolster of aluminum cars
B—Sills, body bolsters, and heating ducts of steel cars

(A)

(B)

excluding the essential difference in material.

The entire body shell of the aluminum car, including side frames and equipment mounts, is constructed of aluminum alloys, with the one exception of the body bolster which is steel. This latter becomes necessary because of space restrictions and vehicle standardization coupled with the low elastic modulus of aluminum.

Additionally, because of the small number of cars involved, the aluminum members were fabricated from standard shapes in many instances where, if quantity permitted, a more advantageous strength-to-weight ratio might have been obtained through the use of special extruded shapes possible with aluminum.

It would appear that, without limitations imposed by the steel prototype and the necessity for standardization for equipment mounting, a lighter aluminum car could be produced within the dimensional framework imposed by the subway structure.

The aluminum alloys used in the aluminum car design varied with requirement. For example, the main structural and other highly stressed members were constructed from an aluminum magnesium silicon alloy containing a small percentage of copper and chromium. The exterior panels, which were to be unpainted, used an aluminum $3^1/_2\%$ magnesium alloy, cold-rolled for strength.

The steel cars were constructed basically from mild steel, although aluminum was used in some cars for roof sheets and doors and in all cars for trim and other decorative purposes. The steel cars were also painted in the standard Commission color scheme.

Figs. 2 and 3, depicting underframe and side-frame construction, illustrate variations in design between the aluminum and steel cars.

Car weights of the 100 steel cars varied because of an increasing use of aluminum in nonstrength locations as car construction progressed. Table I lists car weights for all car types used in the Toronto subway.

Power Consumption

Considering the probable effect of weight reduction on power consumption, the ratio of power to weight saving is an important factor. The fundamental equation of tractive effort: weight × accel-

Table I. Toronto Transit Subway Cars

Car Nos.	Number in Group	Type	Basic Structural Material	Weight, Lbs
5000-5029	30	driving motored	steel	85,525
5030-5099	70	driving motored	steel	83,670
5100-5105	6	driving motored	aluminum	73,250
5100-5115	6	driving motored (dynamic braked)	steel	82,726
5200-5227	28	nondriving motored	steel	76,720

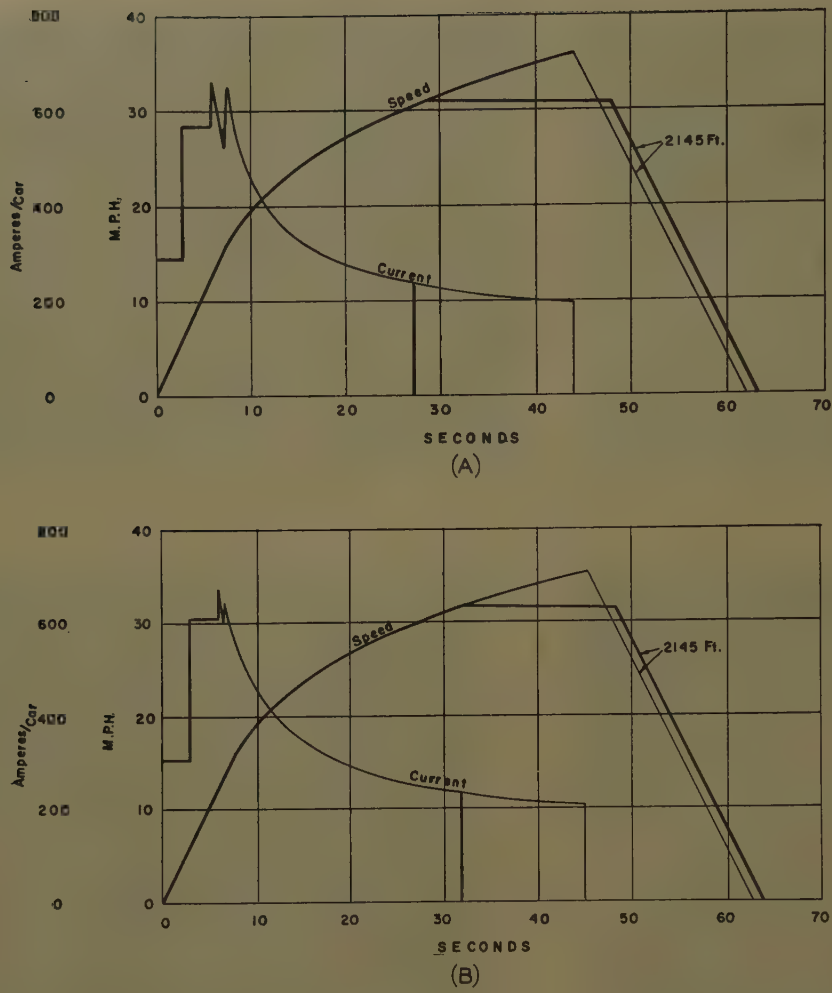

Fig. 4. Speed and current time curves; 10,000-lb load; down 0.56% grade; run length, 2,145 feet

A—Type G2 aluminum cars; 73,250-lb tare
B—Type G1 steel cars; 83,670-lb tare.

eration/g, would suggest that power consumption and weight should vary directly. However, it is equally apparent that other factors, such as losses due to rotating equipment within a vehicle; train resistance as a function of vehicle shape, weight, and speed; and friction at bearings, contribute to modifying the simple relationship of force and acceleration.

Two methods have been employed by the Commission in attempting to obtain power consumption comparison of the steel and aluminum subway cars: (1) calculation and (2) direct measurement (in service through the use of installed meters).

Calculation

For comparative calculation of the effect of weight reduction on power consumption certain conditions were established.

1. Length of run assumed to be 2,145 feet representing the average between-station subway distance on the Yonge Street line.
2. An average run on tangent track of 1.2% up and 0.56% down.
3. Acceleration rates approximately the same on both car types.
4. Tare weight of steel car, 83,670 lbs (pounds).
5. Tare weight of aluminum car, 73,250 lbs.
6. Assumed passenger weight per car, 10,000 lbs.
7. Same schedule speed.
8. Same motors and field shunting.

The cars under consideration were identical in respect to body profile, mounted underbody equipment, trucks, and motors. For comparison, schedule speed or run time was held approximately constant for each car. The motors were identical in characteristics and field shunting; the only effective variable other than weight which might affect energy consumption was accelerating amperes and coasting.

Within the framework of identical time and distance, a number of variations in accelerating amperes and coasting can be obtained. For practical comparison however, the most realistic assumption would be to maintain the same acceleration as much as possible in both cases.

On the basis of the conditions outlined, performance speed time and current time curves for the aluminum and steel cars were developed as noted in Figs. 4(A) and (B). From these curves the data in Table II are derived.

Direct Measurement

With a view to subsequent power-consumption tests, the Commission during car construction arranged for the inclusion of eight resilient mounted watt-hour meters in four steel cars, nos. *5096-5099* and four aluminum cars, nos. *5100-5103* for measuring traction power consumption.

The cars entered service in March 1954 and monthly readings of the meters were taken. The average power consumption obtained through these meters between March 1954 and January 1956 are given in Table III.

Table II

Car Type	Weight Per Car*	% Weight Reduction	Power Consumption, Kw-Hr†/Car Mile	% Power Reduction
Steel cars *5096-5099*	93,670		4.8	
Aluminum cars *5100-5103*	83,250	9.0	4.4	8.3

*Weight is tare plus 10,000-lb load.
† Kilowatt-hours.

Table III

Car Type	Weight*	% Weight Change	Power Consumption, Kw-Hr/Car Mile	% Power Consumption Change
Steel cars *5096-5099*	83,670		4.80	
Aluminum cars *5100-5103*	73,250		4.40	8.3

*In-service weight not known.

Table IV. Load Conditions Journal Bearing Life

% Operating Time	Steel Car Weight, Lbs			Aluminum Car Weight, Lbs		
N)	Tare*	Passenger	Total Weight* (F)	Tare	Passenger	Total Weight* (F)
.51	84,010	21,000	105,010	73,250	21,000	94,250
.96		11,200	95,210		11,200	84,450
.96		7,000	91,010		7,000	80,250
.61		4,200	88,210		4,200	77,450

Steel car weight is average for 100 steel cars.

The comparison between the calculated nd direct-measurement power-consumpon figures indicates identical answers. his accuracy is, we feel, coincidental. irect measurement of power includes ariables of passenger loading, train akeup, and actual coasting. To deterine these figures theoretically, particarly based on an average run calculaon, the accuracy obtained is extremely uestionable. Coincidence in this case probably the answer.

Coasting is another extremely imporant variable. It may be seen from the urves in Fig. 4 that for a very small crease to run time, an appreciable nount of coasting can be inserted hich results in a major reduction in ower consumption.

For the purposes of this study, howver, the actual power saving of 0.40 kwr/car mile will be used.

earing Life

Although both the motor-drive bearings nd the load or journal bearings are ffected by weight reduction, the possible aving in life of drive bearings has been mitted as a negligible factor because of ne bearing cost.

The analysis of the weight effect on earings is, therefore, confined to the ournal bearings, of which there are ght pairs or 16 bearings per car.

The general antifriction bearing forula is:

$$= \left(\frac{C}{P}\right)^{10/3}$$

here

=minimum bearing life, millions of revolutions
'=constant for bearing assembly
=equivalent dynamic load

The minimum bearing life, L, for the oronto aluminum subway cars has been alculated as 1.61 times that for the steel ars.

The load conditions and calculation ethod to determine this factor are ilustrated in Table IV and Appendix I espectively.

The minimum bearing life L, since it represents revolutions, in the case of road wheel can be transposed into miles by calculating the number of revolutions per mile by the 30-inch wheels used on the subway cars. This approximates 150,000 miles for the steel cars and 241,000 miles for the aluminum cars.

The bearing industry subscribes to the theory that "average" bearing life, on which costs are based, can be assumed to be five times the minimum or what is commonly referred to as *B-10* life. On this basis the average expected bearing life on the Toronto subway cars under discussion should be, for steel cars: 750,000 miles, and for aluminum cars: 1,207,500 miles.

If it is assumed that car miles per year = 55,000 and the number of bearings per car = 16, then annual bearing saving per year per car = $0.47R$, where R is the bearing cost.

Factual data are not yet available because of the short service life, so the theoretical figure only is used in subsequent evaluation.

Brake-Shoe Life

Within the normal operating speed limit of 50 mph (miles per hour) on the Toronto subway, the maximum kinetic energy for an 83,670-lb steel subway car with its maximum loading of 31,000 lbs (222 passengers) is determined from the kinetic energy formula

$$KE = \frac{W}{2g} V^2$$

where

W = weight, lbs
V = velocity, ft/sec (feet per second)

This results in a KE value of 960,000 ft-lbs per sec, or 60,000 ft-lbs per sec per shoe.

Within this range of work per shoe, experiments conducted at the University of Illinois Experimental Station have indicated that the relationship of brake-shoe wear, in terms of lbs per 100 million ft-lbs of work, approximates a linear relation to the average rate at which braking is done; see Fig. 5 and Appendix II.

From this relationship it can be derived, as noted in Appendix II, that brake-shoe wear varies directly as the square of the car weight for a vehicle equipped with cast-iron brake shoes.

It would be expected therefore, that in the aluminum cars cast-iron brake-shoe life should be increased by the square of the ratio of car weight or:

Brake-shoe life, aluminum car

$$= \left(\frac{W \text{ steel car}}{W \text{ aluminum car}}\right)^2 \times \text{brake-shoe life, steel car}$$

Assuming a 10,000-lb passenger load in each case:

Brake-shoe life, aluminum cars = 1.24 × brake-shoe life, steel car

Actual tests during 1955 and 1956 showed the following: average brake-shoe life, aluminum cars = 7,550 miles per shoe; average brake-shoe life, steel cars = 6,220 miles per shoe; therefore actual brake-shoe life of aluminum cars = 1.214 × brake-shoe life of steel cars.

The discrepancy between theoretical and actual results may be due to the assumption that the brake-shoe wear varies linearly with the rate of doing work

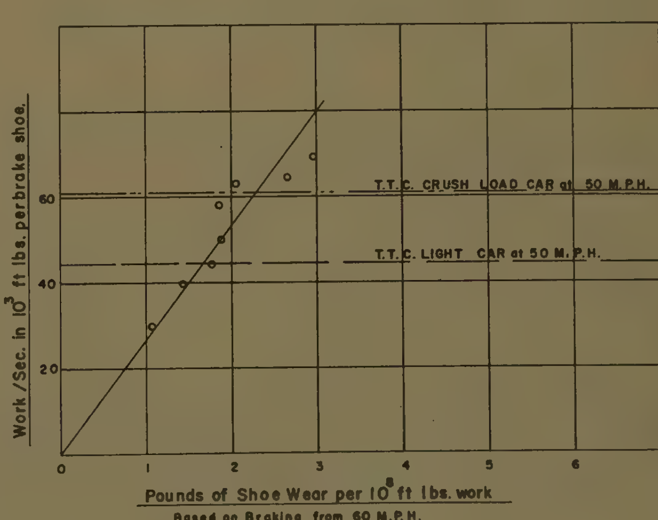

Fig. 5. Relation of Diamond S brake-shoe wear to work done in braking

and validity of the assumption of passenger loading.

Within the test period, because of a change in service train size requirements, the aluminum cars were mixed indiscriminately with steel which resulted in higher work requirements for the aluminum car brake shoes and hence decreased life.

For analysis, however, the agreement appears satisfactory although the in-service performance record will be used to compare savings which come to 21.4%. Since the TTC average brake-shoe consumption per car per year for 104 cars is 118, the annual saving per car per year for the aluminum cars may be stated as: $0.214 \times 118 \times A = 25A$ where A represents the cost per shoe.

Wheel and Track Wear

The effect of weight reduction on wheel and track wear is difficult to determine. Tangential shear components in propulsion, dynamic loading in motion, and tangential effects on wheel and track are all effective factors in wheel and track wear.

In considering the variation in life of wheels and track work due to weight reduction, it is probably safe to assume that since acceleration and braking rates are maintained constant on the steel and aluminum cars the main governing factor would be dynamic effects. For the wheel these effects are generally estimated at 100% of static weight and therefore would be expected to vary directly with weight change.

It has been determined from service operation that 1/16-inch diametral wheel wear represents 5,000 car miles for the aluminum cars and 4,400 car miles for the steel cars. This means the weight reduction due to the use of aluminum has resulted in an increase of wheel life of 13.7%.

Present experience indicates wheel replacement for a steel car to be $2^1/_4$ years or a per-car annual wheel replacement of 32/9 wheels per year. Assuming Z = cost of the wheel, the annual replacement cost of steel car wheels per car = 32/9 Z.

For the aluminum cars, the annual saving per car is 13.7% of this cost or $(0.137 \times 32/9\ Z) = 0\ 49\ Z$.

The variation in wear rate on wheels may reflect similar variations in the rate of rail wear under similar track mounting and operating conditions. With a mixed operation over common rail, actual measurements are not possible. For this study no theoretical evaluation for track wear has been attempted and thus no value has been used in considering relative economies between aluminum and steel cars.

Body Maintenance

Resistance to corrosion of body components is a major factor in body maintenance. The corrosion rate in outer sheets, body posts, sills, purlines, carlines, and other members is the prime factor in establishing economical vehicle life.

Protective coatings are applied to mild steel surfaces during car construction to minimize corrosion. Some of these coatings, such as exterior paint, require frequent renewal and examination to afford adequate protection.

With aluminum a choice of corrosion resistive alloys such as magnesium and magnesium silicons with high corrosion resistance eliminates the necessity for protective coatings.

It is possible to utilize the aluminum alloy in an unpainted condition. If color is desired, suitable paint finishes can be obtained. The natural aluminum oxide film over which paint is applied is inert and this tends to maintain adherence of the paint to the parent metal better than on mild steel sheeting.

The short in-service life of the subway cars has not allowed sufficient time to develop a complete picture of the relative body maintenance costs of steel and aluminum subway cars. However, o[n] the painted steel cars, corrosion at rive[t] heads in certain areas has necessitate[d] paint renewel at these sections.

It appears that the steel subway car[s] will require repainting after 6 years o[f] service. The repainting cost would b[e] approximately $600.00 per car represent-ing a charge of approximately $100.00 pe[r] car per year.

Future experience may show that th[e] figure $100.00 for the reduction in bod[y] costs by the use of aluminum is either to[o] low or too high, but at present it appear[s] reasonable for use in this analysis.

Conclusions

The savings summary, Table V, indi-cates that the operating cost reductio[n] obtained through the use of aluminum i[n] car construction is $565.00 per car pe[r] year. Not all possible savings have bee[n] included, so that the figure represents [a] minimum.

From the savings picture two pertinen[t] facts can be drawn:

1. The weight saved in car constructio[n] that is by reducing weight of a car b[y] 10,414 lbs, represents an annual saving [of] $465.00 which is equivalent to $0.05 per l[b] of weight saved.

2. If cars are amortized over 30 years an[d] money obtained at 5% interest, the annua[l] savings of $565.00 represents the ability t[o] pay approximately $8,700 more on origina[l] capital investment.

It is of interest to note that on th[e] aluminum and steel cars in question, th[e] original delivered purchase price for th[e] aluminum cars was $3,600 higher than th[e] steel. Subsequent tenders for steel an[d] aluminum cars increased this price diffe[r]-ence to $7,700. However, the perform-ance analysis indicates the aluminum ca[r] operating costs would justify these diffe[r]-ences.

It should be realized that the additiona[l] capital investment which could be justi-fied by the annual saving is obviously [a] direct function of current interest rat[e] and would, of course, have to be con-sidered at the time of vehicle purchase.

It should be noted that the weight an[d] body maintenance savings attributed t[o] the use of aluminum cars are not specifi-cally confined to cars constructed with th[e] metal. An analysis could be made fo[r] stainless steels, wherein the inherent corro-sion resistance and extra strength woul[d] bear similar analysis.

The comparisons outlined for th[e] Toronto Transit Commission's aluminu[m] and steel subway cars indicate the ver[y] considerable importance of tare or non-paying weight on a transportation vehicl[e]

Table V. Car Operation Savings Accrued Through Use of Aluminum

Item	Savings: By Calculation	Savings: By Measurement	Factor Value	Annual Saving, Dollars per Car
Power		0.40 kw-hr/car mile	$44.70/kw-year	278.00
Bearings	0.47 R		R = 59.00	28.00
Brake shoes		25 A	A = 4.37	109.00
Wheels		0.49 Z	Z = 102.00	50.00
Subtotal of savings due to weight reduction				465.00
Body maintenance	$66.00			66.00*
Total, all savings				531.00

* The present Commission contract for power calls for a demand payment plus an energy charge over a 30% load factor. In brief, the contract is evaluated to represent an annual charge of $44.70 for d-c kilowatts used at the car. Thus from kw-hrs per car mile and using the average schedule speed of the vehicle a kw demand figure is obtained. This demand figure multiplied by the annual demand charge represents annual power costs.

Average for a system in rush hour including turn-around time 15.56 mph.

Whether weight saving is accomplished either structure redesign or the use alloy, steels, aluminum, or similar etals, the obvious fact is that every und of weight in a vehicle should be refully scrutinized.

On the cars described, certain savings uld be obtained through the use of namic braking, by a reduction in ake-shoe and wheel costs, and weight duction in car heating equipment. ese factors would, of course, have to be nsidered in any car purchase.

Present experience would indicate the e of aluminum in subway-car construcon does result in an appreciable operatg cost reduction and should be given rious consideration in the future.

It is obvious that the acquisition of uminum subway cars has provided a ay to obtain factual data on the merits aluminum in car construction which will rve as a useful guide for future vehicle rchases.

Appendix I

The following calculations are based on e Roller Bearing Engineers Committee port.[1] See Table IV.

$$_{m}=\sqrt[3]{\frac{\Sigma(F^3)N}{100}}$$

ere

=car load

F_m = effective load

N = operating time load is applied

From this:

F_m steel = 92,410 lbs per car or 11,551 lbs per wheel

F_m aluminum = 81,879 lbs per car on 10,235 lbs per wheel

For individual bearing analysis $L=(C/P)$ 10/3 where C = 81,500 lbs for TTC bearing assembly.

$$P=XVF_r-YF_a$$

where

X = radial factor

Y = thrust factor

V = rotation factor

F_r = radial load

F_a = thrust load

For Toronto subway cars P = approximately 1.89 effective load per wheel, therefore, for steel cars:

$$P=1.89\times 11{,}551=21{,}840$$

and for aluminum cars:

$$P=1.89\times 10{,}235=18{,}940$$

$$L \text{ steel}=(C/P)\ 10/3=(81{,}500/21{,}840)\ 10/3=80.48$$

$$L \text{ aluminum}=(81{,}500/18{,}940)\ 10/3=129.1$$

Therefore:

Life rate of aluminum = L aluminum/L steel = 129.1/80.48 = 1.61 times that of steel-car bearings.

Appendix II

The following data are taken from the University of Illinois Station data and graph, Fig. 5.

Pounds of brake-shoe wear/100 million ft-lbs work = K ft-lbs/sec

If W_s = work/wheel/stop in ft-lbs and X = lbs of brake-shoe wear/stop, then:

$$\frac{X}{10^8\text{ ft-lbs}}=K\frac{W_s}{t}$$

and

$$\frac{X}{10^8\text{ ft-lbs}}=\frac{\text{pounds shoe wear/stop}\times 10^8\text{ ft-lbs}}{W_s}$$

Thus,

$$\text{lbs shoe wear/stop}=K\frac{W_s^2}{t\times 10^8\text{ ft-lb}}$$

However, (W_s) = kinetic energy = $1/2(W/g)$-V^2 where W = weight per wheel.

Thus, it is noted shoe wear varies directly as the square of the vehicle weight.

References

1. Method of Evaluating Load Ratings of Roller Bearings, **Roller Bearing Engineers Committee.** Apr. 1, 1954, pp. 8-212–8-215.

2. *Bulletin no. 30*, University of Illinois, Urbana, Ill., May, 1938.

3. Mastering Momentum (book), **Lewis K. Sillcox.** Simmons-Boardman Publishing Corporation, New York, N. Y., 1941.

4. Dynamic Capacity of Roller Bearings, **G. Lundberg, A. Palmgren.** *Acta Polytechnica*, Stockholm, Sweden, no. 7, 1947; no. 96, 1952.

Predictive-Control System Application

H. CHESTNUT
MEMBER AIEE

W. E. SOLLECITO
ASSOCIATE MEMBER AIEE

P. H. TROUTMAN
NONMEMBER AIEE

PREDICTIVE control is used in this report to describe a form of automatic control in which the manipulated variable operating the controlled system is actuated by an estimate of the error which will exist at some future time. Repeated estimations of the future error are obtained by predicting ahead, on a fast-time base, both the reference and the controlled variable as well as some of their lower-order derivatives. Data smoothing and prediction of the reference may be required, and use of a model of the controlled system is needed. By virtue of being able to use fast switching at high energy levels and continually predicting a new value of future error, it is possible to obtain some of the desirable features of the bang-bang "optimum" control as well as the dynamic programming concepts.

One form of the idea of predictive control has been described by Noton and Coales,[1] and work has been done on this method of control by J. C. Lozier of the Bell Telephone Laboratories. In a sense, it is similar to the application of some of the prediction concepts used in fire-control and missile-guidance schemes.

Use of predictive control appears highly attractive with the availability of small, high-speed logic devices and power actuating means. With predictive control, any disturbances or reference input value, whether large or small, can bring to bear the full power capability of the power element. As such, with deterministic inputs, faster speeds of response for a given input and power source can be obtained than for a linear system.

By virtue of the repetitive prediction calculations, including in the model the major nonlinearities or time variations of the process if necessary, higher gain with adequate stability can be obtained than would be possible with linear means. The equivalent speed of response of the system is markedly dependent on the speed of the repetitive predictions as well as by the ability of the system to sense its own performance including its derivatives.

The use of prediction for the reference signal as well as for the model of the process permits the optimum bang-bang concept to be applied to systems in which there is no constant reference input. As a result, the control can achieve a greater correction in a shorter time. Further, evidence points to the fact that an exact model of the process is not necessary and, as illustrated in this paper, a simpler second- or third-order model using equivalent time constants may be used with considerable effectiveness.

Since the predictive control is a nonlinear one, the amount of overshoot to step changes in reference input or disturbance is not proportional to the initial error. The overshoot increases less rapidly with increasing input signals than for the linear control and, as such, more satisfactory performance is obtained where rapid synchronizing is required.

Applications

The characteristics of predictive control make it highly attractive to a large number of computer-control applications. Although eminently suited for on-line digital computers, the method can also be used with analog computing means. Each computing means has certain features that make it attractive for particular cases. Typical application areas where predictive control appears to be well suited are discussed in the following.

Space navigation and rendezvous missions can employ a form of predictive control either to minimize energy expenditure or to minimize the time required to accomplish a correction. Not only may the guidance be made to achieve a certain position and velocity but also it will seek out a means whereby these may be accomplished within the heating or other structural restraints, if this is possible with the power or other conditions available.

Landing of the vehicles to prescribed flight paths, within structural or aerodynamic limitations, can be done effectively with predictive control. Since errors in the initial conditions or disturbances during landing can be eliminated as rapidly as can be accomplished with the full torque or force capability of the controlled system, this control means has performance superior to linear systems. An example of the application of predictive control to the aircraft landing problem is discussed in this paper.

The ability of predictive systems to operate with inexact models makes it highly desirable for use in dynamic chemical-control processes. The work of Eckman and Lefkowitz[2] has shown the results to be relatively insensitive to model inaccuracies. Thus the control of chemical processes in which the characteristics change with time or other parameters in ways difficult to measure, can be made to advantage with predictive control. If necessary, it should be possible to combine predictive control with slower speed changes in the model, as through such self-checking procedures as those of Eckman and Lefkowitz.[3]

From studies of the sort described in the material that follows, it appears that predictive control can be used to advantage in general, on-line, computer control.[4]

Description of Predictive-Control Systems

Predictive-control systems are similar to nonlinear optimum switching systems in that they control the polarity of the actuating signal such that the output of a plant, or other controlled system synchronizes with a given reference input in minimum time. The means by which this controlled switching is performed is by the use of a fast-time model and control logic as shown in Fig. 1. The actuating signal can be a constant, a ramp, a set of pulses, or whatever predeter

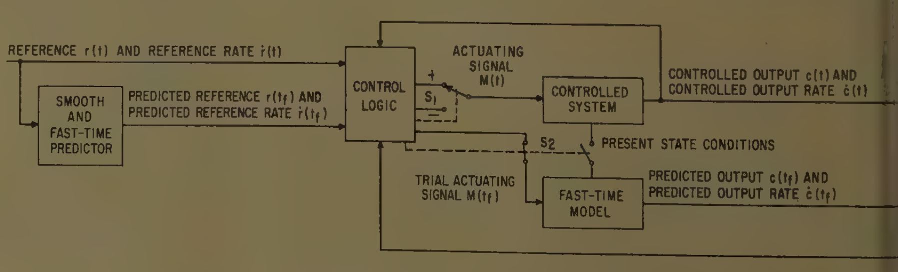

Fig. 1. Block diagram of predictive control system

Paper 61-12, recommended by the AIEE Feedback Control Systems Committee and approved by the AIEE Technical Operations Department for presentation at the AIEE Winter General Meeting, New York, N. Y., January 29–February 3, 1961. Manuscript submitted June 14, 1960; made available for printing November 7, 1960.

H. Chestnut, W. E. Sollecito and P. H. Troutman are with the General Electric Company, Schenectady, N. Y.

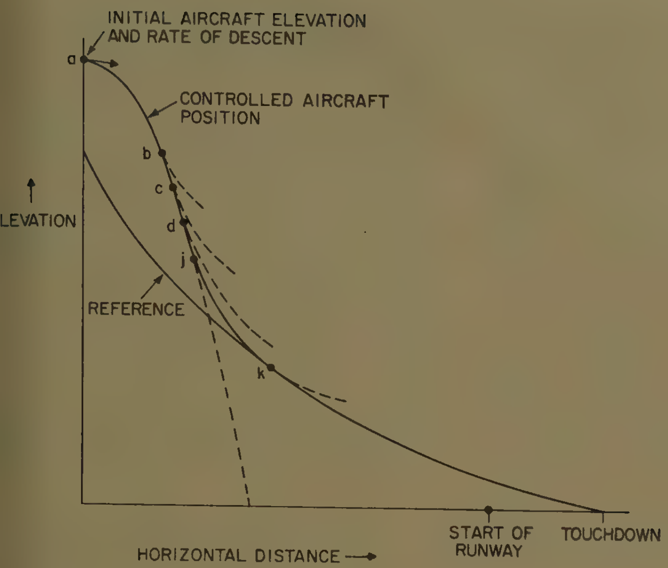

Fig. 2. Predictive control applied to automatic landing of aircraft

ined characteristic is obtainable. The ontrol logic determines the polarity and uration of the actuating signal that is pplied to the controlled system and also he switching sequence by observing the ehavior of the predicted error and error ate in the event of reversing the actuating ignal polarity at the present time. The redicted error and error rate in the uture are obtained by smoothing and rediction of the reference input and by he fast-time simulation of the controlled ystem.

Fig. 1 shows that the actuating signal, $I(t)$, is applied to the controlled system ia switch S_1 and the trial actuating signal $I(t_f)$ to the fast-time model via switch S_2. Switch S_2 also applies to the present-tate conditions existing in the controlled ystem at the present time on a variable-requency repetitive basis. During syn-hronization, switch S_2 operates much nore frequently than S_1. During close ollowing, S_1 and S_2 operate at approxi-nately the same rate.

The control logic maintains a given ctuating signal polarity until such time s the predicted error and error rate reach ero together. At this time, switch S_1 perates to reverse the actuating signal olarity.

Consider the case shown in Fig. 2 which escribes the controlled landing of an ircraft and employs a variable-frequency epetitive prediction basis. The refer-nce shows a certain desirable path to ollow in order to touch down on the run-vay at the right point with an acceptably mall downward velocity. At point a the ircraft is too high and descending too lowly. The control logic immediately alls for a negative polarity actuating ignal which causes the aircraft to follow he trajectory as shown. The dotted curve proceeding directly downward from point j indicates the trajectory in the event that the polarity is never reversed. At point b, where the error and error rate become of the opposite polarity, the fast-time model determines the trajectory in the event of polarity reversal at that time. The dotted curve starting at b indicates this predicted trajectory which is extended until the predicted error rate is equal to zero. Since this trajectory does not intersect the reference where the predicted error rate equals zero, this is not the proper time to switch. A second prediction is made at point c with the same conclusion. The prediction is repeated until finally, at point j, the predicted error and error rate reach zero (or some acceptably small value) together. The control logic switches the actuating signal polarity at this point. The trajectory therefore follows the solid curve to point k. Beyond k a small hunting exists about the reference.

The error phase-plane portrait for the situation shown in Fig. 2 is shown in Fig. 3. At starting point a, the error is negative because the output is greater than the reference and the error rate is negative because the negative output rate is less than the negative reference rate. The actuating signal is held negative through point j. At point b the first prediction is made to observe the value of $e(t_f)$ when $\dot{e}(t_f)$ reaches zero in the event of a polarity reversal. Successive predictions are made until finally, at point k, the predicted error changed its sign from minus to plus when $\dot{e}(t_f)$ reached zero. This information is used by the control logic to switch the actuating signal polarity at point j.

The actual error phase-plane trajectory passes from point a through b, c, d, j, and k. Along this curve time takes on real-time dimensions. The predicted trajectories shown dotted in Fig. 3 are obtained from the fast-time model and along these trajectories time takes on computer-time dimensions.

It will be noted that the predicted trajectory starting at b is much shorter than the one starting at d. This occurs because the next prediction is started when the previous predicted error rate reached zero. This results in a variable-frequency prediction rate, which means that, for large error and error rates, the prediction rate is slowest. For small error and error rates, the prediction rate is fastest. This situation is desirable because it results in tightest control when it is needed most.

Beyond point k there exists a limit cycle about the origin. The magnitude and frequency of this limit cycle depend in large part upon the prediction repetition rate. Because this rate is relatively high, the magnitude of oscillation can be small and the frequency high depending

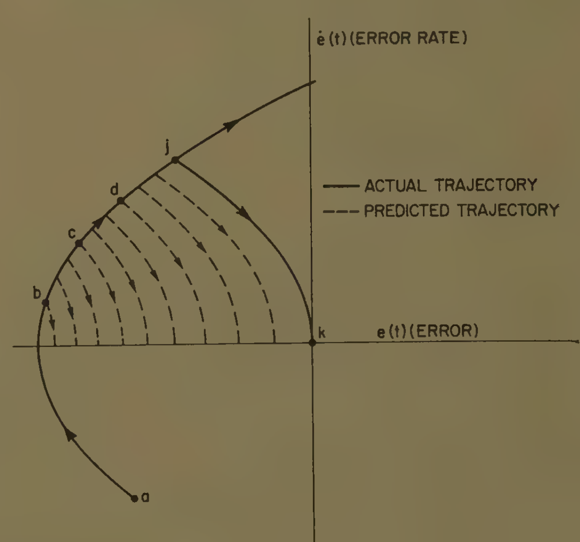

Fig. 3. Phase-plane portrait for aircraft landing of Fig. 2

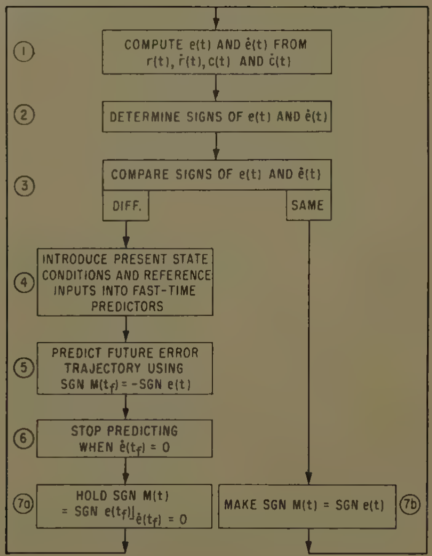

Fig. 4. Logic flow chart

on the nature of the controlled system and the speed of the equipment to perform the switching functions.

Sophistication of the control logic can provide means for reducing the limit-cycle magnitude or for removing it entirely. For example, in one of the cases described later, use is made of the principle of reducing the magnitude of the limit cycle by reducing the amplitude of the actuating signal when the present error and error rate are less than certain threshold values. A number of other more elaborate methods might also be employed to reduce the limit-cycle amplitude.

The preceding description employed the variable-frequency prediction method which is associated with analog computing equipment. In similar fashion, the fast-time prediction and comparison, if done on a digital computer, will probably be done on a time-sampled basis and the comparison made at discrete instances of future time. In this event, the time when this prediction is started is more rigidly prescribed and a somewhat different format for performing the control logic must be employed.

Control Logic

The heart of the predictive-control system is the logic section. In many ways the control logic in a predictive system and the controller in a linear feedback system perform similar functions except that each accomplishes its ultimate goals based on different judgment rules.

In its simplest form the control logic is just a means of mechanizing the switching criteria that were introduced in the previous section. This procedure is summarized in a logic flow chart which is shown in Fig. 4. From this chart it can be seen that the first step in applying the logic is to compute the present values of $e(t)$ and $\dot{e}(t)$ from the present values of $r(t)$, $\dot{r}(t)$, $c(t)$, and $\dot{c}(t)$. After determining the signs of $e(t)$ and $\dot{e}(t)$ they are compared for the same or different sign.

If the signs of $e(t)$ and $\dot{e}(t)$ are the same, the controlled variable is moving away from synchronization; thus the sign of $M(t)$ is made the same as the sign of $e(t)$. This will insure that the controlled system is driving toward synchronization as quickly as possible. The choice of polarity for $M(t)$ is apparent so that no prediction is necessary. It is of interest to note that a linear control or human operator would also react in the same manner. An example of this condition would be segment a through b in Figs. 2 and 3.

When the signs of error and error rate are different, the controlled variable is moving toward synchronization. If the actuating signal, $M(t)$, is switched at precisely the correct time, a deadbeat response will result. Thus the predictive system logic calls for repetitive computations to determine if future synchronization would occur if the polarity of the actuating signal were switched at the present instant of time. For this information a fast-time scale model is used to predict the future response of the controlled variable and a fast-time scale predictor (or extrapolator) is used to predict the future values of the input. Since both the model and extrapolator are synchronized and predict at the same fast-time scale, a subtraction process is used to determine when the future error rate is equal to zero. When this occurs, (at time t_f), the sign of future error is stored and used as the basis for selecting the sign of the actuating signal $M(t)$ for the next instant of time. If this value of future error falls short of synchronizing, no action is taken. If, on the other hand the future error overshoots synchronizing the polarity of $M(t)$ is switched immediately. Thus the switching action will occur properly if the polarity of the actuating signal is made the same as the future error signal evaluated when the future error rate equals zero. An example of this type of operation is also seen in Figs. 2 and 3. Predictions for trial switchings are made at points l through j. When the response reaches point j, the logic indicates future synchronization will occur if $M(t)$ is switched immediately. Finally, it may be seen that synchronization does occur at point k.

When a digital computer is used to perform the logical processes just described, the computer flow diagram is very similar to the logic flow chart. Only in such finer points as establishing prediction and sampling rates need there be any difference. On the other hand, the circuitry for the analog computer logic is not as obvious when given only the logic flow chart. Fig. 5 shows a typical form of analog logic.

By comparing Figs. 4 and 5 it is apparent that the mechanization of Fig. 5 performs the logic of Fig. 4. Thus at *1*, present error and error rate are computed, at *2* their signs are determined, at *3* the signs of error and error rate are compared. If the signs are the same, switch S_1 is energized and at *7b* the sign of the error is used for the sign of the actuating signal applied to the controlled system. If the signs are different, at *4* the present state condition switches open and at *5* the fast-time model predicts the future error trajectory. When the predicted error rate becomes zero, at *6*, the sign of the predicted error is sampled and held. This sign is then applied at *7b* as the sign of the actuating signal into the controlled system. Thus the analog logic mechanizes the logic flow chart.

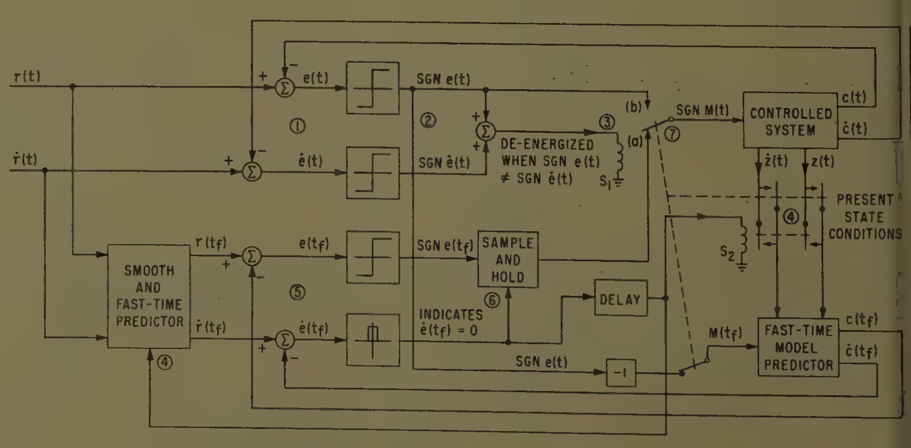

Fig. 5. Analog mechanization of control logic for predictive control

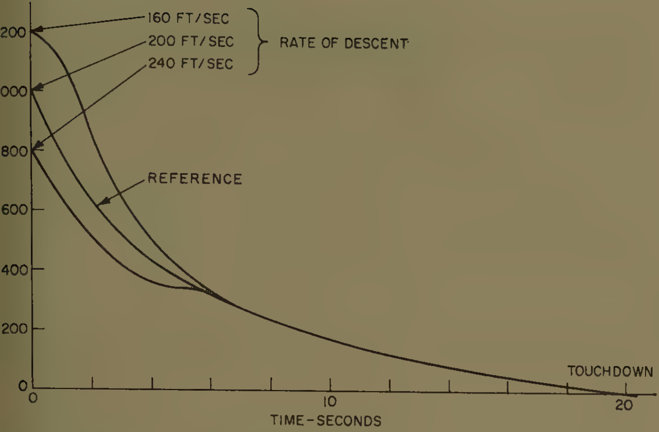

ig. 6. **Typical aircraft landing responses to initial errors in elevation and rate of descent**

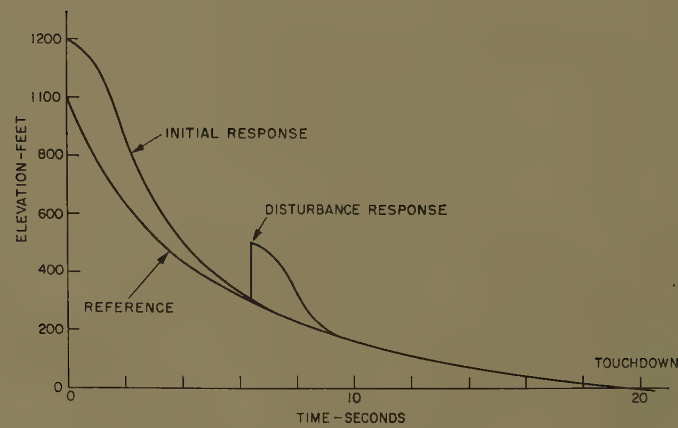

Fig. 7. Aircraft landing response to disturbance

It was noted earlier that a variable pre-ction rate is an excellent method of ducing the size of the limit cycle about e point of synchronization. This mode operation in an analog simulation re-iires a suitable time delay to insure a lf-triggering action when prediction is ecessary. Fig. 5 was described for this pe of operation and the delay unit fol-wing step *6* make possible a reiterative op between steps *6* and *4*. Thus the ıalog simulation can easily work in the ariable prediction mode with only the switch pickup time (6 milliseconds) pro-ding sufficient delay.

Thus it can be seen that the mechaniza-on of the control logic can be accom-ished by either digital or analog means. theory, both methods obtain the same sults since they use the same set of gical criteria. In practice, the digital mputer is more accurate and the ana-g computer is considerably more eco-mical.

imulation Results

As a typical example for which the pre-ictive-control method can be used to advantage, a simplified aircraft landing problem was chosen. Fig. 3 depicts the case where the reference is an exponentially decaying curve and where the aircraft was initially too high and descending too slowly. This particular problem was chosen because the reference is time-varying and the results can be readily interpreted for the various effects of initial condition errors, model inaccuracies, load disturbances, vehicle acceleration constraints, and magnitude variations in the actuating signal. Such effects as ground cushion, nonlinear lift and drag, etc., were not included in the description of the aircraft kinematics.

Before describing the results obtained with the use of a predictive control for this aircraft landing problem flying a prescribed exponential flight path and having a ± 2 g lateral acceleration limit, it is interesting to note some other control approaches that might be employed to solve this problem.

These approaches might include use of a linear system, or a final-value control system in which the touch-down point is the final value, or some sort of a nonlinear adaptive system.

If one were to use a linear-control system, one finds that the actual flight path lies under the desired exponential path. This, of course, means that the plane touches down before the proper landing position and does so at a higher than desired touch-down rate. The presence of a rather low loop gain and a limited lateral acceleration aggravates these conditions. Although one might bias the desired path to compensate for the control-system lags, the amount of bias will change with aircraft speed and other control parameters.

The use of a final-value control-system approach means that the controller must consider at each instant of time, the plane's path from the present to the time of touch-down. This requires that the amount of information handled by the controller be greater than for the predictive control which only need consider the plane's flight path from the present until the time in the future when the error rate is zero with maximum control effort used throughout. Using the final-value approach, there is a possibility that wind gusts may later throw one off-course such that the acceleration required to land

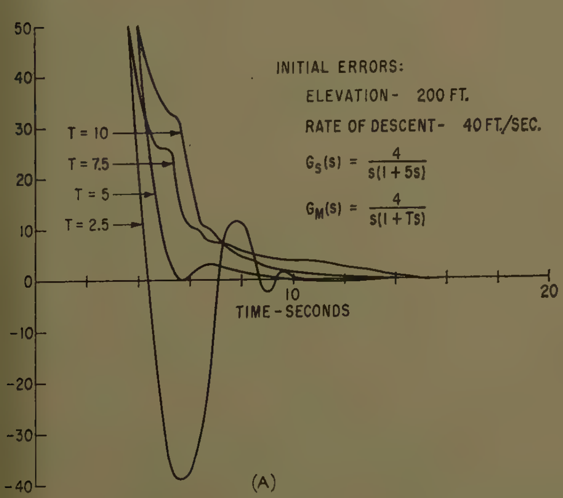

Fig. 8. Aircraft landing error response for inaccurate model

A—Time constant

B—Gain and time constant

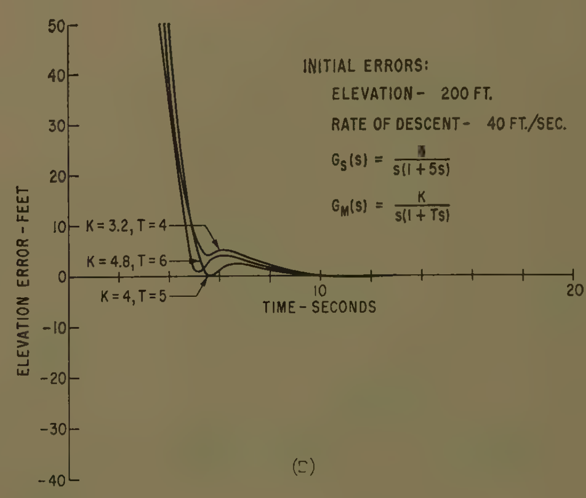

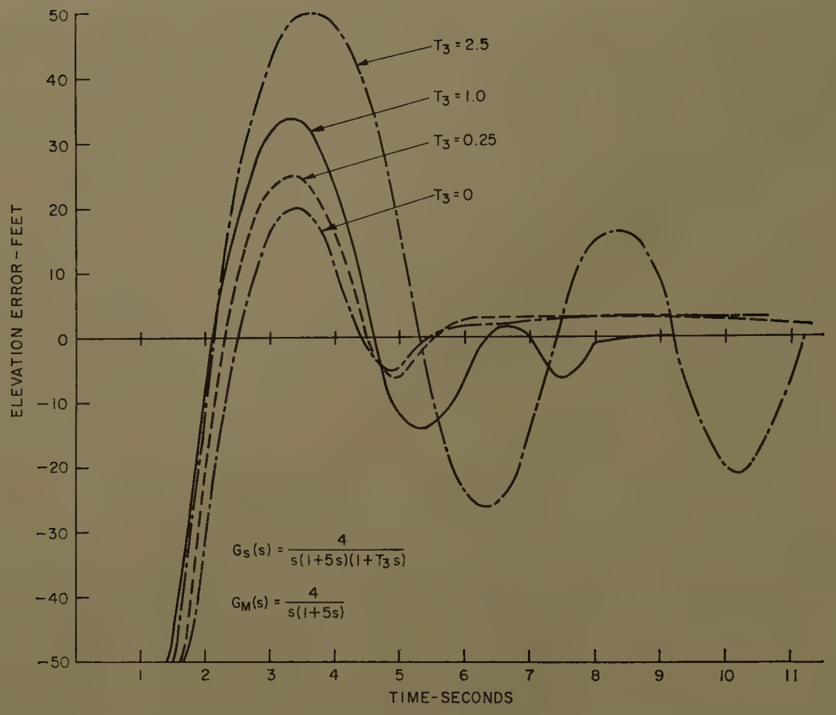

Fig. 9. Error responses when neglecting various third-order system terms in model

properly is greater than that which is available.

Use of a nonlinear or adaptive-control system has been shown to improve the flight-path performance over a similar linear system but the performance still fell short of the results described later for a predictive system. Naturally, some nonlinear systems are better than others and extensive effort was not made to obtain a "best" system. Frequently, considerable effort is required to obtain a suitable adaptive control whereas the predictive-control design means tend to be more direct and require less time.

Second-Order Controlled System

In its simplest form, the controlled system of Fig. 1 for the aircraft landing problem was taken to be of the form:

$$G(s) = \frac{C_{(s)}}{M_{(s)}} = \frac{K}{s(Ts+1)} \tag{1}$$

Fig. 6 shows the type of response obtained for the case where the aircraft initially has initial condition errors of $\pm 20\%$ in elevation and $\pm 20\%$ in rate of descent and for a model that has the proper time constant and gain. For purposes of simplicity, the reference was taken as an exponential in time. This assumes that the horizontal velocity remains constant. Examination of this figure shows the fast synchronizing and close follow-up characteristics of predictive control.

Fig. 7 shows the rapid recovery from load disturbances. It is characteristic of a predictive control to provide fast response characteristics in removing initial errors and disturbance effects and to follow closely time-varying input commands because it is capable of using full power capabilities for even minor corrections. Since the logic network is not affected by past history, except through the present-state conditions that are repetitively applied to the model, predictive control tends to be an optimum type of control in the sense that it tries to reduce an erro[r] and its derivative to zero in minimum time. Since the parameters of the controlled system will, in general, not b[e] known exactly, consideration was give[n] to the effect of inaccuracies in the tim[e] constant and/or gain of the second-orde[r] controlled system. Fig. 8(A) compare[s] the error response of the controlled sys[-]tem for the model having its time constan[t] 50% fast, 50% slow, 100% slow, as we[ll] as the same value as the actual controlle[d] system with the initial elevation 20% low.

Fig. 8(B) illustrates the error respons[e] when the model has an inaccuracy of $\pm 20\%$ in gain and time constant fo[r] comparable initial conditions of Fig. 8(A). It can be seen that these cause rela[-]tively little difficulty. The basic effect[s] of model inaccuracies can be summarize[d] as follows:

1. If the system is more sluggish (lowe[r] gain and/or slower time constants) tha[n] the model assumed, an overshoot whos[e] magnitude is related to this degree of in[-]accuracy will occur.

2. If the system is faster (higher gai[n] and/or faster time constants) than th[e] model assumed, a deadbeat system havin[g] the basic response of the model will result.

If the exact system characteristics ar[e] either unknown or time variable, it is bes[t] when designing for minimum settlin[g] time and minimum overshoot, to hav[e] the system somewhat faster than th[e] model.

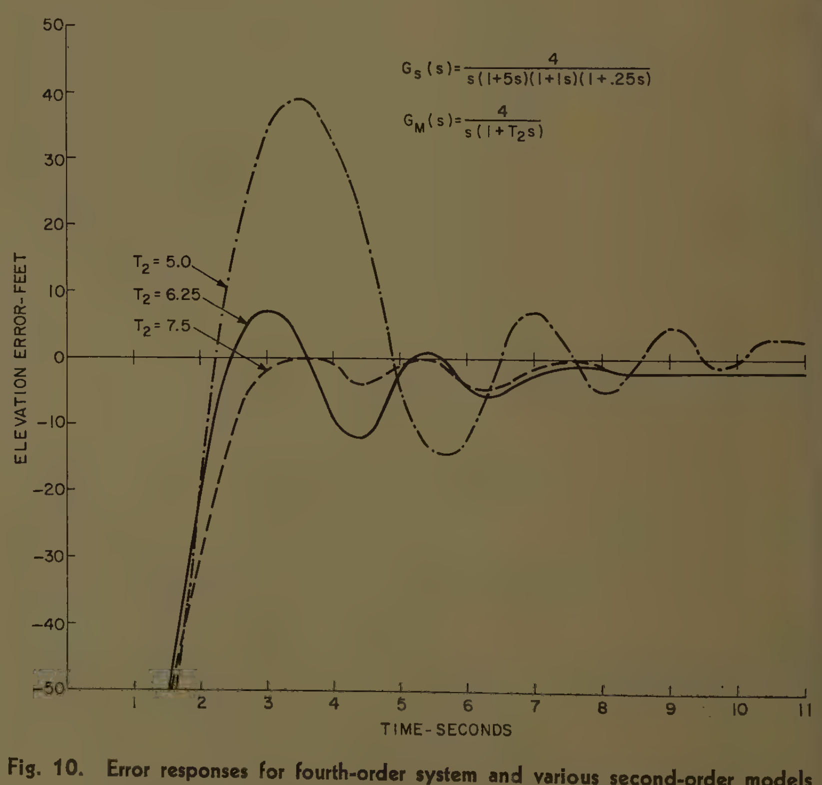

Fig. 10. Error responses for fourth-order system and various second-order models

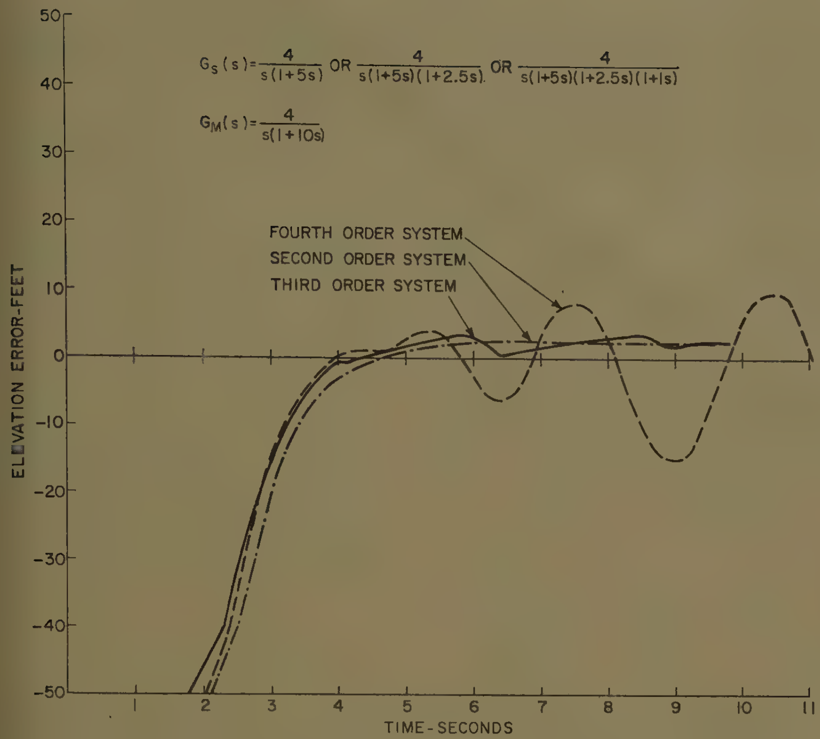

. 11. **Error responses for a second-, third-, and fourth-order system with sluggish second-order model**

GHER ORDER CONTROLLED SYSTEM

The representation of a controlled sys-n as a second-order system is generally rather simplified assumption. In the ults that follow, the controlled systems nsidered have transfer functions of the m:

$$s) = \frac{C_{(s)}}{M} = \frac{K}{s(T_2s+1)(T_3s+1)(T_4s+1)} \quad (2)$$

ere $T_4 = 0$ represents a third-order sys-n.

It is possible to control in a near timum manner such a third- or fourth-der system with only a second-order odel. It should be pointed out that for third-order system a phase-space form model and logic is necessary for true timum performance; however it was cided to investigate what penalties ere would be by keeping the much npler second-order logic-control system.

It can be seen in Fig. 9 that the effect adding an additional significant time nstant to the system with no model mpensation, is to increase initial ershoot and settling time and, if rried to an extreme, even causes sus-ined oscillation of the system in the eady-state condition. The small steady-ate errors shown in Figs. 9, 10, and 11 ere caused by drift in the unstabilized alog computer used to evaluate these ns.

By increasing the dominant time con-ant of the model it is possible to com-nsate for the effect of an additional system time constant as shown in Fig. 10. Thus, as the model time constant gets slower, the responses are less oscillatory although somewhat more sluggish.

In Fig. 11 the model time constant was made twice as large as the dominant time constant of several system configurations. From the transient responses it is seen that all systems have the same initial transient response even though the transfer function of the controlled system is quite different. However, it is also seen that even though the fourth-order system has an almost deadbeat initial response, it eventually remains in a sustained limit cycle.

Finally, in Fig. 12, the effects of compensating a third-order system with a third-order model using second-order logic can be seen. The stabilization effect on the response by including an additional time constant in the model with present-state conditions applied to it is very noticeable in this figure.

One of the decided disadvantages of a bang-bang type of control system is the excessive wear and power drain caused by the power element banging back and forth, even when the error is small. For this reason the magnitude of the actuating signal was reduced by 75% when the error and error rate became less than 8 feet and 8 feet/second as shown in Fig. 13. The results obtained were what would be expected in the sense that full power capability would be applied during large errors while smaller power signals would be applied during times of small errors. If at any time a load disturbance or change in input would increase the error beyond this narrow band, full power would be immediately applied for correction.

It was seen from this relatively simple example of an aircraft landing problem that the predictive control will: (1) follow

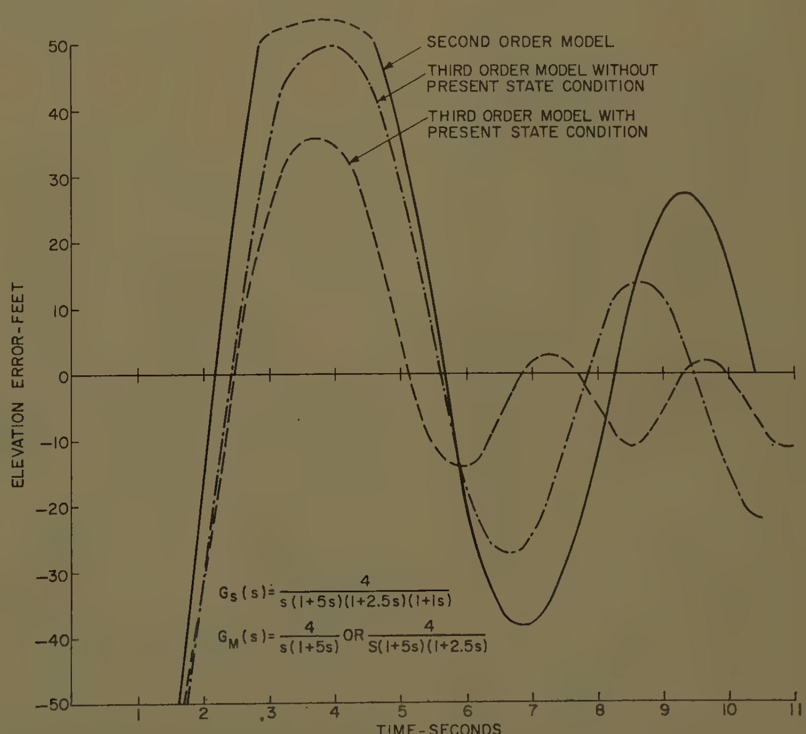

Fig. 12. Error responses for fourth-order system with second- and third-order models

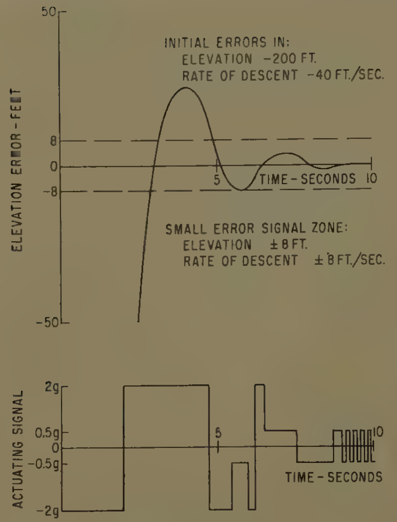

Fig. 13. Aircraft landing response using variable actuating signal

closely a time-varying input; (2) react in a near optimum manner to correct any errors that might be caused by either initial conditions or load disturbances; (3) work successfully for a wide variation in model inaccuracies; and (4) operate at reduced power capabilities when the errors were less than a specified minimum.

Conclusions

The experience gained over the last 2 years in applying predictive control to various control applications indicates that this form of control has definitely desirable characteristics for many high performance control systems. Because a maximum actuation signal is used, the maximum force capabilities of the controlled system are used to remove initial condition errors and disturbance effects. This allows rapid synchronization with and close correspondence to a wide range of command signals. The conventional stability considerations do not seem to be a major consideration. Rather, the basic limitation lies in the speed of computation and in the accuracy of the measurement of the present-state conditions.

A major disadvantage of this form of control lies in the need for a fast-time simulator and a fairly elaborate control logic. A trade-off must be made between rapid, accurate response and equipment complexity.

The simulator may be of either the analog or digital form. The analog approach offers economy, small size, reliability, and fast response. The digital approach offers accuracy and is most practical when the computer is used for a multiplicity of purposes.

The logic used in this paper represents an improvement over past techniques in that it is somewhat simpler and uses a variable-frequency repetition rate for prediction which is highest when the controlled variable is close to the command signal. This effect improves the spee of response and accuracy of the system an reduces the magnitude of any limit cyc that may exist.

It was found that the model need no be an exact replica of the plant to provid good control. Time constants and gain can be in error by 2 to 1 and more with out excessive loss of performance. I general, to avoid overshoot, the fast-tim model should be made to simulate a sys tem slower than the actual controlle system.

When approximating higher ord systems with a lower order model, th model may be made more effective wh its most dominant time constant is pr portional to the sum of the time constan in the higher order controlled system.

References

1. An On-Off Servomechanism with Predict Change-Over, J. F. Coales, A. R. M. Not *Proceedings*, Institution of Electrical Enginee London, England, vol. 103, pt. 10, July 1955, 449–62.

2. Application and Analysis of a Comput Control System, I. Lefkowitz, D. P. Eckma *Journal of Basic Engineering*, New York, N. Dec. 1959.

3. Principles of Model Techniques in C timizing Control, D. P. Eckman, I. Lefkowi *Proceedings*, International Federation of Automa Control Congress, Butterworth's Scientific P lications, London, England, 1961.

4. A Comparison of Predictive and Explo tory Modes of Computer Control for I dustrial Processes, M. Phister, Jr. *Ibid.*

Discussion

J. F. Coales (University of Cambridge, Cambridge, England): This is an excellent and concise description of the single-variable predictive-control system. The simplification of the logical rules and the provision for resetting as soon as the error rate is reduced to zero are valuable refinements. In our early work we had established that the accuracy of the plant simulation could be quite crude, mainly because, as the instant of changeover is approached, the time over which the prediction is made is reduced so that at the only time that is operationally important, the actual instant of changeover, the prediction error is small even when the prediction is crude. It is most valuable to have quantitative results on this important matter. Because of the short prediction time at the actual instant of changeover, the prediction of future input and input rate can also be quite crude, so that simple linear extrapolation is usually adequate when the input is not predetermined as in the controlled landing case when the input (or desired output) is a random process, it is possible to design quite simple predictors to give the most probable future values of input and input rate, provided that the autocorrelation function of the input is known. It is probable that, for this purpose, the autocorrelation functions of most inputs met in practice can be adequately represented by exponential functions, in which case quite simple Laguerre function predictors can be used to give the most probable future values of the input and its derivative.

We have recently done some work with predicted changeover when the load is subjected to random disturbances such as gusts of wind on a radar aerial. Such disturbances can result in great changes in the trajectories in the $e/\dot{e}$ phase plane. This can introduce large errors and unsymmetrical limit cycles which, when smoothed out, result in a steady-state error. The use of Laguerre function predictors can become important under these conditions because, with a large unknown torque opposing motion, the time from changeover to alignment may be increased several times and the accuracy of prediction must therefore be improved.

In Cambridge we are now turning our attention to multivariable systems and it is hoped that it will be found possible to use simple logical rules to drive these to the optimum as fast as the constraints allow. If the systems can be made noninteracting by the techniques of Boksenbom and Hood,[1,2] there is really no problem, since all controls can be driven to their desired values independently and simultaneously. This, however, is not necessarily the best procedure because the networks required to make the parameters noninteracting m make the system inherently more sluggis The requirement is therefore to find metho of applying predictive control to interacti multivariable systems by the applicati of simple logical rules, and it is this that are investigating.

It does not seem to be generally appr ciated that the limit cycle, which is inevit ble in "bang-bang" control of this typ need only appear at the output of the rela There is no objection to putting a filt between the relay and prime mover smooth out the oscillation, but this will, course, introduce a delay. However, t authors have shown that adding an addi tional delay has little effect, even if n simulated, provided it is only about 1/ that of the dominant time delay. Thu to reduce chatter to about the same lev as that in a linear system, it is necessa only to insure that the prediction time a delays around the relay circuit are suf ciently short to keep the limit-cycle peri short enough that it can be smoothed o with an integrator of a time constant 1/20 that of the dominant time delay of the pla In general, the filter can be at a low pow level and, if its characteristics are includ in the high-speed simulator, it will have effect on performance unless the limit cyc is too great, in which case it may increase t time the actuating force takes to do maximum.

FERENCES

A. S. Boksenbom, R. Hood. *Technical Report* , National Advisory Committee for Aeronautics, shington, D. C., 1950.

Engineering Cybernetics (book), H. S. en. McGraw-Hill Book Company, Inc., New k, N. Y., 1954, p. 53.

n C. Lozier (Bell Telephone Laboratories, ippany, N. J.): The authors are to be gratulated on their success in mechaniz- a practical form of optimum switching h a minimum of analog computing ipment. There have been many papers the theory of optimum switching, all olving about the idea that an nth order tem with a limited driving function can duce a deadbeat step response (the error all of its n-1 derivatives simultaneously ng to zero) in minimum time with n-1 ersals of the maximum driving function. wever, as far as I know, no one has pre- ted a practical realization of the general imum switching case for higher order tems.

The simplifying aspect of approach used the authors is the concentration on null- just the error and its first derivative, ich is done here with a single reversal of driving function. It would appear that a practical system where noise is present s simplified optimum should realize most the advantage gained from the optimum itching approach. I would be interested having the authors' comments on this nt.

My associates and I have been doing ilar work using a digital computer chanization and have found it advan- eous to be able to predict the system re- nse with both polarities of drive. This is pful, for example, in cases where the first que reversal was premature. (A pessi- stic model will cause the system to itch early.) Under these conditions the tem will undershoot with a correspond- ly poor transient response unless it can k with the same polarity of drive that it using, see that it will cross the error axis the phase plane short of the origin, and itch the torque back again. Predicting th the opposite polarity of torque will not lp in this situation for the simple reason t the predicted trajectories will not cross error axis, and hence the switching cri- ion has no information to go on until it too late to prevent the undershoot. The ves for $T=7.5$ and $T=10$ in Fig. 8(A) monstrate this effect. Perhaps this ility to look both ways could be added thout too much complication.

One of the most interesting aspects of an timum-type system is its small-signal rformance after the transient phase is er. This criterion is one that will work th any amplitude of input signal. Fur- ermore it is one that seeks to drive the tem so that the input and output meet ngentially; one would thus expect the all-signal performance to be very good. fact, if the input were constant, such a tem could conceivably oscillate about the sired value at a frequency determined marily by the response characteristics of high-speed model. It is clear that such a forcement of the stability considerations m the properties of the actual system is ated to the model's ability to predict.

Unfortunately, with this simple criterion the prediction is only to the crossing of the error axis in the phase plane, and thus becomes negligibly short when the error is very small. Consequently one would expect that some intermediate oscillating condition would obtain between that dictated by the dynamics of the system and that dictated by the dynamics of the model. Furthermore one would expect that this effect would be greater in higher order systems where the need for a lead in the switching times is greater. A full-scale analysis of this problem would be very difficult but it would be interesting to have the authors' experience with this small-signal mode of operation. In particular, it would be interesting to know what oscillating frequency was obtained for the fourth-order system and how it compared with the oscillating frequency of the system without prediction.

L. F. Kazda (University of Michigan, Ann Arbor, Mich.): The authors are to be complimented on their excellent paper on the application of predictive control to practical systems. They have taken known concepts and have investigated the many ramifications of these concepts which are necessary before this approach can be applied to a practical system. Review of the paper reveals that the authors have not defined the type of system which they considered amenable to their method of analysis. For example, are pure stochastic inputs prohibited? What happens to the performance of this type of system if the aircraft suddenly receives an extremely large sharp-edged-vertical gust, which may result in a major change in the performance characteristics of the aircraft? Would the performance deteriorate or would the system become unstable? In short, has stability in the large been given any detailed study in these applications? Given a particular application, it would have been helpful if the authors had outlined a format which could be followed by others in applying the ideas developed in this paper to a new problem.

Frederick A. Russell (Newark College of Engineering, Newark, N. J.): The authors are to be congratulated on an interesting and well-presented description of an application of a predictive-control system. This is a form of automatic control which holds great promise for further development, especially in situations where a computer is required for other purposes.

While the authors discuss the attractive characteristics of this system in resisting load disturbances, they give only passing consideration to the effects of noise in the reference signal, and perhaps some comment on this phase of the problem would be useful. I have worked with a very similar control system in which reference signal noise could be the determining factor in the size of the limit cycle. When $e(t)$ and $\dot{e}(t)$ have been reduced to small values, it can be seen from Fig. 3 of the paper that an impulse of noise can readily cause an incorrect switching decision on the part of the logic block of Fig. 1.

If random noise is present in the reference signal, $r(t)$, it will be amplified in $\dot{r}(t)$ by differentiation. If we imagine the control system stationary at zero error and zero error rate, it is easy to see that the control logic will be actuated by the spurious noise into making random decisions as to the direction in which the output should be ordered to move. An average of a large number of these excursions can be found for a given amplitude of noise, and this motion can be called a limit cycle.

The amplitude of this limit cycle due to noise depends also on the torque exerted by the bang-bang controller, and one great advantage of limiting the driving torque to a small value as the error and error rate become small is that the system will have a smaller limit cycle due to noise, although it becomes more sensitivie to load disturbances.

Filtering, especially of $\dot{r}(t)$, can be used to reduce the amount of noise. However, the filtered reference signal is a delayed version of the reference signal which the control system is required to follow; hence filtering also tends to cause incorrect decisions on the part of the control logic, because decisions are being made on "stale" data.

We conclude then, that in the presence of a noisy input, a compromise must be made among three parameters: the amount of filtering, the amount of torque reduction, and the sensitivity to load disturbances. Optimization of these factors is an area which should be very attractive for further research.

W. M. Gaines (General Electric Company, Phoenix, Ariz.): The use of a mathematical model in process-control computers has proved to be a very effective means of accomplishing process optimization and control. This paper is another excellent example of how a mathematical model can be used effectively to improve the performance of a dynamic system.

It is useful to separate the types of optimization into two classes: (1) steady-state optimization; and (2) transient optimization.

In "steady-state" optimization the objective is to determine the optimum settings of the process-control variables to obtain a long-term "optimum" performance. Once the model has been developed there are a number of methods of determining the best performance. Linear programming can be used when performance can be approximated by linear relationships. Gradient methods (methods of steepest ascent or hill climbing) or other iterative techniques can be used in nonlinear cases. (Such methods have been adapted to utilize the process itself as the model and by repeated perturbation and measurement to achieve optimum performance.) A review of the literature will indicate that the majority of applications of process-control computers has been in the area of steady-state optimization.

In transient optimization we are interested in minimizing the cost during a transient. This may be a transient introduced by external disturbances or it may be the result of a long-term management decision to change product characteristics. Mathematically the result is the desire to minimize an integral of the form shown in equation 3:

$$I(m, t_1)=\int_{t_1}^{t_2} F\,(Q_n, q_n, M_n, m_n), \tau)d\tau \quad (3)$$

where Q_n and M_n are the desired output

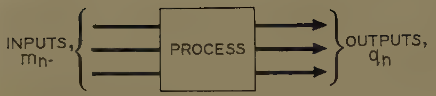

Fig. 14. Nomenclature for equation 3

and input. The nomenclature is defined in Fig. 14.

To date there has been very little general analysis of this type of problem which has led to practical on-line solutions. Dynamic programming offers a method of solution but in most practical situations results in a very formidable requirement on computer speed and memory. The work of Dr. Merriam[1] provides a possible solution in those instances where a more restrictive class of transient optimization can be met. The greatest progress, however, has been made in the restrictive class of problem wherein the objective is to minimize the elapsed time of the transient. The paper is a significant contribution as is the work which has been done at the Case Institute.[2] Hopefully, we will see this type of effort continued and further progress in the analysis of the more general problem of transient optimization.

The paper has several subtle implications which can be of considerable use in industrial process control; and I would like the authors to comment upon the following items:

1. In many industrial processes the input variables are not changed in the stepwise manner indicated in the paper. They are limited to rather slow rates of change either because of physical constraints upon the variables themselves or because of process limitations which make it mandatory to increase or decrease the variables more slowly. It would seem in instances where this is the case that the predictive technique could still be utilized effectively. I would like the authors' comments upon any experience they might have had with cases where input-manipulated variables are not changed in a stepwise manner.

2. In most process-control situations we are concerned with a multivariable problem and there is usually considerable coupling between the variables. It would seem that in this instance the dimensionality of the process model would similarly have to be increased. While it is still possible in this instance to represent the dynamics by second-degree equations, in all likelihood the model would now constitute a set of simultaneous second-order differential equations. I would like to ask the authors how this particular problem can be handled and what complexity it may introduce.

3. Difficulty can be encountered in on-line applications of process-control computers in obtaining sufficiently fast sampling and real-time computational rates to obtain the degree of stability desired. (Such sampling rates can be determined in linear operation by the use of z-transforms or other linear methods of stability analysis.) It appears quite possible that by using predictive-control systems the sampling rate required during the course of a transient can be drastically reduced. The amount of reduction appears to be a function of the correctness (or exactness) of the process model; i.e., if the model were perfect it would be necessary to sample the output only once. I would like the authors' comments on this particular potential of the predictive technique.

References

1. Use of a Mathematical Error Criterion in the Design of Adaptive Control Systems, C. W. Merriam, III. *AIEE Transactions*, pt. II (*Applications and Industry*), vol. 78, 1959 (Jan. 1960 section), pp. 506–12.

2. Optimizing Control of a Chemical Process. D. P. Eckman, I. Lefkowitz. *Control Engineering*, New York, N. Y., Sept. 1957.

A. M. Hopkin (University of California, Berkeley, Calif.): The development of the general concept of "optimum" relay control systems has resulted in much more paper analysis than in actual hardware. This situation probably exists because, in spite of the attractive features of the optimum relay type of system, its practical realization usually seems to involve too much complication and cost to compete economically with alternative systems. With this fact in mind, the authors are to be congratulated on seeking to find systems which combine sufficient simplicity with sufficient performance to be practical.

The authors point out that they are following up the work of Noton and Coales (reference 1 of the paper) and of Lozier. It might be of interest to note that about 8 years ago Otto J. M. Smith suggested the use of a somewhat similar procedure. This suggestion was not widely circulated, but one of his students did write a thesis concerning an analog computer study of the idea,[1] and one of this discusser's students later wrote a thesis on a similar topic.[2]

The authors are quite careful to indicate that they are approximating the actual system behavior by a simple model, and that the criterion which determines the switching-control logic applies strictly only to the control of systems described by second-order equations. I would like to consider the example given with the purpose of indicating situations where the second-order criterion, based on error and error rate, might well prove inadequate.

In the example in the paper, the aircraft transfer functions, equations 1 and 2, were assumed to have only real poles and to possess no zeros. I feel that possibly a more realistic transfer function for the elevation control of a tail-steered aircraft would be of the approximate form:

$$G(s)=\frac{C(s)}{R(s)}=\frac{K}{s^2}\frac{(s+Z_1)\ (s+Z_2)}{(s^2+2\zeta\omega_n s+\omega_n^2)} \qquad (4)$$

where it is assumed that the elevator is positioned by a hydraulic cylinder. For equation 4 it is possible that one of the zeros may be in the right-hand s-plane, and ξ may be 0.2 or less, resulting in lightly damped complex poles.

For this case both the presence of lightly damped complex poles and the presence of zeros, particularly those in the right-hand half-plane, render the higher order system less likely to give good behavior with a switching logic based on a second-order criterion. These two factors also require that care be used in selecting a simple fast-time model to predict system behavior. The procedure followed by the authors of the paper of carefully checking system behavior say on an analog computer, would most certainly be called for.

References

1. A Predictor Servomechanism, N. C. Walkl *M.S. Thesis*, University of California, Berkele Calif., June 1953.

2. A Taylor's Series Approach to the Desi of a Predictor Servomechanism, G. F. Aroy *M.S. Thesis*, University of California, Jan. 1957

Irmgard Flügge-Lotz (Stanford Universit Stanford University, Calif.): After readi this very interesting paper, I have two que tions which concern an extension of t method.

1. I wonder how predictive contr works for a system which has complex real and complex poles. For the secon order case the optimum switching curve h a rather simple character for real chara teristic roots. For complex roots, howev this curve is more complicated (see B shaw's original work as re-presented Tsien[1]). I would like to know how predi tive control works in such a case, and pa ticularly, whether it will be necessary limit the magnitude of the initial distur ance in such a way that only the first an of the optimum switching curves near t origin of the phase plane are used.

2. What experience do the authors ha with systems with zeros in the transf function?

Reference

1. Engineering Cybernetics (book), H. Tsien. McGraw-Hill Book Company, Inc., N York, N. Y., 1954, pp. 155–57.

J. J. Jonsson (Polytechnic Institute Brooklyn, Brooklyn, N. Y.): The com bination of prediction and optimum nu time using a bang-bang controller shou make this system extremely attractive f future applications. It therefore represen a valuable contribution. Two commen seem pertinent.

1. Fig. 3 shows the actual trajecto from j to k. The paper seems to indica and it would be true in practice, that t model trajectories cannot be accomplishe in zero time. Therefore, if the system is state j when the model trajectory is ini

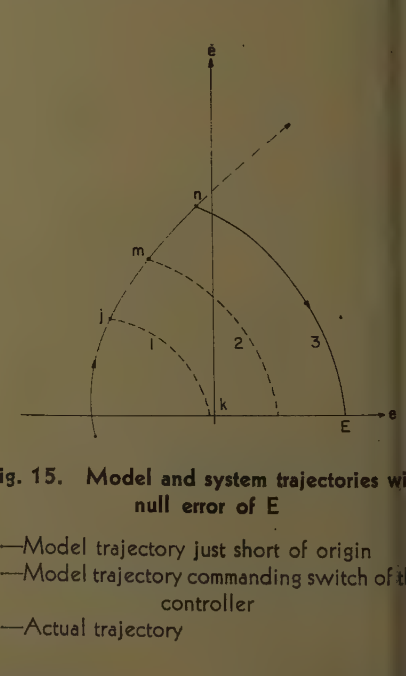

Fig. 15. Model and system trajectories wi null error of E

1—Model trajectory just short of origin
2—Model trajectory commanding switch of th controller
3—Actual trajectory

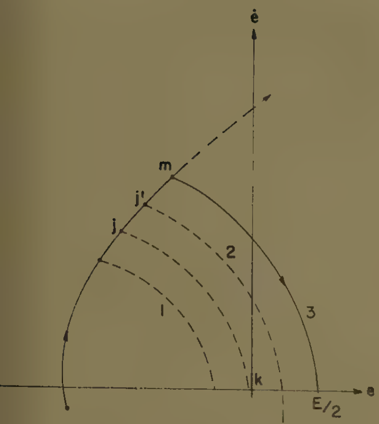

. 16. Model and system trajectories with null error of E/2

See subcaption of Fig. 15

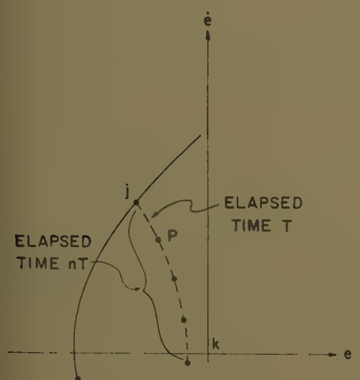

. 17. Discrete time model trajectory

ted, the actual system will continue up-rd and to the right until the model ches point k and the system logic com-nds a change of controller sign. In fact, the model trajectory passed just to the of the origin by a very small amount, entire new model pass must be made ore switching can occur. This will result a maximum null error of E as shown in . 15. For a given model speed, E may be uced by a factor of 2 with a slight dification as indicated in Fig. 16. If system is at state j, the actual trajectory predicted ahead on a fast-time basis to nt j', mid-way between j and m. A tching command will result from model jectory *2*, giving trajectory *3* with a ximum null error of $E/2$. Extending the j' prediction beyond half the j to m tance does not seem advisable since the sibility of a null error of less than $-E/2$ n exists.

. As so many others, this paper is pri-rily concerned with large signal perform-e and, therefore, the challenge of the 0 Joint Automatic Control Conference sents itself again, namely: How may describe or anticipate small-signal be-rior near the origin of the phase plane? sider the model trajectory of Fig. 17. e shortest possible fractional part of this jectory, j to p, represents an elapsed e T, the entire trajectory being made of n parts. Such a limiting value of T exist in a practical sense in the case of ital simulation, and probably for analog

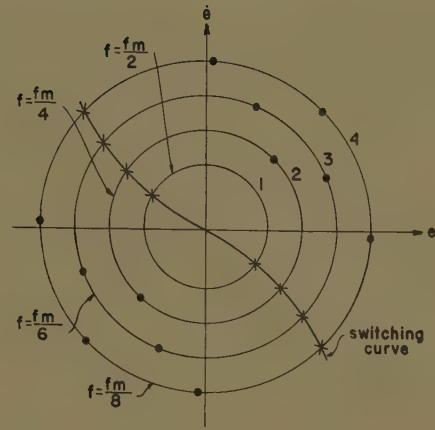

Fig. 18. System switching curve and possible trajectories

Computer decision synchronized with required system switching

+ Proper switch point

● Other possible switch points

simulation also. This implies a maximum limit cycle frequency for the actual system of $1/2T$; that is, at its highest possible frequency of steady-state oscillation the model must command two symmetrical controller switchings per system cycle. The actual system trajectory for this condition is shown in Fig. 18, curve *1*, where

$f_m = \frac{1}{T}$ = the model frequency

f = actual limit cycle frequency

The system under consideration is third order of form

$$\frac{A}{s(s+a)(s+b)}$$

It is conceivable that the system may also lock in at

$$f = \frac{f_m}{4}, \frac{f_m}{6}, \frac{f_m}{8}, \text{ etc.}$$

to give the symmetrical trajectories shown in Fig. 18, switching decisions being made at the end of every second, third, fourth, etc., model cycle T, respectively. Discrete orbital modes, not necessarily circles, are illustrated together with the proper steady-state switching curve.

The effect of sampling the actual system state variables must also be taken into account, i.e., $KG(s)$ is replaced by a sampling transfer function $KG^*(s)$ where

$$KG^*(s) = \frac{1}{T} \sum_{n=-\infty}^{+\infty} KG(s+j\,n\omega_m)$$

with

T = sampling time

ω_m = model frequency

The effect will be that of requiring a shift, primarily in phase, of the switching curve of Fig. 18 to anticipate the sampling influence.

In general computing, sampling, and logical decision to switch is done on an arbitrary time base, with discrete switchings being possible at points *1*, *2*, *3*, etc., with respect

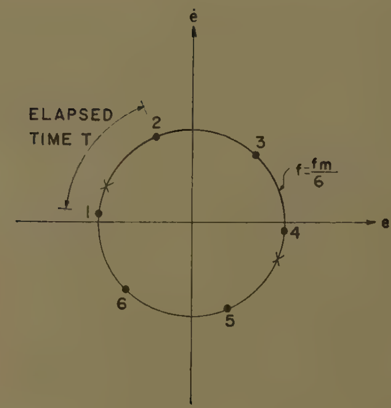

Fig. 19. Discrete computer decisions asynchronous to required system switching

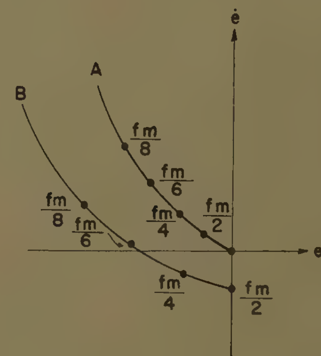

Fig. 20. Continuous switching curve as modified by sampling and relay holding

A—Switching curve for continuous system

B—Switching curve with effect of sampling and controller hold included

to the proper switch points X of Fig. 19. Therefore, there is no assurance that the control logic is synchronized to the points X of the phase plane. Switching should not be done at point *1* because this is too early and yet point *2* is too late. On the average, the time delay is one half of a computing cycle. If the delay is referred to the actual system then

Average controller holding delay

$$= 90° \frac{f}{f_m/2}$$

That is, if $f = f_m/2$ the delay is 90 degrees; for $f = f_m/4$ the delay is 45 degrees, etc. Such a delay must be anticipated by shifting the switching curve of Fig. 18.

The complete system transfer function must include the original transfer function, the effect of sampling, and also the effect of controller holding. While the gain is affected very little, a significant change occurs in the phase characteristic. In fact at $f = f_m/2$ the transfer function for the third-order system cited above lies at 270 degrees. Curve *B* of Fig. 20 indicates the new average switching contour. It is important to note that this is an average curve since the actual controller holding delay may vary anywhere from zero to the full time T, or zero to 180 degrees.

It is therefore apparent that switching criteria near the origin of the phase plane may be quite different from those used for

large signals. What this should be is not altogether clear because of the arbitrary time relationship between the discrete model behavior and the fixed switching points of the actual system. The $(n-1)$ switching usually associated with an n-order system is replaced by a single switch in the $\dot{e}-e$ phase plane in this paper when driving to zero from large errors. For third-order, and higher, systems one would hope that most of the stored energy in the system would have been removed with this technique which indeed represents a very commandable practical approach to the n-dimensional switching problem, but the same reasoning does not apply at the origin. Indeed (unless zero forcing function is admissible as a controller possibility) it would be desirable to have the system oscillate with minimum error, namely, trajectory *1* of Fig. 18. But what will be the actual path in the $e-\dot{e}$ phase plane? It is suspected that the mode of operation will skip from one trajectory of Fig. 18 to another in some statistically random fashion. Additional research is necessary to estimate the limits of error and error rate. There will be some tendency to ignore this problem by reverting to a linear mode of operation near the origin or else simply increasing the model simulation frequency. The first solution still leaves the above questions to be answered. The second solution has economic implications and physical limitations since systems are now in existence where communication between computer and the actual control system is done with discrete pulses at a repetition rate which cannot be economically increased.

H. Chestnut, W. E. Sollecito, and **P. H. Troutman:** We are pleased with the large number of interesting and worthwhile discussions on our paper. In a number of cases the discussers have had a long and scholarly association with this problem, and we are delighted they are willing to share their experiences and comments with us.

We agree with Mr. Coales that the bang-bang aspect of predictive control is not essential when the errors are small. Use of a filtering scheme such as Mr. Coales suggests, or of a decreased bang-bang amplitude signal, or perhaps going to a very small linear control range in the vicinity of zero error are all possibilities that might be employed for the small-signal case.

We are interested to hear of the work that Mr. Coales is doing on the subject of disturbances which may result in large changes in the trajectory. We feel that these random disturbances can best be considered as specific inputs (pulses, steps, or ramps) rather than that one should design for them on any over-all statistical basis.

We also feel that the work on the multivariable systems is extremely important and are glad to learn that Mr. Coales and others are doing work on this problem. We, too, are concerned with the possibility of using predictive controls for this application.

Mr. Lozier has pointed out that our work as described deals entirely with the noise-free reference signal condition. We feel this to be valid because in many industrial processes the signal-to-noise ratio can be brought more fully under the designer's control and thus it is worthwhile to study the noise-free case first. However, as he points out, the presence of noise would tend to complicate the logic involving higher order prediction terms and as such the simple first-order prediction could be of practical importance for signals containing noise.

We are interested to learn that Mr. Lozier and his associates have been doing a digital computer mechanization of the predictive-control problems and found it advantageous to use prediction with both polarities. We feel that for some conditions it might be nice to try to use both polarities of drive at each prediction time but for reasons of simplicity we did not feel it worth the added complexity. We have, however, incorporated in our signal polarity for the undershoot conditions described by Mr Lozier, the ability to see that we will cross the error axis in the phase plane short of the origin and we do switch the torque back. For the case described in Fig. 8(A), the real problem is that the curves for $T=7.5$ and $T=10$ describe a situation in which the model is off by 50 and 100% respectively.

The problem of the small-signal limit cycle was not significant because the oscillations in the controlled variable were within prescribed acceptable limits. Our feeling has been that to reduce the oscillations we would go to either a lower elevator force on the airplane or to a small range of linear operation about the zero point.

In the case of analog prediction, the frequency becomes extremely high for the small-signal condition as was described by Mr. Coales. Hence, the small limit cycle is attributable to a combination of the prediction time and the time constants in the process.

Although the significance of the closed-loop oscillating frequency asked for by Mr. Lozier was not studied in detail, it is our feeling that the oscillating frequency of the system without prediction of necessity would be much lower than that which will be realized with the prediction employed.

In regard to Professor Kazda's inquiry regarding stochastic signals, it is our purpose in the predictive control to operate with signals in which the deterministic portion is much larger than the stochastic one. Our emphasis has been upon handling individual disturbances as they arrive and reducing them as quickly as possible. Fig. 7 of the paper indicates the nature of the treatment of disturbances. Our investigation of the effect of model inaccuracy was directed at determining the effect of changes in the processes. Our consideration of stability in the large has been directed at determining the effect of large initial errors, disturbances, and inaccuracies in a model of the magnitude of those studied in the paper. The various values for these initial errors for model inaccuracies were studied for the purpose of determining the maximum deviations which might be expected and evaluating the performance on the basis of these magnitudes.

Regarding Professor Kazda's request for a general format to be applied by others, it was our intent that the procedure outlined in Figs. 1, 4, and 5 would serve this purpose. Our objective was not to consider the general nth order system, and therefore the logic and general approach may appear somewhat limited.

It is our feeling that in the control of many systems commonly encountered in practice probably one or two integrati[...] due to the process might reasonably be e[...] pected. The remaining time constants [...] delays would probably be caused by t[...] time of response due to the controls o[...] which the designer has presumably so[...] influence. Because the designer has this [...] fluence, it is reasonable to expect that [...] would choose them in such a way that th[...] would not become dominate in influenc[...] the over-all response of the control and t[...] process. For this reason our attention [...] been concentrated on relatively low-or[...] process systems and a general considerat[...] of the nth order system has been given lit[...] attention.

It is of interest to note that the obser[...] tions of Mr. Russell are so similar to th[...] of Mr. Coales when he discusses the [...] fects of random input signals and load [...] turbances for the small error region. [...] also agree with Mr. Russell's conclusi[...] that a compromise must be made am[...] input filtering, torque reduction for sm[...] errors, and sensitivity to load disturban[...]

Mr. Gaines has very nicely summari[...] the state of the art concerning pro[...] optimization and control. We will ans[...] his questions in the order in which he p[...] sented them.

It is true that the input-manipula[...] variable need not be changed in the st[...] wise fashion described in the paper and t[...] the predictive technique can be effectiv[...] utilized where it is mandatory that [...] variables increase or decrease less abrup[...] In such instances it is necessary to kn[...] the time relationships of the manipula[...] variables in order to so generate them in [...] predictive portion of the control.

We are in whole-hearted agreement t[...] the multivariable problem is importa[...] It also appears that the model dim[...] sionality would have to be increased, [...] that another set of logic would proba[...] have to be formulated. Mr. Coales [...] indicated that his group is currently [...] vestigating this area of interest.

It appears that where the process can[...] adequately described by linear equati[...] it is possible that, by the judicious use[...] predictive control, the sampling rate [...] quired during the course of a transient [...] be reduced. This possibility exists beca[...] in the calculation of the predicted respon[...] the exponential form of the time respo[...] can be used and the response at requi[...] times in the future can be calculated q[...] rapidly without recourse to time-consum[...] integration procedures.

The discussions by Mrs. Flügge-Lotz [...] Mr. Hopkin both raise important questi[...] in application areas in which we made [...] limited investigations. Since their excel[...] discussions are closely related, both [...] be answered simultaneously.

Using predictive controls for second-or[...] systems having lightly damped complex [...] pairs should result in good switch[...] characteristics since the predictor will se[...] immediately upon entering a new quadr[...] whether switching should occur immedia[...] (i.e. the trajectory overshoots the ori[...] or be delayed until the predicted traject[...] passes through the origin. Thus in[...] disturbances are not limited to the in[...] arcs of the optimum switching curves.

Third- and higher order systems [...] definitely more difficult to control. Re[...] studies were made of a fourth-order sys[...]

ntaining two poles at the origin in dition to a lightly damped complex pole ir. It was found that simple phase-ane switching logic was incapable of oducing a stable system since the higher rivatives were uncontrolled; neverthe-ss, it was of interest to note that during ch revolution of the diverging limit cycle e trajectory would pass through the ase-plane origin. Thus it appears ap-rent that additional studies should be ade to include higher order systems.

A transfer function having a zero in the t-hand s-plane was investigated and esented little difficulty. However, rticular care must be taken to insert the proper present-state conditions into the model prior to each prediction. Zeros in the right-hand s-plane were not investigated.

Mr. Jonnson's discussion indicates that he has done considerable work in the area of predictive controls. The idea of shifting the prediction time from j to j' is an effective way of counteracting time delays in the system.

Mr. Jonsson's analysis of the small-signal operation has served to clarify the nature of the problem when digital computers are used for predicting system responses. For analog prediction, this prediction time becomes very short and additional considerations enter the picture concerning the small-signal limit cycles. We agree that small-signal performance is somewhat different in nature from large-signal performance.

We also feel that introducing a linear range of operation for small errors is attractive when physically practical. For the case where a linear range is impractical, it is necessary to find other ways to reduce the small-error limit cycles when extreme accuracy is a requirement.

In closing we should like to re-emphasize our appreciation for all the constructive comments offered by the discussers. We feel that their contributions have added considerable value to the paper.

Electromagnetic Brake with Controllable Torque

C. A. LISTER
MEMBER AIEE

MANY LARGE materials handling machines and processing machines quire smooth, accurate stopping. In e past, accurate stopping has usually en accomplished by the use of hydraulic akes. Recently, an electromagnetic ake has been developed to perform the me functions and to overcome some dis-vantages of hydraulic brakes, such as e need for hydraulic lines and slow re-ase of parking torque by a foot-operated draulic pump. The electromagnetic ake can be readily controlled from small ot devices and can be fed through llector bars so that the operator need t be on the same structure as the drive d brake. Thus, the new brake offers creased flexibility in application.

inciples of Operation

For most applications in industry a ake used mainly for smooth stopping ist also provide a holding torque when e drive is stopped and must apply ergency braking torque if failure of ntrol power occurs. Thus, the main requirements for a controllable torque brake are:

1. With no power applied, the brake must exert a holding or parking torque to prevent the equipment on which it is mounted from being moved by external forces such as wind.
2. Means must be provided for releasing the holding torque to permit the drive to run and to reapply the holding torque when desired by the operator.
3. If the power supply to the drive is interrupted, the brake should apply emergency braking torque and holding torque.
4. With the holding torque released, means must be provided to apply retarding torque in the amount and at the time desired by the operator.

The first three of these requirements are the same as those for the spring-set magnetic-release brakes used widely on crane hoists and other industrial drives.[1-3] The fourth requirement, controllable torque, may be accomplished by coupling an electromagnet to the brake mechanism to apply torque in proportion to the force of the magnet. Thus, the marriage of a spring-set magnetically released brake and a magnetically applied brake is indicated. The brake of Fig. 1 is an embodiment of this principle, and the partially sectioned views of Figs. 2 and 3 illustrate how the mechanism fulfills these requirements.

Those parts of the brake needed to meet the first three requirements are shown in Fig. 2. With no power applied to the brake, a main spring applies force to a "whiffletree" linkage which in turn applies equal forces to the two brake shoes which are in contact with the brake wheel. Application of power to auxiliary coil PB causes the auxiliary armature to close and compress the main spring allowing the retractor springs to release the shoes from the wheel and permitting the drive to run. Whenever current to the auxiliary magnet is interrupted, either by action of the operator or upon power failure, the armature will be released and the main spring will set the brake. It should be noted that the auxiliary armature is not coupled directly to the shoe linkage mechanism but is arranged to compress the spring and to decouple the spring from the mechanism. If it were not for the retractor springs, the closing of the auxiliary armature would result in physical separation of the armature from bearing surface P on the linkage.

per 59-645, recommended by the AIEE Indus-l Control Committee and approved by the EE Technical Operations Department for sentation at the AIEE Fall General Meeting, cago, Ill., October 9–14, 1960. Manuscript mitted February 19, 1959; made available for nting January 10, 1961.

A. LISTER is with the Square D Company, veland, Ohio.

e author gratefully acknowledges the contribu-ns of Dr. J. D. Leitch who conceived the arrange-nt of a single magnet housing and two armatures, those of S. K. Shu, W. W. Schneider, and E. S. gers who did the design and testing work on the ke.

Fig. 1. Electrically energized controllable torque brake

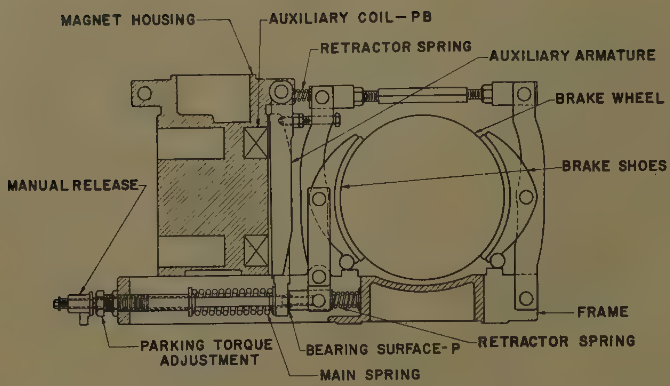

Fig. 2. Spring-set magnetically-released portion of brake with frame and magnet sectioned

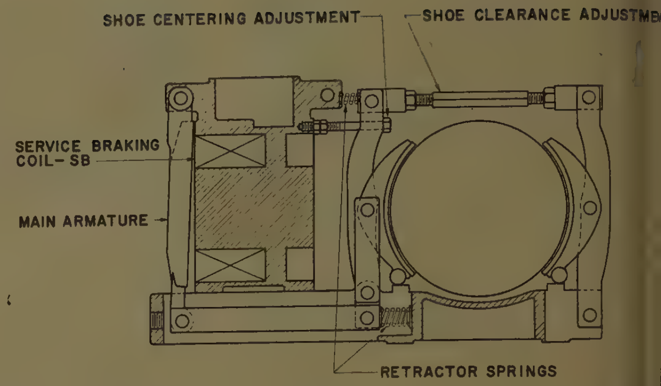

Fig. 3. Controllable torque portion of brake with frame and mag sectioned

In Fig. 3, the parts of the brake used in the application of controllable torque are shown. With the main coil de-energized, retractor springs hold the shoes away from the wheel. When the coil is energized, the main armature is attracted, the retractor springs are overpowered, and the shoes are set against the wheel. Increasing the current in the main coil increases the force on the armature and the torque developed by the brake.

In the usual operation of the complete brake, the auxiliary coil is first energized to decouple the main spring, and then the brake is essentially an electrically applied brake as illustrated in Fig. 3.

Control

A d-c constant potential controller and a multipoint foot switch used with the brake are shown in Fig. 4(A), and the elementary diagram for this controller is shown in Fig. 4(B). Operator's controls also include a push-button station for control of parking torque application.

In use, the operator first presses a Release push button to close relay *BR1* to apply power to auxiliary coil *PB* to release the parking mechanism of the brake. After the current in the auxiliary magnet has increased enough to release the brake, current relay *BR2* opens to insert a protective resistor in series with the auxiliary coil. With the parking mechanism released, the drive may be operated normally and braking power may be applied, as required, by operating the master switch to close relays *BR3*, *BR4*, and *BR5* to apply successively increasing amounts of excitation to the main coil and therefore greater amounts of braking torque. Field trials have indicated that three torque points are sufficient for most applications, but additional points may be added when necessary. When the operator wishes to apply parking torque, he pushes the Set button to drop out relay *BR1* which de-energizes both the auxiliary coil and the main coil. The same result is obtained when power fails.

In many cases a normally open electrical interlock of relay *BR1* is used in the drive-controller circuit to prevent energizing the drive motor until the parking torque is released. Similary, an additional contact is sometimes provided in the brake master switch to cause de-energization of the drive motor before controlled braking can be applied. Both of these provisions are made to avoid driving through the brake.

In cases where repeated and prolonged braking is necessary, the control has b arranged to establish service dyna braking by the motor as the first brak point and to have this operate in para with the controlled braking.

While the controller is shown with a f switch, the brake has also been app to a floor-operated crane with cont from a pendant master switch.

Design Considerations

The brake shown in Fig. 1 was signed to have certain dimensions, same as those standardized for spring brakes with 13-inch-diameter wheel listed in the standards of Association Iron and Steel Engineers (AISE) National Electrical Manufacturers As ciation (NEMA).[4,5] The standard dimensions assure that the brake mount the same way as a spring-set br and that a wheel suitable for a spring brake can also be applied with the c trollable torque brake.

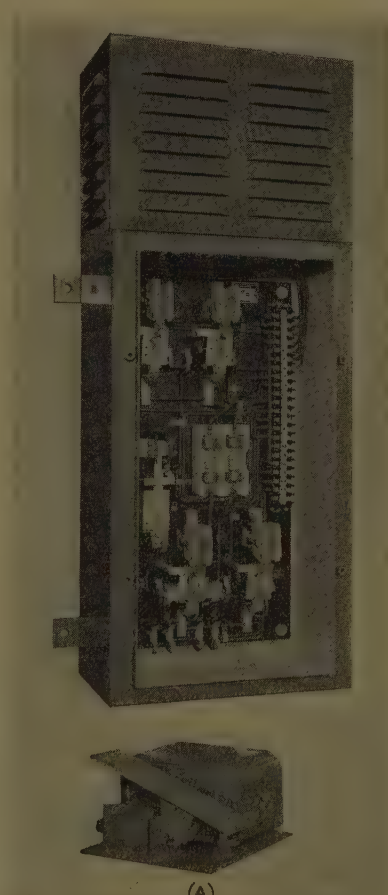

(A)

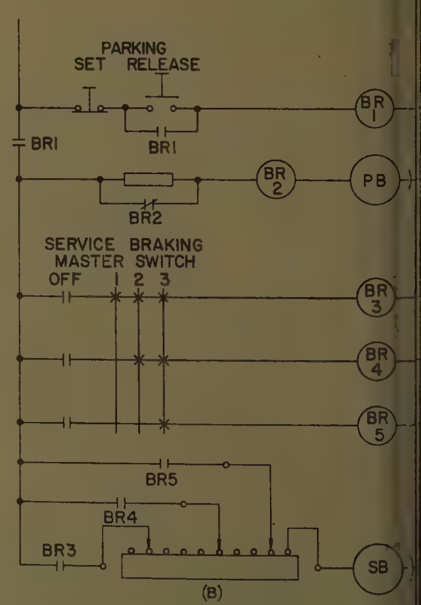

(B)

Fig 4. A—Brake controller and foot switch. B—Controller elementary diagram

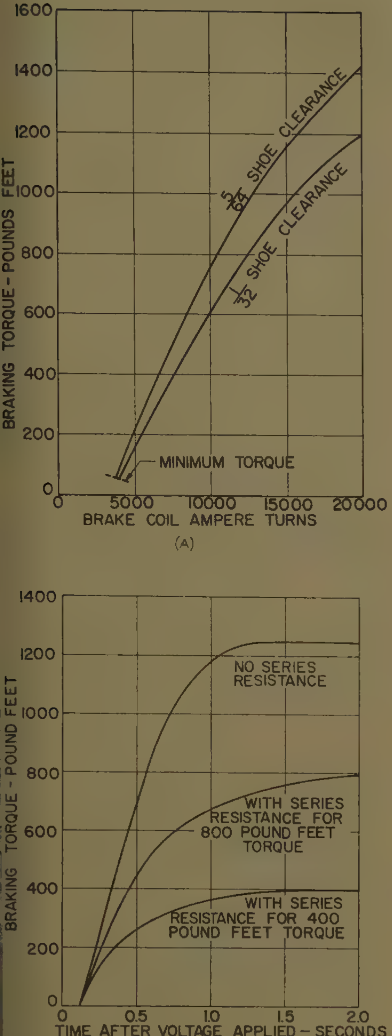

. 5. A—Service braking torque versus coil :itation. B—Service braking torque versus time

Maximum emergency braking torque of : brake is 550 pound-feet, the same as it of a 13-inch spring-set brake meeting SE–NEMA Standards. This torque 1 be adjusted down to as low as 150 ınd-feet by turning the calibrated park- torque adjustment shown in Fig. 2.

The new brake has been designed for a ximum controllable torque of 1,100 ınd-feet, twice the torque rating of a inch spring-set brake. It is antici- ed that this maximum torque will be uired infrequently and then only for rt periods of time. Consequently, the to provide 1,100 pound-feet maximum que has been designed for a 10-minute ing. For most applications, a maxi- m torque of 550 pound-feet will be quate, and a coil for this torque rating a 30-minute rating.

'he main magnet has been designed h a rather large air gap. This has two antages. First, it permits consider- y more than usual shoe wear between ustments. As the shoes wear, the magnet closes more and more; if the magnet were finally to close completely, the brake would no longer apply torque and would require adjustment. Second, the large air gap reduces the effect of manufacturing tolerances and that of shoe wear on the torque developed by the brake This reduction in torque variation is highly beneficial when it is desired to have two brakes share load equally, or when brakes are mounted on each end of a moving bridge which is to be stopped without skewing.

Equal clearances on the two shoes, when the brake is released, are obtained by turning the Shoe Centering Adjustment near the top of the auxiliary magnet armature. This screw serves as a stop for the top of the inner shoe lever as indicated in Fig. 3.

To adjust for shoe wear, a shoe clearance adjustment is provided as indicated in Fig. 3. The arm over the brake wheel is hexagonal in cross section and is provided with right-hand threads at one end and left-hand threads on the other so that the shoes can be drawn together or moved apart by turning this arm.

The Manual Release shown in Fig. 2 provides a means to compress the main spring without power permitting the retractor springs to move the shoes away from the wheel. With the brake manually released, maintenance work such as changing brake shoes and removing a motor armature and brake assembly may be accomplished easily.

Service Braking

Service braking torque is shown as a function of coil ampere-turns in Fig. 5(A). The lower curve shows the torque which is developed when the brake is adjusted, as recommended, for a shoe clearance of 1/32 inch. The upper curve shows the torque which is developed when the shoes have worn to the point where shoe clearance is 5/64 inch, the point at which the clearance should be readjusted to 1/32 inch. Some force is required to overcome the force of retractor springs when braking is applied, and since the force of the magnet increases as the armature moves toward the closed position in applying the shoes, the minimum torque which can be applied during service braking is limited. This minimum torque is indicated in the figure.

Because the brake coil is highly inductive, some time is required for the current to reach its final value, and the application of torque is correspondingly gradual. Fig. 5(B) shows torque as a function of

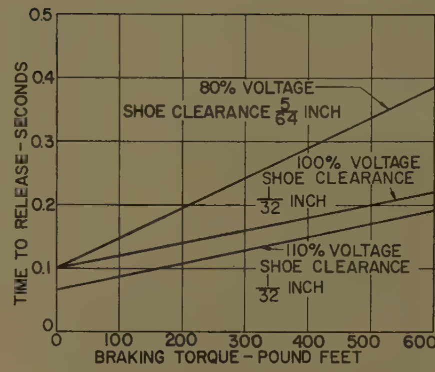

Fig. 6. Time to release parking torque

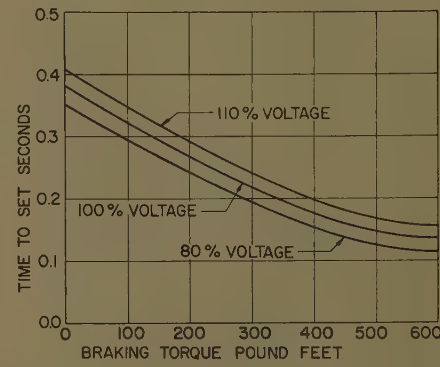

Fig. 7. Time to apply torque after power failure

time when full voltage is applied directly to the service braking coil and also when full voltage is applied to series arrangements of the service braking coil and appropriate resistances to give approximately two-thirds and one-third rated torque. Maximum service braking torque shown on the diagram is higher than rated because the tests were made with a relatively cold coil. However, the times to reach all except the highest values of torques are nearly the same when the

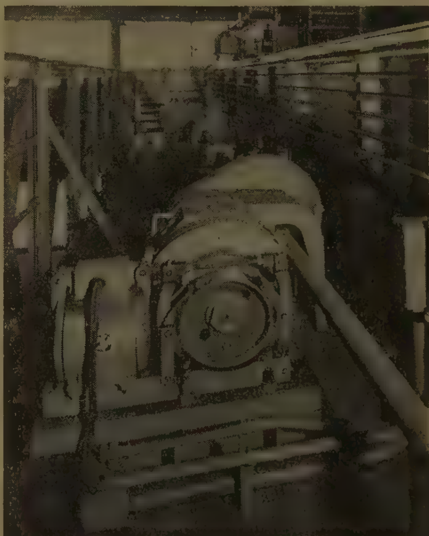

Fig. 8. Controllable torque brake mounted on bridge drive of overhead travelling crane

brake coil is hot as when it is cold because, although the ultimate torque is less, the inductance to resistance ratio is smaller when the coil is hot. It is evident that the time to develop torque is acceptably small for ordinary applications, and field tests have confirmed this.

To obtain the torque-versus-time characteristics, strain gages were mounted on a connecting lever between the service braking armature and the inner shoe lever, and oscillographic records of strain versus time were made. Strain in the connecting lever is directly proportional to shoe force and, assuming constant shoe friction, to brake torque.

At the same time that a strain proportional to torque was measured with strain gages, service braking coil current was also recorded. A torque-versus-time curve was then derived from this curve as well as the statically determined relationship between torque and current. Agreement between the directly obtained torque-versus-time curve and the curve based on the current-versus-time curve was good, indicating that there is no appreciable time lag between current and the torque corresponding to this current under steady-state conditions. Also, it is clear that derivation of the torque-versus-time curve from the easily determined current-versus-time curve is acceptable for practical purposes.

Parking and Power-Failure Braking

The time to release the parking mechanism of the brake is shown as a function of parking torque setting in Fig. 6. The middle curve shows the characteristic when rated voltage is applied to a hot coil and when the brake is adjusted for the recommended shoe clearance of 1/32 inch. The other two curves show the extremes of the characteristic for a voltage range of 80 to 110% of rated voltage and for a shoe clearance range of 1/32 inch to 5/64 inch.

Fig. 7 shows emergency set time as a function of parking torque for the rated voltage range of 80 to 110%. Emergency set time is practically independent of shoe clearance since most of the time is required for initial release and relatively little time for movement of the linkage.

Both release and set times of the parking section of the brake are comparable to those of spring-set magnetic-release brakes which are widely used, and thus these characteristics should be generally acceptable.

Applications

Fig. 8 shows one of two controllable torque brakes applied to the bridge drive of a manned trolley crane located in a steel mill shipping department. Here, accurate spotting of loads on trucks is accomplished by controlled braking. Since the operator moves with respect to the bridge, the brakes are connected to the control through collector bars.

The controllable torque brake has been applied to a coke pusher where accurate stopping of the pushing machine is necessary to line up a ram with an oven door. In this case, the auxiliary magnet is c energized each time the pusher machi is lined up with an oven to hold t machine against movement while t pusher ram is passing through the oven

Another typical field application is o floor-operated crane controlled from pendant master switch.

Conclusions

Development of an electromagne brake with controllable torque provi industry with a means to obtain smoo and accurate stopping of large drives w control from a small electric pilot devi Release of parking torque is accomplish quickly and with very little effort by t operator. Substitution of electric wi for hydraulic or air lines increases fle bility and reduces maintenance. Pe formance predicted by tests at the facto have been confirmed by applications the field.

References

1. Controllers for Electric Motors (bo H. D. James, L. E. Markle. McGraw-Hill B Company, Inc., New York, N. Y., 1945, pp. 123

2. Control of Electric Motors (book), P Harwood. John Wiley & Sons, Inc., New Y N. Y., third edition, 1952, pp. 479–97.

3. Magnetic Control of Industrial Mot (book), G. W. Heumann. John Wiley & S Inc., second edition, 1954, pp. 538–53.

4. D-C Mill Motor Brake Standard. *St ard no. 11*, Association of Iron and Steel Engine Pittsburgh, Pa.; also, *AISE Proceedings*, 1957, 836–37.

5. Industrial Control. *Publication No. 1 1959*, National Electrical Manufacturers Asso tion, New York, N. Y., pt. 20, June 1959, pp.

Random Linear Systems: A Special Case

ARTHUR R. BERGEN
ASSOCIATE MEMBER AIEE

IN CONTROL SYSTEMS, elements are frequently used whose "gain" is a function of variables outside of the primary control loop. For example, the gain of an armature controlled servomotor depends on the motor field current. The gain of a hydraulic valve (with respect to flow rate as output and valve displacement as input) depends on the static head on the valve. The effectiveness of a control surface in turning a body moving in a turbulent medium varies with time: The gain from control surface deflection to turning torque may be assumed to vary randomly with time.

It is interesting to know how a random gain affects a control system's performance. Even in those cases in which the external variables ffecting system gain are regulated, the effects of imperfect regulation are of interest. Thus, since regulators are ordinarily more effective in attenuating disturbances which are slowly varying rather than rapidly varying, the related gain variations in the primary control loop may be assumed to be broad band in some cases of interest. This assumption, basic in the analysis which follows, suggests a tractable model for a random parameter system.

Analysis

The system considered is linear time invarient except for a single r domly-varying gain. Fig. 1s hows system with the input and output of gain element exposed. The system m not be a feedback system, but this is case of interest.

The random gain $k(t)$ is assumed to a stationary random process with mea and varying component $a(t)$. Clea

Paper 61-72, recommended by the AIEE Feedb Control Systems Committee and approved by AIEE Technical Operations Department for sentation at the AIEE Winter General Mee New York, N. Y., January 29–February 3, 1 Manuscript submitted October 31, 1960; available for printing November 23, 1960.

A. R. Bergen is with the University of Califo Berkeley, Calif.

This research was supported by the Electr Research Directorate of the Air Force Cambr Research Center, Air Research and Develop Command, under Contract *AF 19 (604)-5460*.

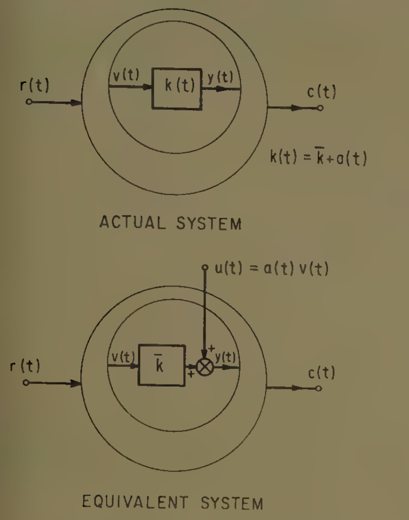

g. 1. Equivalent representation of random gain

t) has zero mean. In Fig. 1 an equiv-ent system is shown; the variable $y(t)$ the equivalent system is the same as at of the original system. A new riable $u(t)$ is defined which can be eated as a system input. Except for is dependent input, the system now pears to be a linear time-invariant stem.

Suppose now the system error is to computed. Treating $u(t)$ as a system put, by superposition

$$)=\int_{-\infty}^{t} h_{er}(t-\tau)\,r(\tau)\,d\tau+\int_{-\infty}^{t} h_{eu}(t-\tau)\,u(\tau)\,d\tau \quad (1)$$

so, this time, writing $u(t)$ explicity as) $v(t)$

$$)=\int_{-\infty}^{t} h_{vr}(t-\tau)\,r(\tau)\,d\tau+\int_{-\infty}^{t} h_{vu}(t-\tau)\,a(\tau)\,v(\tau)\,d\tau \quad (2)$$

equations 1 and 2 $h_{ji}(t)$ is the response the closed loop system at the point elled j to a unit impulse applied at the nt labelled i, with all other inputs zero. The solution of equation 2 is intractable ause of the presence of the $a(t)$ term. wever the mean-square error may be nd readily if the following assump-ns are made:

The input $vr(t)$ and the varying com-ent $a(t)$ of the random gain are statisti-y independent stationary random proc-s.

$a(t_1)$ and $a(t_2)$ are statistically independ-random variables for all t_2 not equal to $a(t)$ is a process with a constant spectral sity.

$h_{vu}(0)=0$, i.e., the application of an ulse at u does not cause a response at v antaneously.

f these assumptions the second is the t restrictive. Nevertheless, the problem is of interest since its solution (which is easily obtained) should suggest the types of behavior possible for systems in which the gain variation is not white but only broad band.

With these assumptions it may now be established that $E[a(t)v(t)r(t_1)]=0$ for all t_1, E denoting the expectation. The reason follows.

From equation 2, $v(t)$ can depend only on past and present values of $a(t)$. But, by Assumption 3 only past values of $a(t)$ can affect present values of $v(t)$. Then the present value of $v(t)$ is causally independent of the present value of $a(t)$. Finally, since by Assumption 2 past and present values of $a(t)$ are statistically independent random variables, present values of $a(t)$ and $v(t)$ also are statistically independent. In this case

$$E[a(t)v(t)r(t_1)]=E[a(t)]E[v(t)r(t_1)]=0 \quad (3)$$

since $a(t)$ has zero mean.

By the same token (assume $t_2\geq t_1$), $a(t_2)$ is independent of all the other variables and

$$E[v(t_1)a(t_1)v(t_2)a(t_2)]=0 \quad t_2\neq t_1$$
$$E[v(t_1)a(t_1)v(t_2)a(t_2)]=E[v^2(t_1)]E[a^2(t_1)] \quad t_2=t_1 \quad (4)$$

Assuming that the spectral density of the $a(t)$ process has a constant values S_0, it may be presumed on the basis of equation 4 that

$$E[v(t_1)a(t_1)v(t_2)a(t_2)]=E[v^2(t_1)]S_0\delta(t_2-t_1) \quad (5)$$

and this representation may be established.

The expected value of $v^2(t)$ may now be found as a preliminary to finding the mean-square system error. Squaring equation 2 and using equations 3 and 5

$$E[v^2(t)]=\overline{v_0^2}+S_0\int_{-\infty}^{t} h_{vu}^2(t-\tau)\times E[v^2(\tau)]d\tau \quad (6)$$

the square and average of the first term of equation 2 results in the constant term denoted by $\overline{v_0^2}$. It is a constant independent of time since $r(t)$ is assumed a stationary process. $\overline{v_0^2}$ is the mean-square value of $v(t)$ if $a(t)$ is zero. The cross terms of the square of equation 2 average to zero by virtue of equation 3. The square and average of the second term of equation 2 yields a double integral which reduces to the single integral in equation 6 by virtue of equation 5.

Equation 6 may be solved directly for $E[v^2(t)]$ if it is known to approach a constant value in the steady state. This, however, may not be assumed *a priori*; the stationariness of $r(t)$ and $a(t)$ do not insure this.

It is thus necessary to investigate the limiting behavior of $E[v^2(t)]$. For this purpose assume that although the input $r(t)$ has been turned on sufficiently far in the past to obtain steady-state conditions by the time $t=0$, $a(t)$ is only turned on at $t=0$. Then for positive time $E[v^2(t)]$ starts from the value v_0^2 and obeys the equation

$$E[v^2(t)]=\overline{v_0^2}+\int_0^t h_{vu}^2(t-\tau)E[v^2(\tau)]d\tau \quad (7)$$

Equation 7 differs from equation 6 in the lower limit of the integral and is appropriate for considering the transient behavior of $E[v^2(t)]$.

The solution of equation 7 is found by using the Laplace transform. Let $V^*(s)$ be the Laplace transform of $E[v^2(t)]$ while $H^*(s)$ is the Laplace transform of $h^2_{uv}(t)$. Transforming equation 7 and solving for $V^*(s)$

$$V^*(s)=\frac{\overline{v_0^2}}{s(1-S_0H^*(s))} \quad (8)$$

The behavior of $E[v^2(t)]$ depends on the roots of $1-S_0H^*(s)$. If all the roots are in the left-half plane (excluding the imaginary axis) there are transient terms which decay exponentially; $E[v^2(t)]$ tends to a steady-state value. If any of the roots are in the right-half plane $E[v^2(t)]$ diverges; the system is unstable. With roots on the imaginary axis, except at the origin which leads to divergence because of the double pole, an oscillatory behavior is possible.

In Appendix I it is shown that a sufficient condition for all the zeros of $1-S_0H^*(s)$ to be in the left-half plane is

$$S_0H^*(0)<1 \quad (9)$$

while in Appendix II this condition is also shown to be necessary. If

$$S_0H^*(0)\geq 1 \quad (10)$$

there is at least one root at the origin or on the positive real axis and the system is unstable in the mean square. Clearly a sustained oscillatory mode is not possible in this system.

Assuming equation 9 is satisfied, a constant quantity $\overline{v^2}$ may be defined and evaluated using the final value theorem of the Laplace transform

$$\overline{v^2}=\lim_{t\to\infty} E[v^2(t)]=\frac{\overline{v_0^2}}{1-S_0H^*(0)}=\frac{\overline{v_0^2}}{1-S_0\int_0^\infty h_{vu}^2(\tau)d\tau} \quad (11)$$

This result can also be obtained (now that the steady-state constancy has been established) from equation 6 by assuming the limiting value $\overline{v^2}$.

Equation 11 is valid as long as $\overline{v^2}$ is positive. Nonrealizable negative values

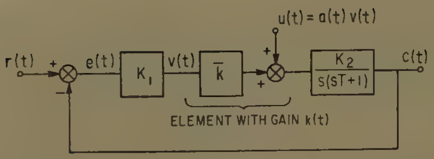

Fig. 2 (left). Servomechanism of the example

Fig. 3 (right). Effect of random gain on system rms error

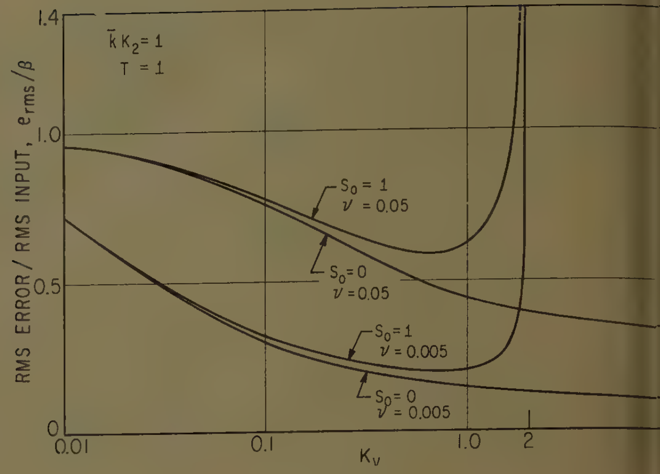

for $\overline{v^2}$ on the other hand imply instability; see equation 10.

Now it is possible to compute the steady-state mean-square error. Taking the square of equation 1, noting equations 3 and 5, and substituting the value of $\overline{v^2}$ found in equation 11

$$\overline{e^2}=\overline{e_0^2}+\frac{\overline{v_0^2}S_0\int_0^\infty h_{eu}^2(\tau)d\tau}{1-S_0\int_0^\infty h_{vu}^2(\tau)d\tau} \tag{12}$$

Here $\overline{e_0^2}$ is the mean-square error if $a(t)$ is zero. This result is valid provided the denominator is positive. It may be noted that $\overline{e^2}$ increases monotonically as a function of S_0. A random gain always deteriorates the system's performance.

In the special case that $v=K_1e$ equation 12 may be simplified.

$$\overline{e^2}=\overline{e_0^2}\frac{1}{1-S_0\int_0^\infty h_{vu}^2(\tau)d\tau} \tag{13}$$

Example

A second-order servomechanism with a random gain is shown in Fig. 2. The equivalent representation for the random gain has been introduced. Assume the input is a rectangular wave with values $\pm\beta$, the input makes independent random crossings from one value to the other. The autocorrelation function in this case is[1]

$$\phi_{rr}(\tau)=\beta^2e^{-2\nu|\tau|}$$

where ν is the average switching rate and β is the rms value of the input. If $a(t)$ is zero (the nonrandom gain case) the system mean-square error is

$$\overline{e_0^2}=2\nu\beta^2\frac{(K_v+2\nu)T+1}{K_v+2\nu+4\nu^2T} \tag{14}$$

$K_v=K_1\bar{k}K_2$ is the velocity constant. This result is derived by Newton, Gould, and Kaiser.[2] Curves of the mean-square error are shown in Fig. 3 labeled $S_0=0$.

Assume now the gain has a varying component $a(t)$ which satisfies assumptions 1 and 2 of this paper; Assumption 3 is satisfied by the servomechanism under discussion. Equation 13 may therefore be used to evaluate the mean-square error.

The computation of the integral in equation 13 is facilitated by using tables of integrals, for example, those in reference 1. Assuming a positive velocity constant K_v, the poles of $H_{vu}(s)$ are in the left-half plane and there are also more poles than zeros; the integral in equation 13 therefore converges and Parceval's theorem may be used to evaluate it, i.e.,

$$\int_0^\infty h_{vu}^2(\tau)d\tau = \frac{1}{2\pi j}\int_{-j\infty}^{j\infty}H_{vu}(s)H_{vu}(-s)ds$$

Substituting

$$H_{vu}(s)=\frac{-K_1K_2}{Ts^2+s+K_v}$$

and using the tables

$$\int_0^\infty h_{vu}^2(\tau)d\tau=\frac{(K_1K_2)^2}{2K_v}=\frac{K_v}{2\bar{k}^2}$$

By use of equation 13

$$\overline{e^2}=\frac{\overline{e_0^2}}{1-\frac{S_0K_v}{2\bar{k}^2}} \tag{15}$$

$\overline{e_0^2}$ is given by equation 14. Curves of equation 15 are shown in Fig. 3. Note that there is now a minimum which occurs for

$$K_v<\frac{2}{S_0/\bar{k}^2}$$

The larger the ratio of $S_0/\bar{k}^2$ the smaller the realizable K_v. $S_0/\bar{k}^2$ is a measure of the relative variability of gain and is an appropriate normalization of S_0.

Conclusions

The mean-square error of a linear control system of arbitrary order subjected to a random input and in the presence of a single random gain within the loop may be evaluated by conventional techniques under the following circumstances:

1. The input $r(t)$ and the varying component $a(t)$ of the random gain are statistically independent stationary random processes.

2. The random gain $a(t_1)$ and $a(t_2)$ are statistically independent random variables for all t_2 not equal to t_1.

3. $h_{vu}(0)=0$.

Under these conditions the following co[n]clusions may be drawn.

The mean-square error may converge[to] a constant value or diverge but sustai[ned] oscillations of the mean-square error [are] not possible. The effect of the rand[om] component of gain is to increase the sy[s]tem mean-square error. Any appar[ent] decrease of mean-square error is unreali[za]ble and indicates that instability in [the] mean-square has occurred.

Appendix I

If

$$S_0H^*(0)=S_0\int_0^\infty h^2(\tau)d\tau<1$$

then $1-S_0H^*(s)$ has all its zeros in the l[eft-] half plane. $H^*(s)$ is the Laplace transf[orm] of $h^2(t)$.

Starting with the definition

$$H^*(s)=\int_0^\infty h^2(\tau)e^{-s\tau}d\tau = \int_0^\infty h^2(\tau)e^{-\alpha\tau}e^{-j\omega\tau}\ldots$$

Using the triangle inequality and no[ting] that on the imaginary axis or in the ri[ght-] half plane where α is positive or zero

$$|H^*(s)|\le\int_0^\infty h^2(\tau)e^{-\alpha\tau}d\tau\le \int_0^\infty h^2(\tau)d\tau=H\ldots$$

Finally, introducing the hypothesis, ...

$$S_0|H^*(s)|\le S_0H^*(0)<1$$

on the imaginary axis or the right-half pl[ane].

As a consequence $1-S_0H^*(s)$ cannot [have a] zero in the right-half plane or imagin[ary] axis; all the zeros must be in the left-[half] plane.

Appendix II

If

$$S_0H^*(0)=S_0\int_0^\infty h^2(\tau)d\tau\ge1$$

then $1-S_0H^*(s)$ has at least one real [zero in] the right-half plane or at the origin.

ssume a real-axis zero of $1-S_0H^*(s)$ oc-
s for α, a real value of s. If $s=\alpha$ is a root

$$^*(\alpha)=1$$

hypothesis

$$^*(0)\geq 1$$

1

$$(0)\geq H^*(\alpha)$$

Noting that

$$\frac{d}{d\alpha}H^*(\alpha)=-\int_0^\infty \tau h^2(\tau)e^{-\alpha\tau}d\tau$$

is negative for all α, and that $H^*(\alpha)$ tends to zero as α tends to infinity, there is an $\alpha\geq 0$ for which $S_0H^*(\alpha)=1$. This proves that $1-S_0H^*(s)$ has a real root at the origin or in the right-half plane if $S_0H^*(0)\geq 1$.

The sufficient condition for $1-S_0H^*(s)$ to have only left-half plane zeros is therefore also necessary.

References

1. Analytical Design of Linear Feedback Controls (book), G. C. Newton, Jr., L. A. Gould, J. F. Kaiser. John Wiley & Sons, New York, N. Y., 1957, pp. 100–02.

2. *Ibid.*, pp. 126–133.

Time Domain Design of Sampled-Data Control Systems

M. P. PASTEL
MEMBER AIEE

G. J. THALER
MEMBER AIEE

CONTROL ENGINEER usually begins the design of a sampled-data dback control system with two sets of a. These are the fixed components t the system must include and the cifications which the final system must et. The fixed components, which will referred to as the plant, are inherent he process to be controlled and in many es are not subject to change. The nmonest specifications are generally terms of time-response and may inde rise time, peak overshoot, and ady-state position errors. In gen-l, the plant will not, of itself, satisfy specifications; hence, the designer's blem is to select such additional com-ents as will produce the desired sys-n. These components, called the npensator, may then give the final tem the form shown in Fig. 1, where s) represents the transfer function of plant and $G_c(s)$ is the compensator. termination of this compensator is the tral problem in feedback control sys-n design.

With the specifications given in terms over-all system performance, the logical proach to selection of the compensator uld seem to be from the closed-loop ction. Unfortunately, this generally uires laboriously finding roots of h-degree polynomials and computing transients. As a result of these difficulties, the classical method is to work directly with the open-loop function.[1] A compensator is chosen to reshape the Bode or Nyquist diagram according to certain tenuous relationships between the frequency and time domain. For continuous control systems, the easy application of this method compensates for the uncertain final performance of the closed-loop system.

er 61-77, recommended by the AIEE Feedback trol Systems Committee and approved by the E Technical Operations Department for presation at the AIEE Winter General Meeting, v York, N. Y., January 29–February 3, 1961. nuscript submitted January 4, 1960; made ilable for printing December 6, 1960.

P. Pastel and G. J. Thaler are with the U. S. val Postgraduate School, Monterey, Calif.

authors wish to express their gratitude to the ce of Naval Research for the use of a desk caltor.

However, in the case of sampled-data systems, the introduction of a compensator, not employing a sampler, requires the calculation of a new z-transfer function for the compensator and the parts of the plant into which it is cascaded. Not only does this involve a great deal of additional labor, but the choice of the compensator and its effect on the open-loop transfer function is more difficult to predict than for continuous systems.

These difficulties indicate that design of sampled-data systems should be based on a broader and more systematic procedure than that described, and it should include elements of synthesis rather than trial and error, since the latter involves much numerical calculation for sampled-data systems.

Systematic Design Methods

A design procedure is shown in the form of a flow chart in Fig. 2. The various blocks represent steps, and the letters beside each arrow identify the operation required to advance to the next step. The chart is headed by blocks representing available data at the start of the design: the time specification, and the plant. Thus the procedure may be initiated from either block depending on the emphasis. If final time performance must be secured, the chart should be entered with the time-specification block. If the plant involved must be preserved in its entirety, initiation should be from the plant-function block. In most cases, however, a compromise procedure can be used. This is discussed later.

If the chart is entered with the time specification, the specifications are interpreted in terms of a closed-loop pole-zero configuration on the z-plane by means of correlation theorems, discussed in Appendix I. From the pole-zero configuration the open-loop root locus yields the corresponding open-loop pole-zero configuration. The term open-loop root locus has been introduced to distinguish this root locus method, which finds the open-loop poles from the closed-loop function, from the conventional root locus technique first introduced by Evans.[2,3] This latter method of finding the closed-loop poles from the open-loop function is referred to in this method as the closed-loop root locus. The rules for preparing an open-loop root locus are prescribed in Appendix II.

With the open-loop function which will satisfy the time requirements known, the designer can either:

1. Proceed directly to determination of the compensator, or

2. Attempt to conciliate the differences between the poles and zeros of the open-loop function and those of the plant so that, at least, the major poles and zeros of the plant are included in the final open-loop function.

By the first method, the procedure is straightforward. The desired open-loop z-transform is converted into its equiv-

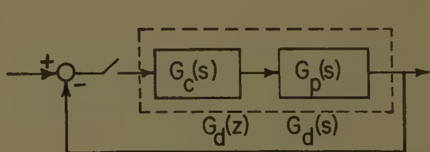

Fig. 1. A compensated sampled-data control system

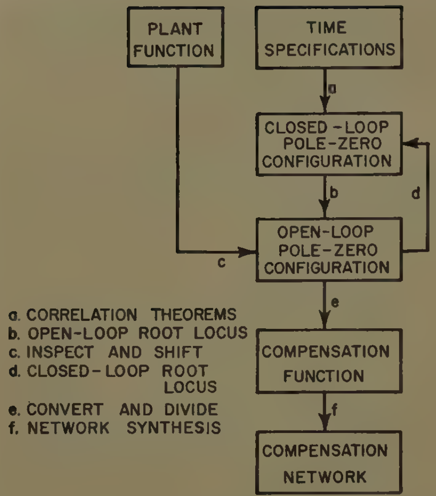

Fig. 2. Synthesis flow chart

alent Laplace transfer function. The transfer function of the compensator may now be found by simple division

$$G_c(s)=\frac{G_d(s)}{G_p(s)} \tag{1}$$

where $G_d(s)$ is the open-loop or "desired" transfer function, corresponding to the selected closed-loop function. The actual compensating network may be determined by standard network synthesis procedure.

A study of equation 1 reveals that the compensator will, in general, cancel out each pole and zero of the plant, as well as add the poles and zeros of the desired function. In practice, complete cancellation of the poles and zeros of physical components such as electric and hydraulic motors is impossible, since their precise characteristics are never known over the full range of operation. Fortunately, system performance is not significantly changed as long as the pole and its cancelling zero lie near each other. This situation gives rise to a pole and zero placed close together in the closed-loop function, and the resulting residue is negligible.

A more serious objection to method 1 is the impossibility of cancelling out equipment time constants and expecting the equipment to function in a linear mode over a large range of input values. Cancelling out a motor time constant and replacing it with a much smaller one cannot be expected to result in an increase in the actual maximum obtainable acceleration, and the motor and gear combination will not be able to follow a ramp which exceeds its maximum speed. For these reasons, the designer is strongly urged to proceed according to the second method.

In method 2, the designer compares the poles and zeros of the desired open-loop with that of the plant. By shifting location of the closed-loop poles-zeros, the major poles and zeros of the plant can usually be brought into the desired open-loop transfer function. The open- and closed-loop root locus furnish a graphical way of bringing about this correspondence. The impossibility of incorporating the major components of the plant into the desired open-loop function does not imply failure of this design method. Actually, this is a signal to the designer that the fixed plant is incapable of providing the performance demanded by the specifications. This means that the plant must be improved or, if this is not practical, the specifications must be changed to concede the realities of the situation. Thus, method 2 increases the designer's circumspection.

If the compensator can be cascaded to the plant through a sampler, the preceding steps may still be taken, and the compensator can be found directly from

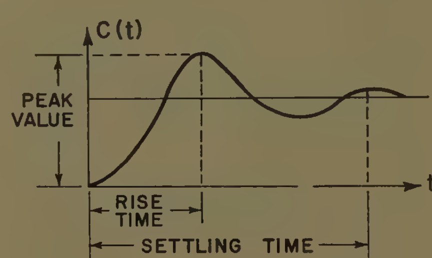

Fig. 3. Typical transient response to unit step input

the z-transform of the system, that is,

$$G_c(z)=\frac{G_d(z)}{G_p(z)} \tag{2}$$

An alternate method is to start the design with the plant, first forming the open-loop pole-zero configuration and then the closed-loop root locus. The optimum performance possible without compensation can be determined by use of the correlation theorems. In general, additional open-loop poles and zeros will be required to satisfy the time requirement, their effect on the time response being ascertained readily by use of the root locus and correlation theorem technique.

Time Response and Basic Pole-Zero Configuration

The critical step in this procedure involves choosing the proper pole-zero configuration. The typical time requirements for a transient response to a step is shown in Fig. 3. The steady-state error to a ramp and parabolic input a[re] shown in Fig. 4. Numerous pole-zer[o] arrangements can be found to satisfy [a] particular set of time specification[s]. However, the correlations theorems f[or] transient response listed in Appendix [I] are based on a dominant pair of comple[x] poles. A pole-zero spaced close togeth[er] and near the point $1+j0$ in the z-plan[e] provides control over the steady-sta[te] error. With this, the basic pole-zer[o] configuration in the z-plane is that show[n] in Fig. 5.

While all specifications cannot [be] satisfied by third-order systems, the sy[n]thesis can be handled initially in th[is] way in many cases. As a last step in th[e] design, more poles or zeros may have [to] be added if the compensator is to [be] physically realized. This is discusse[d] in greater detail in Appendix III. If th[e] poles and zeros have large real parts [in] the s-plane, they will give rise to z-plan[e] poles and zeros near the origin and hav[e] little effect on the previously determine[d] results. Fig. 6 shows a typical pol[e-]zero configuration.

Control of time response extends on[ly] to the sampling instants. This generall[y] is satisfactory. However, a complet[e] description of the output between the[se] instants may be secured by employin[g] the modified z-transform technique [in] the final system.

Plants with poles and zeros in the righ[t-]hand half of the s-plane require speci[al] consideration. The poles will hav[e] images outside the unit circle in the [z-]plane, as will the zeros in most case[s]. Rather than attempt to cancel these pol[es] and zeros, they should be included [as] part of the final open-loop transfer func[]tion.

The general methods of this present[a]tion have been extended to sample[d-]data systems which do not possess [a] sampler in the error channel.[5] Th[is] class of system does not enjoy a close[d]

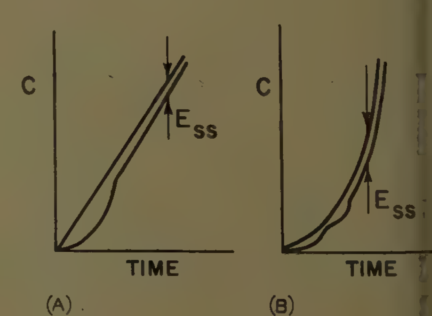

Fig. 4. Steady-state errors to ramp [...] parabolic input

A—Ramp input
B—Parabolic input

p transfer function independent of the
ut function.

ıstrated Example

As an example of using the proposed sign procedure, consider the design of a stem to certain specifications.

The plant has a sampler in the error annel operating with period of 0.1 second l a transfer function given by

$$(s)=\frac{K(s+19)}{s(s+3.7)(s+8)(s+25)} \tag{3}$$

The time domain specifications are

≤ 0.35

≤ 4

≤ 10

$^{*}=\infty$

$^{*}\geq 60$

Two items which must be decided be- e selection of the closed-loop pole-zero nfiguration are the difference in the mber of z-plane poles and zeros of the nt and how many of each are to be ained in the desired transfer function. r the first item, the plant has one sam- r, no delays, and a numerator 3 de- es less than the denominator; hence, z-transfer function of the plant will ve one more pole than zero. A dis- sion of the required minimum number z-plane poles and zeros and the re- red difference between the number of h is given in Appendix III.

For the second item, the retention of nt poles and zeros is frequently de- dent on the physical equipment. In case, an infinite value for K_p^* re- res the pole at the origin to be retained l, arbitrarily, the pole at 3.7 will also retained. With these constraints, the plest pole-zero configuration can be a r of complex poles and one real zero. e first choice of pole-zero selection is

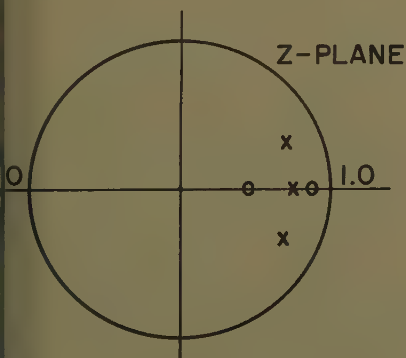

5. **Basic closed-loop pole-zero configuration**

made with poles at $0.5-j0.45$ and a zero at 0.3. Using the correlation theorems

$M=0.21$

$n_p=3.0$

$n_s=8$

$K_v^*=13$

The transient response requirements are met with sufficient margin to permit realization of a higher velocity error-constant by introduction of a dipole. First, however, the open-loop poles must be ascertained by the open-loop locus shown in Fig. 7. The gain is fixed by including one pole at point 1.0, and the remaining pole is found at 0.64.

The s-plane pole of 3.7, which is to be included in the final open-loop function, corresponds to a z-plane pole of 0.691. Since the first try has produced a pole, not too far removed from this location, a closed-loop locus is now formed in Fig. 8.

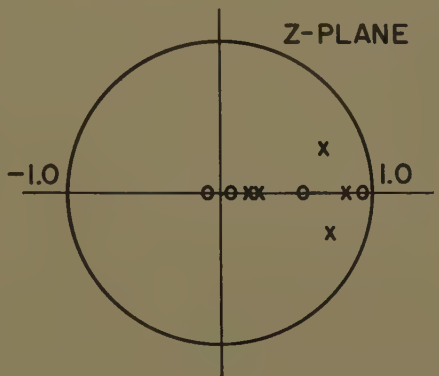

Fig. 6. **Typical closed-loop pole-zero configuration**

Choosing on the locus poles at $0.55\pm j0.46$ gives the time specifications

$M=0.28$

$n_p=3$

$n_s=9$

$K_v^*=13$

With the gain determined, the open-loop function is

$$G(z)=\frac{0.591(z-0.3)}{(z-1)(z-0.691)} \tag{4}$$

A dipole is now employed to raise the steady-state error constant. But the required close spacing of the pole and the zero will render graphical methods impractical. An alternate procedure, avoiding this difficulty, works directly with the open-loop function. An open-loop pole at 0.99 and a zero at 0.95 increases the steady-state error constant to 65.

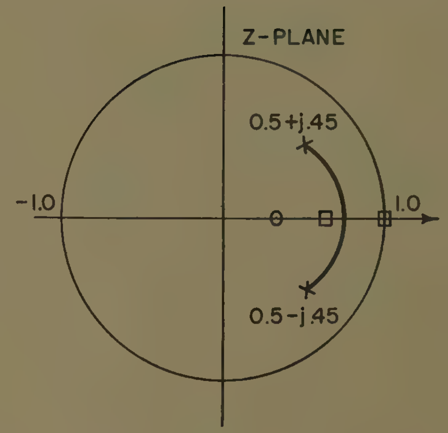

Fig. 7. **First selection for closed-loop configuration and open-loop root locus**

Realization of the open-loop function as a continuous one, without time delays, requires a zero at the origin. To retain the difference of one between the number of poles and zeros, an additional pole is added at 0.001. This pole was purposely placed near the origin to cancel the effect that the zero may have on the transient response. The desired open-loop system is thus described by the transfer function

$$G(z)=\frac{KA(z)}{B(z)}$$
$$=\frac{0.591z(z-0.95)(z-0.3)}{(z-1)(z-0.99)(z-0.691)(z-0.001)} \tag{5}$$

Inclusion of the additional poles and zeros will result in a shift of the complex poles and a change in the transient response. The new pole positions could be determined by analytical methods and the correlation theorems employed once again. But a simpler method would be to form the output z-transform function $C(z)$ to a unit step directly from $G(z)$ as

$$C(z)=\frac{z}{z-1}\times\frac{KA(z)}{KA(z)+B(z)} \tag{6}$$

By simple division, the output at the sampling instant is, in this case,

$$C(z)=0.591u_0(t-0.1)+1.087u_0(t-2)+1.33u_0(t-3)+1.34u_0(t-0.4)+1.212u_0(+-0.5)+1.065u_0(+-0.6)+0.988u_0(t-0.7)+0.935u_0(t-0.8)+0.955u_0(t-0.9)+0.995u_0(t-1.0)$$

The transient specifications are now

$M=0.34$

$n_p=4$

$n_s=9$

Converting the z-transfer function to its equivalent Laplace transform, with poles in the primary strip, is the next step. This involves taking a partial-fraction expansion of $G(z)/z$, multiply-

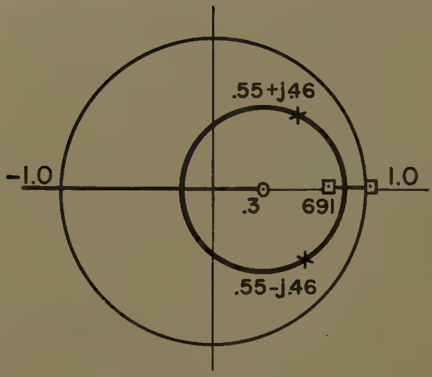

Fig. 8. Adjusted pole-zero configuration and closed-loop locus

ing through by z, converting term by term to Laplace transform with the aid of tables, and, lastly, collecting the terms over a common denominator. In this case the final result is

$$G(s)=\frac{20.95(s+0.512)(s+15.94)}{s(s+0.1)(s+3.7)(s+69)} \tag{7}$$

The compensation is now determined by dividing the derived transfer function, equation 7, by the plant equation 3, yielding

$$G_c'(s) =\frac{20.95(s+0.512)(s+8)(s+15.94)(s+25)}{(s+0.1)(s+19)(s+69)} \tag{8}$$

The network is not realizable in its present form, but addition of a fourth pole far out on the negative axis has a negligible effect on the transient response, and yields a realizable compensation function

$$G_c(s) =\frac{620(s+0.512)(s+8)(s+15.94)(s+25)}{(s+0.1)(s+19)(s+30)(s+69)} \tag{9}$$

This function is realizable in terms of resistance and capacitors by standard network synthesis procedures.

Conclusion

The foregoing operation furnishes an integrated and systematic method of designing sampled-data feedback control systems to required time response through use of root locus techniques and correlation theorems. Its flexibility permits emphasis on either the fixed components of the plant or on the time-performance of the closed-loop system. The method increases the designer's circumspection into the effect of closed-loop and open-loop poles and zeros on the time response. This is particularly important in the design of sampled-data systems because of the additional numerical work involved in taking the z-transform and the complication of determining a new transform function whenever a compensator is added without a sampler.

Appendix I. Correlation Theorems

If the transfer function is denoted

$$G(z)=\frac{KA(z)}{B(z)} \tag{10}$$

The closed-loop transfer function $W(z)$ can be denoted

$$W(z)=\frac{KA(z)}{B(z)+KA(z)}=\frac{KQ(z)}{P(z)} \tag{11}$$

or

$$W(z)=\frac{K(z-q_1)(z-q_2)\dots(z-q_n)}{(z-p_1)(z-p_2)\dots(z-p_n)} \tag{12}$$

Then the main characteristics of a transient sequence of samples, as shown in Fig. 3, can be determined from the closed-loop poles and zeros with a predominant pair of poles, z_0, as[4,5]

$$n_p=\frac{1}{\phi_0}\left[\frac{\pi}{2}-\text{ang } Q(z_0)+P(z_0)\right] \tag{13}$$

where

$$\phi_0=\tan^{-1}\frac{\text{imag }(z_0)}{\text{real }(z_0)}$$

M=(product of distance from all poles to the point $1+j0$, excluding distances from the two predominate poles to the point $1+j0$)/(product of distances from all poles to predominate poles excluding the distance between predominate poles) $\times$ (product of distances from zeros to the predominate pole)/(product of distance from all zeros to the point $1+j0$) $|z_0|^{n_p}$.

$$n_s=\frac{\log D}{\log |z_0|} \tag{14}$$

where D is the difference between unity and the accepted settled value, for a unit step input. (D is 0.05 in the illustration.)

The steady-state error constants K^*_p, K_v^*, and K_a^* for a unit step, unit ramp, and unit parabolic input[5] are in terms of the closed-loop poles and zeros.

$$K_p^*=\frac{K\prod_{k-1}^{w}(1-q_k)}{\prod_{i=1}^{m}(1-p_i)-K\prod_{k=1}^{w}(1-q_k)} \tag{15}$$

$$K_v^*=\frac{1/T}{\sum_{i=1}^{m}\frac{1}{1-P_i}-\sum_{k=1}^{w}\frac{1}{1-q_k}} \tag{16}$$

$$K_a^*=\frac{2/T^2}{\sum_{k=1}^{w}\left(\frac{1}{1-q_k}\right)^2-\sum_{i=1}^{m}\left(\frac{1}{1-P_i}\right)^2} \tag{17}$$

In terms of open-loop poles and zeros, th error constants are[6]

$$K_p^*=\lim_{z\to 1} G(z) \quad (1$$

$$K_v^*=\frac{1}{T}\lim_{z\to 1}(z-1)G(z) \quad (1$$

$$K_a^*=\frac{1}{T^2}\lim_{z\to 1}(z-1)^2G(z) \quad (2$$

Appendix II. Open-Loop Roo Locus

For a system such as Fig. 1, the ope loop function $C(z)$ and closed-loop functi $W(z)$ are related by

$$W(z)=\frac{G(z)}{1+G(z)} \quad (2$$

Solving for $G(z)$ gives

$$G(z)=\frac{W(z)}{1-W(z)} \quad (2$$

Hence, the poles on root of $G(z)$ are t solution of the equation

$$W(z)=1 \quad (2$$

Alternately, equation 23 may be writt as

and $W(z)=0+2h\pi$ (2

where h may be any integer or zero and

$$|W(z)|=1 \quad (2$$

The approximate root locus genera can be found quickly by applying fu similar to those for the conventional r locus and by employing a spirule.

Some helpful facts regarding approxima construction of the open-loop root lo are[5]

1. The loci are continuous curves, starti at a pole for zero gain and terminating zero or at infinity for infinite gain.
2. The loci exist on a part of the real a where an even number of poles plus ze are found to the right.
3. If the number of poles w exceeds t number of zeros m, there are w-m branch which go to infinity. Further, the directi of the infinite asymptotes with respect t the real axes are

$$\frac{2h\pi}{w-m} \quad h=1, 2, 3\dots \quad (2$$

4. All asymptotes intersect at a point on the real axis.

$$u=\frac{\sum_{i=1}^{m}p_i-\sum_{k=1}^{w}q_k}{w-m} \quad (2$$

5. The angle at which a locus emana from a complex pole or terminates upo complex zero is found by summing the ang to all other poles and zeros. When emanat from a pole, the angles from the poles taken negative. When terminating on zero, the angles from the zeros are tak negative.

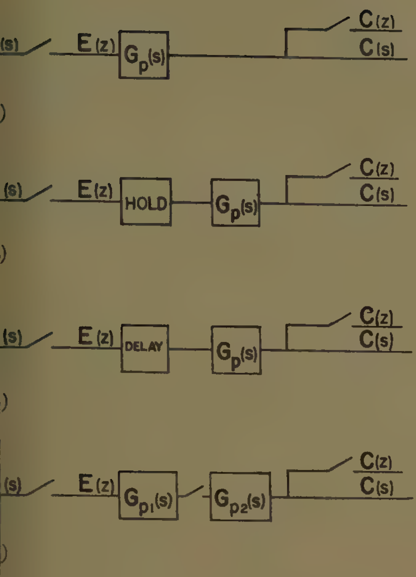

Fig. 9. Various types of plants

\—Plant is continuous network
—Plant includes hold network
—Plant contains pure delay
—Parts of plant are separated by samplers

Appendix III. Required Number of Poles and Zeros

The general location of the poles and zeros achieve various requirements have been scussed. However, at the start of the nthesis procedure, knowing the minimum mber of poles and zeros needed by a given plication is required. Although mathatically permissible, a practical compensar cannot possess poles at infinity. Consently, the excess of poles over zeros for the mpensated or desired open-loop function ust be at least equal to the excess for the plant $G_p(s)$. Since the closed-loop function zeros are the same as those of the open-loop and the number of poles are the same for either open- or closed-loop function, it can be said that

$$(\text{number of poles}-\text{number of zeros})_{W(z)} \geq (\text{number of poles}-\text{number of zeros})_{G_p(z)} \tag{28}$$

It would be advantageous to avoid the the lengthy process of taking the z-transform from the Laplace transform in order to determine the number of zeros of the plant. This number usually can be found by inspection, as will be illustrated by considering the open-loop systems shown in Fig. 9. When the continuous system, as shown in Fig. 9(A), has two poles in excess of the zeros, output will be available at the second sampling; i.e., $n=1$.

Since the value of the output can be determined at the sampling instant by dividing the denominator of $G(z)$ into the numerator, an output at this sampling instant requires that the number of z-plane zeros be only one less than the number of z-plane poles. The number of zeros equals the number of poles when the Laplace transform poles exceed the zeros by only one. Also, in these cases, a zero is found at the origin. If a hold network is employed, as shown in Fig. 9(B), the same process of reasoning indicates that the number of poles exceeds that of zeros by one; however, a zero need not necessarily be at the origin. A plant including a delay, such as Fig. 9(C) of less than one sampling period, will give rise to the same z-plane pole-zero difference as discussed for Fig. 9(A) except the zero generally will not be found at the origin.

For every complete sampling period that the delay involves, poles are placed at the origin without any additional zeros. The over-all transfer function for Fig. 9(D) is the product $G_{p1}(z)\,G_{p2}(z)$, and the difference between the poles and the zeros of each function is additive in the final transfer function. If the poles and zeros differ by one, then the over-all transfer function will have an excess of two poles more than the zeros. This is in accordance with physical expectation, since the second network does not receive an input until the second sampling instant.

References

1. Analysis and Synthesis of Sampled-Data Control Systems, E I. Jury. *AIEE Transactions*, pt. I (*Communication and Electronics*), vol. 73, Sept. 1954, pp. 332–46.

2. Graphical Analysis of Control Systems, W. R. Evans. *Ibid.*, vol. 67, 1948, pp. 547–51.

3. Root Locus Method of Pulse Transfer Function for Sampled-Data Control Systems, M. Mori. *Transactions*, Professional Group on Automatic Control, Institute of Radio Engineers, New York, N. Y., Nov. 1957.

4. Correlation Between Root-Locus and Transient Response of Sampled-Data Control Systems, E. I. Jury. *AIEE Transactions*, pt. II, (*Applications and Industry*), vol. 74, 1955 (Jan. 1956 section), pp. 427–34.

5. The Closed-Loop Pole-Zero Synthesis of Sampled-Data Feedback Systems, M. P. Pastel. *Doctoral Dissertation*, U. S. Naval Postgraduate School, Monterey, Calif., 1959.

6. Additions to z-Transformation Theory for Sampled-Data Systems, G. V. Lago. *AIEE Transactions*, pt. II (*Applications and Industry*), vol. 73, 1954 (Jan. 1955 section), pp. 403–08.

Discussion

T. J. Higgins (University of Wisconsin, Madison, Wis.): The discusser has read this interesting and clearly written paper with profit. A rational means of designing compensating networks for sampled-data systems to meet prescribed response, rather than dependence on earlier used trial-and-error procedures, is most desirable. The authors are to be congratulated on their successful effort.

The Synthesis of Optimum Systems from Nonideal Components

J. K. WOLF
NONMEMBER AIEE

T. R. WILLIAMS
NONMEMBER AIEE

J. B. THOMAS
MEMBER AIEE

HE USEFULNESS of statistical techniques in the synthesis of optimum ntrol systems has been amply justid,[1–7] and a voluminous literature ists on the subject. A wide class of ch synthesis problems are those where e basic circuit is fixed and the designer ust choose values for a finite number parameters. It is usually assumed that ese parameters relate to components hich possess exactly their nominal lues. In such cases, once a design criterion has been established, the optimization procedure is straightforward.

It is the purpose of this paper to consider situations where the actual values of the components differ from the nominal values in some random fashion, i.e., the components have either associated tolerances or associated drift characteristics. In the following discussion, such components will be called "nonideal."

If the components to be used are nonideal, then the optimization parameters can be treated as random variables whose probability densities have one or more variable moments. For example, consider the case where one of the parameters is represented by the value of a single resistor which has a $\pm 10\%$ tolerance. If there is an equal probability of the resistance R falling anywhere within $\pm 10\%$ of the nominal value R' (and zero probability of falling elsewhere), the following density function would be assigned to the random variable representing the resistance value:

Paper 61-86, recommended by the AIEE Feedback Control Systems Committee and approved by the AIEE Technical Operations Department for presentation at the AIEE Winter General Meeting, New York, N. Y., January 29–February 3, 1961. Manuscript submitted October 14, 1960; made available for printing December 16, 1960.

J. K. Wolf is with the U. S. Air Force Rome Air Development Center, Griffiss Air Force Base, N. Y., and T. R. Williams and J. B. Thomas are with Princeton University, Princeton, N. J.

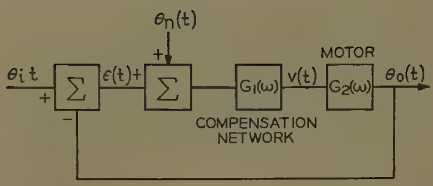

Fig. 1. Block diagram of servomechanism

$$p(R)=5/R',\ 0.9R'\leq R\leq 1.1R' \qquad (1)$$
$$=0,\ \text{elsewhere}$$

For this example, R' is the mean value of the random variable R and is the variable moment specified in designing the system. In other cases, other moments or characteristics of the density function might be used. The particular moment or characteristic which corresponds to the nominal value of the parameter to be specified will be called the zero tolerance variable (ztv). In general, all the moments of the density function could be functions of the ztv, but it will be assumed that the density function can be written as an explicit function of this parameter. For purposes of notation, the ztv corresponding to the parameter α_i will be denoted by α_i'.

If more than one parameter is involved in the optimization, a joint density function must be specified. However, in many cases, the tolerances associated with the different parameters will be statistically independent so that the joint density function can be written as the product of the individual density functions.

Analysis

In any statistical synthesis procedure, a criterion for optimization must be established. In accordance with the great majority of literature in this area, the minimum mean-squared error (mse) criterion will be used.

It is necessary first to examine briefly the problem of designing a system with ideal components. The system will be assumed fixed except for the values of q parameters, $\alpha_1,\ \alpha_2,\ \ldots,\ \alpha_q$. The mse can then be calculated in terms of these q parameters provided that the correlation functions of the input signals and disturbances are known. Formally, there is no difficulty in calculating the mse; in fact, the values of certain integrals which occur frequently in these calculations have been tabulated.[8] The optimum values, $\alpha_{10},\ \alpha_{20},\ \ldots,\ \alpha_{q0}$, of the parameters $\alpha_1,\ \alpha_2,\ \ldots,\ \alpha_q$ are then determined by standard minimization techniques.

For systems with nonideal components, it is assumed, as before, that there are q parameters to be specified and, in addition, that these parameters correspond to components with statistically independent tolerances. The density function for the ith parameter α_i will be written $p(\alpha_i;\ \alpha_i')$ where α_i' is the ztv of this density function. The average mse* is then

$$\overline{\epsilon_a^2}(\alpha_1',\ \ldots,\ \alpha_q')=\int_{-\infty}^{\infty}\cdots\int_{-\infty}^{\infty}$$
$$\overline{\epsilon^2}(\alpha_1,\ \ldots,\ \alpha_q)\prod_{i=1}^{q}p(\alpha_i;\ \alpha_i')d\alpha_1\ldots d\alpha_q \qquad (2)$$

where $\overline{\epsilon^2}(\alpha_1,\ldots,\ \alpha_q)$ is the mse that would result if the components were ideal. Thus, in equation 2, the average mse is used as the new optimization criterion and the statistics of the random parameters must be taken into account as well as those of the signals and disturbances.

The remaining procedure is, in principle, straightforward. The quantity $\overline{\epsilon_a^2}$ is minimized with respect to the ztv $\alpha_1',\ \alpha_2',\ \ldots,\ \alpha_q'$ by the usual methods of the calculus. The values of the ztv which produce this minimum will be denoted by $\alpha_{10}',\ \alpha_{20}',\ \ldots,\ \alpha_{q0}'$.

Equivalence of Solutions

It is interesting to determine the conditions for which the minimum average mse choices of the ztv are numerically equal to the minimum mse choices of the parameter values for ideal components, i.e., the conditions for

$$\alpha_{i0}=\alpha_{i0}' \qquad i=1,\ 2,\ \ldots q \qquad (3)$$

It is shown in the Appendix that, for components with statistically independent tolerances, the following conditions are sufficient for equation 3 to hold:

1. The probability density functions are symmetric about their respective ztv.

2. The mse $\overline{\epsilon^2}(\alpha_1,\ \ldots,\ \alpha_q)$ for ideal components is symmetric about its minimum (i.e., about the point-defined by $\alpha_i=\alpha_{i0},\ i=1,\ 2,\ \ldots,\ q$).

These conditions are sufficient but not necessary for the equivalence of solutions.

Example

The following example is taken from the control literature[9] where it first appeared, with ideal components a[…]sumed. A simple compensation netw[…] is to be designed for a servomechanis[…] The input $\theta_i(t)$ is a series of step displa[…]ments of random amplitudes occurri[…] at random time intervals. The rand[…] process defined by the time derivative [of] this input is a white noise[10] with t[…] constant power spectrum S_0.

The block diagram of the system [is] given in Fig. 1. In this figure, a d[…]turbance $\theta_n(t)$ is shown which is assum[ed] to be independent of the input signal a[nd] to have the flat power spectrum […] The motor is represented by the differe[n]tial equation

$$J\ddot{\theta}_0(t)+K_2\dot{\theta}_0(t)=K_3v(t)$$

so that its transfer function is

$$G_2(s)=\frac{K_3}{s(Js+K_2)}$$

The compensation network has a fix[ed] time constant T_1 and an adjustable ga[in] K_1; thus

$$G_1(s)=\frac{K_1}{1+sT_1}$$

The problem is to specify the va[lue] of K_1 which minimizes the statistic[al] expectation of the square of the er[ror] $\epsilon(t)$.

It is convenient to define the follow[ing] parameters:

$$\alpha\triangleq(T_1+J/K_2)K_1K_3/K_2$$

$$A\triangleq\frac{T_1(J/K_2)}{(T_1+J/K_2)^2}$$

$$L\triangleq\frac{N_0}{S_0(T_1+J/K_2)^2}$$

$$K_0\triangleq(T_1+J/K_2)S_0/4 \qquad ($$

If all the components are ideal, [the] mse is shown[9] to be

$$\overline{\epsilon^2}(\alpha)=K_0\frac{1+\alpha(1-A)+L\alpha^2}{\alpha(1-A\alpha)},\ 0<\alpha<\frac{1}{A} \qquad ($$

If α is outside the interval (0, $1/A$) the system is unstable and the mse [is] infinite. All parameters are assum[ed] fixed except for K_1 which occurs linea[rly] in α. Thus equation 11 can be mi[ni]mized with respect to α. The result [is]

$$\alpha_0=[A+(A+L)^{1/2}]^{-1} \qquad ($$

which specifies the optimum value of [K_1] for the ideal case. The mse[9] is

$$\overline{\epsilon^2_{\min}}=K_0[A+2(A+L)^{1/2}+1] \qquad ($$

Let us now consider the nonid[eal] case and assume that α is a rand[om] variable described by the density funct[ion]

$$p(\alpha,\ \alpha')=1/2\beta,\ \alpha'-\beta\leq\alpha\leq\alpha'+\beta$$
$$=0,\ \text{elsewhere} \qquad ($$

* Although the term "average mse" may appear redundant, it is used to indicate that the squared-error is averaged over both the statistics of the random inputs and the statistics of the random parameters.

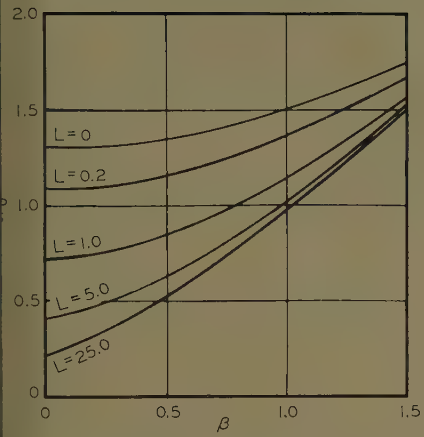

g. 2. **Optimum nominal gain as function of half-width of density function**

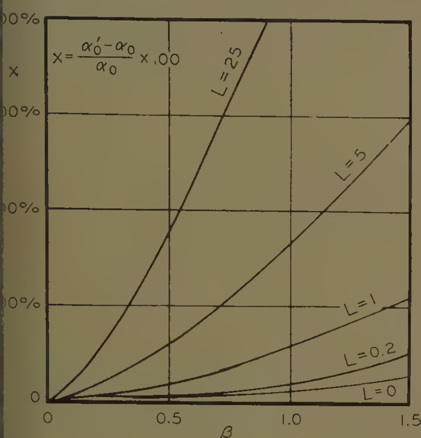

g. 3. **Percentage change in nominal gain s function of half-width of density function**

here β is a constant. Here the ztv is the mean of the distribution. The erage mse is now

$$(\alpha')=\int_{\alpha'-\beta}^{\alpha'+\beta}\frac{K_0}{2\beta}\left[\frac{1+\alpha(1-A)+L\alpha^2}{\alpha(1-A\alpha)}\right]d\alpha \tag{15}$$

hich becomes after integration

$$(\alpha')=\frac{K_0}{2\beta}\left[\left(\frac{L}{A^2}+\frac{1}{A}\right)\times \log_e\frac{[1-A(\alpha'-\beta)]}{[1-A(\alpha'+\beta)]}+\log_e\frac{\alpha'+\beta}{\alpha'-\beta}-\frac{2L\beta}{A}\right] \tag{16}$$

quation 16 is a minimum with respect α' when

$$'=\frac{A-[(A+L)+\beta^2(A^2-A-L)^2]^{1/2}}{A^2-A-L} \tag{17}$$

α_0' satisfies the inequality

$$\leq\alpha_0'\leq\frac{1}{A}-\beta \tag{18}$$

If inequality 18 is not satisfied, a lution may exist but the fact that the se is infinite outside the limits of ability must be considered. If β is too large, there is no solution and an infinite mse results independent of α.

For small β, i.e., small tolerances, an expansion of equation 17 in a power series in β yields

$$\alpha_0'=\frac{1}{A+(A+L)^{1/2}}-\frac{(A^2-A-L)}{2(A+L)^{1/2}}\beta^2+\frac{(A^2-A-L)^3}{8(A+L)^{3/2}}\beta^4-\ldots \tag{19}$$

For $\beta=0$, it is seen that $\alpha_0'=\alpha_0$.

The results of the calculations in connection with this problem are shown in graphical form in Figs. 2 through 4 for the case where the two time constants T_1 and J/K_2 are equal (as assumed in the original problem[11]) From equation 8 it is seen that, for this case, the parameter A has the numerical value 0.25. To consider reasonable values of L, the ratio S_0 to N_0 was taken to be 4.0 seconds^{-2}. (The choice of the ratio S_0 to N_0 has been previously made by Newton, et al.[12]) For this ratio and for typical time constants in the range 0.05–1.0 second, the parameter L lies in the range 0.0625 to 25.0.

In Fig. 2, the optimum nominal value α_0' of the parameter α is plotted versus the half-width β of the density function of equation 14, for $L=0$, 0.2, 1.0, 5.0, and 25.0. The optimum value α_0' increases with an increase in β. It should be noted that the y-axis intercepts are the optimum values α_0 for the ideal case. Fig. 3 gives the same information as Fig. 2 except that the ordinate is the percentage change in the optimum value α_0' from its value for ideal components. The largest percentage change in α_0' for a fixed β occurs for the largest value of the parameter L.

Fig. 4 shows, for the same five values of L, the percentage increase in average mse as a function of the tolerance parameter β. It can be seen that large tolerances (large values of β) are required to give appreciable error since the feedback system is relatively insensitive to gain variations. It should be kept in mind that the average mse has been calculated on the assumption that the optimum value of α, i.e., α_0' given by equation 17, is used in the system. For any other value of α, e.g., α_0 given by equation 12, the average mse would necessarily be greater.

Conclusions

A method has been presented for the minimum mean-squared error synthesis of systems built from components with associated tolerances or drift characteristics. The departures of component values from their nominal values have been treated as random variables. Synthesis is shown to involve not only the signal and noise power spectral densities, as in the usual case where the component values are assumed to be exact, but also the density functions characterizing component value variations.

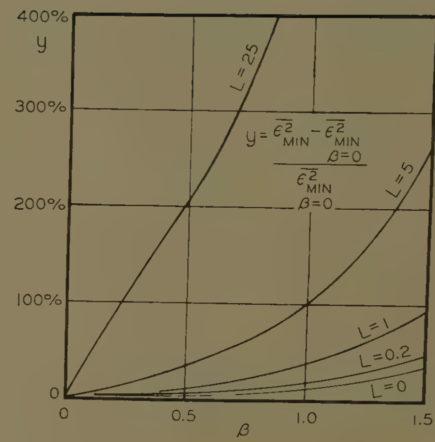

Fig. 4. Percentage increase in mean-squared error as function of half-width of density function

Appendix

From equation 2, the average mse $\overline{\epsilon_a^2}$ can be written in terms of the mse $\overline{\epsilon^2}$ for ideal components as

$$\overline{\epsilon_a^2}(\alpha_1',\ldots,\alpha_q')=\int_{-\infty}^{\infty}\ldots\int_{-\infty}^{\infty}\times\ \overline{\epsilon^2}(\alpha_1,\ldots,\alpha_q)\left[\prod_{j=1}^{q}p(\alpha_j,\alpha_j')d\alpha_j\right] \tag{20}$$

Let the quantity $g(\alpha_1',\ldots,\alpha_i,\ldots,\alpha_q')$ be defined by

$$g(\alpha_1',\ldots,\alpha_i,\ldots,\alpha_q')\triangleq\int_{-\infty}^{\infty}\ldots\int_{-\infty}^{\infty}\times\ \overline{\epsilon^2}(\alpha_1,\ldots,\alpha_q)\left[\prod_{\substack{j=1\\j\neq i}}^{q}p(\alpha_j,\alpha_j')d\alpha_j\right] \tag{21}$$

Then, equation 20 can be written

$$\overline{\epsilon_a^2}(\alpha_1',\ldots,\alpha_q')=\int_{-\infty}^{\infty}g(\alpha_1',\ldots,\alpha_i,\ldots,\alpha_q')p(\alpha_i,\alpha_i')d\alpha_i \tag{22}$$

The average mse will be a minimum with respect to the variables $\alpha_1',\ldots,\alpha'_q$, when

$$\frac{\partial\overline{\epsilon_a^2}}{\partial\alpha_k'}=0\qquad k=1,2,\ldots,q \tag{23}$$

If, in equation 22, the partial derivative of $\overline{\epsilon_a^2}$ is taken with respect to α_i', the result is

$$\frac{\partial\overline{\epsilon_a^2}}{\partial\alpha_i'}=\int_{-\infty}^{\infty}g(\alpha_1',\ldots,\alpha_i,\ldots,\alpha_q')\frac{\partial}{\partial\alpha_i'}[p(\alpha_i,\alpha_i')]d\alpha_i \tag{24}$$

Now, if $\overline{\epsilon^2}$ is symmetrical (the symmetry must be even since $\overline{\epsilon^2}$ is an extremum at α_{k0}) about the point $\alpha_k=\alpha_{k0}$ for $k=1,\ldots,q$, then $g(\alpha_1',\ldots,\alpha_i,\ldots,\alpha_q')$ has even

symmetry about the point $\alpha_i=\alpha_{i0}$ and can be expanded in the Taylor series

$$g(\alpha_1',\ldots,\alpha_i,\ldots,\alpha_q')=\sum_{m=0}^{\infty}\frac{(\alpha_i-\alpha_{i0})^{2m}}{(2m)!}\times\left[\frac{\partial^{2m}g}{\partial\alpha_i^{2m}}\bigg|_{\alpha_i=\alpha_{i0}}\right] \qquad (25)$$

From the binomial theorem, the term $(\alpha_i-\alpha_{i0})^{2m}$ can be written

$$(\alpha_i-\alpha_{i0})^{2m}=\sum_{n=0}^{2m}(\alpha_i-\alpha_i')^n(\alpha_i'-\alpha_{i0})^{2m-n}\frac{(2m)!}{(2m-n)!n!} \qquad (26)$$

The substitution of equations 25 and 26 into equation 24 results in

$$\frac{\partial\overline{\epsilon_a^2}}{\partial\alpha_i'}=\sum_{m=0}^{\infty}\left[\frac{\partial^{2m}g}{\partial\alpha_i^{2m}}\bigg|_{\alpha_i=\alpha_{i0}}\right]\times\sum_{n=0}^{2m}\frac{(\alpha_i'-\alpha_{i0})^{2m-n}}{(2m-n)!n!}\int_{-\infty}^{\infty}(\alpha_i-\alpha_i')^n\frac{\partial}{\partial\alpha_i'}[p(\alpha_i,\alpha_i')]d\alpha_i \qquad (27)$$

If $p(\alpha_i, \alpha_i')$ is symmetrical about the point $\alpha_i=\alpha_i'$, then the integral

$$\int_{-\infty}^{\infty}(\alpha_i-\alpha_i')^n\frac{\partial}{\partial\alpha_i'}[p(\alpha_i,\alpha_i')]d\alpha_i$$

is equal to zero for even values of n. Thus equation 27 can be expanded:

$$\frac{\partial\overline{\epsilon_a^2}}{\partial\alpha_i'}=a_1(\alpha_i'-\alpha_{i0})+a_3(\alpha_i'-\alpha_{i0})^3+a_5(\alpha_i'-\alpha_{i0})^5+\ldots \qquad (28)$$

It is apparent from this expression that a root of

$$\frac{\partial\overline{\epsilon_a^2}}{\partial\alpha_i'}=0 \qquad (29)$$

is $\alpha_i=\alpha_{i0}$. In other words, the optimum value of α_i' (which is written α_{i0}') is equal to α_{i0}.

Since the index i is arbitrary, it is true that $\alpha_{i0}'=\alpha_{i0}$ for $i=1, 2, \ldots, q$, which is the desired result.

References

1. Theory of Servomechanisms (book), H. [...] James, L. B. Nichols, R. S. Phillips. McGra[w-]Hill Book Company, Inc., New York, N. Y., 19[..] chaps. 6–8.

2. Probability Criterion for the Design [of] Servomechanisms, J. R. Ragazzini, L. A. Zade[h]. *Journal of Applied Physics*, New York, N. [Y.,] vol. 20, Feb. 1949, pp. 141–44.

3. Application of the Statistical Techniq[ue] to the Servomechanism Field, M. J. Pelegr[in]. *Automatic and Manual Control*, Butterwor[ths] Scientific Publications, London, England, 19[..] pp. 123–37.

4. The Determination of the Best Form [of] Response for a Servo, S. Jones. *Ibid.*, [pp.] 139–58.

5. Control System Synthesis (book), J. [G.] Truxal. McGraw-Hill Book Company, chaps. 7,[..]

6. Random Processes in Automatic Contr[ol] (book), J. H. Laning, Jr., R. H. Battin. McGra[w-]Hill Book Company, Inc., 1956.

7. Analytic Design of Linear Feedba[ck] Controls (book), G. C. Newton, Jr., L. A. Gou[ld], J. F. Kaiser. John Wiley & Sons, Inc., New Yo[rk,] N. Y., 1957.

8. *Ibid.*, Appendix E.

9. See reference 1, pp. 321–28.

10. *Ibid.*, p. 299.

11. *Ibid.*, pp. 326–27.

12. See reference 7, p. 398.

On the Design of A-C Servo Lead Networks

GERALD WEISS
MEMBER AIEE

PARALLEL-T and bridged-T *R-C* (resistance-capacitance) networks are often used for the lead compensation of carrier-type servomechanisms. Presently available design methods require the use of cumbersome charts and do not readily permit evaluation of the relative gain. This paper carries out an analysis based on considerations of realizability. For each type of structure a realizability curve is determined. The analysis leads to equations relating the zero-frequency gain of the *R-C* networks to that of the *R-L-C* (where *L* is inductance) resonant damper. Finally, a very simple design method is derived, based on the conventional low-pass prototype, with no curves required.

The Bilinear Compensating Function

A great many feedback compensation problems can be handled by the bilinear transfer function or doublet

$$G(p)=k\frac{p+a}{p+b} \qquad (1)$$

called a leading doublet for $a<b$ and a lagging doublet for $b<a$. The function is easily realized by the simplest electric network, a single *R-C* L-section. For the lead network the maximum value of the constant multiplier k is unity; for the lag network it is b/a. Viewed in the complex plane, the lead network is used as a cancellation network; i.e., the zero at $(-a)$ is used to cancel the most objectionable real axis pole of the loop transmission. The lag network is used as a dipole close to the origin in type 1 control systems; it does not affect the root loci except in a minor way, but it increases the zero-frequency gain.

For purposes of design, the frequency response point of view is probably more practical. At real frequencies $p=j\omega$, the network function becomes

$$G(j\omega)=k\frac{a+j\omega}{b+j\omega} \qquad (2)$$

The phase angle θ of $G(j\omega)$ is related to frequency by

$$\tan\theta=\frac{\omega(b-a)}{ab+\omega^2} \qquad (3)$$

The maximum phase angle occurs at

$$\omega_m=\sqrt{ab}$$

and equals

$$\tan\theta_m=\frac{b-a}{2\sqrt{ab}}=\frac{1}{2}\left(\sqrt{\frac{b}{a}}-\sqrt{\frac{a}{b}}\right)$$

The zero-frequency gain of the lead ne[t]work is a/b, and the infinite-frequen[cy] gain of the lag network function is $b/[a]$. Hence the behavior of these networks [is] completely determined by the frequen[cy] span a/b and the (geometric) center f[re]quency $\sqrt{ab}$.

In the frequency domain, the se[ries] lag network is basically a low-pass filt[er,] its ultimate purpose being to reduce t[he] gain at phase crossover without affecti[ng] the latter. The phase lag of the netw[ork] interferes with this stabilizing acti[on.] Hence the attenuation must be int[ro]duced at a very low frequency. As [...]

Paper 61-14, recommended by the AIEE Feedb[ack] Control Systems Committee and approved by [the] AIEE Technical Operations Department [for] presentation at the AIEE Winter General Meeti[ng,] New York, N. Y., January 29–February 3, 19[61.] Manuscript submitted May 23, 1960; made av[ail]able for printing November 7, 1960.

Gerald Weiss is with the Polytechnic Instit[ute] of Brooklyn, Brooklyn, N. Y.

This work is an extract from the dissertat[ion] "Carrier-Frequency Networks" submitted in par[tial] fulfillment of the requirements for the degree [in] Electrical Engineering at the Polytechnic In[sti]tute of Brooklyn. The dissertation was sup[er]vised by Dr. John G. Truxal, whose encourageme[nt] and support are gratefully acknowledged. [The] research on which the paper is based was carri[ed] out at the Microwave Research Institute and [was] supported by the U. S. Air Force, Rome [Air] Development Center, under Contract *AF-30(60[2])-1648.*

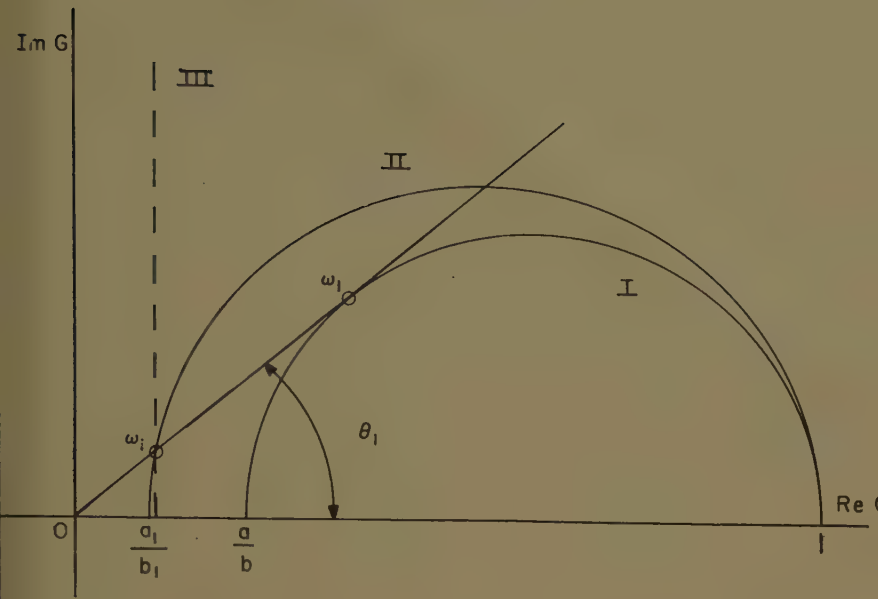

Fig. 1. Comparison of lead networks on basis of gain

I—"Optimum" low-pass prototype $G(j\omega)=\frac{j\omega+a}{j\omega+b}$

II—Modified low-pass prototype $G_1(j\omega)=\frac{j\omega+a_1}{j\omega+b_1}$

III—Approximation $G_1(j\omega)=\frac{j\omega+a_1}{b_1}$

xample, consider a simple instrument ervomechanism with a mechanical time onstant of 1/30 second. The lag net-ork values of a and b should be about 3 adians per second and 0.3 radian per sec-nd respectively.

The lead network is used to reduce the hase lag at gain crossover; hence the alues a and b straddle the crossover oints. The compensation requirements re then usually couched in the following orm: We require θ_1 degree of phase lead t ω_1 radians per second. In other words, ust one point on the frequency charac-eristics of the network is specified.

Equation 3 then becomes a relationship etween the unknown network parameters and b and the specified θ_1 and ω_1. his is one equation in two unknowns, ence the required θ_1 and ω_1 are satisfied y an infinite number of networks, e.g., urves I and II of Fig. 1. All these net-orks have phase lead θ_1 at frequency ω_1, ut they differ in their maximum achiev-ble phase lead and in their zero-frequency ain. Out of the infinity of networks here is one (Fig. 1, curve I) which accom-lishes the desired phase lead in the most conomical way, with the maximum zero-equency gain; this network has its *aximum* phase lead at the desired fre-uency. θ_1 and ω_1 are then given by quations 4 and 5 respectively, and these re the design formulas for a d-c lead net-work. Solving for θ_1 and ω_1 yields

$$\frac{a}{b}=\frac{1-\sin\theta_1}{1+\sin\theta_1} \tag{6}$$

$$a=\omega_1\frac{1-\sin\theta_1}{\cos\theta_1} \tag{7A}$$

$$b=\omega_1\frac{1+\sin\theta_1}{\cos\theta_1} \tag{7B}$$

A-C Compensating Networks

Compensating networks for a-c servos must have an *envelope* transfer function of the form of equation 1. It is readily shown[1] that a linear network cannot have such a transfer function. The familiar low-pass band-pass transformation

$$\frac{p}{\omega_c}=\frac{1}{2}\left(\frac{s}{\omega_c}+\frac{\omega_c}{s}\right) \tag{8}$$

yields a realizable network with transfer function

$$G(s)=\frac{s^2+2as+\omega_c^2}{s^2+2bs+\omega_c^2} \tag{9}$$

The corresponding envelope transfer function is a biquartic, closely approximating the desired bilinear envelope function. In the case of the lead network, $a<b$, the biquartic function has one dominant zero near $(-a)$.[2]

The function represented in equation 9 is always physically realizable; an *R-L-C* realization can be immediately obtained from a low-pass prototype.[3] The practicability of the realization depends on the effective Q, which is $\omega_c/2b$ or $\omega_c/2a$ for lag and lead networks respectively. With the use of a 400-cps (cycle-per-second) carrier, the previous example would require Q's of the order of 4,000 for a lag network and 40 for a lead network. Hence a-c lag networks are completely ruled out, and lead networks are the only passive a-c compensating networks used in current a-c servo practice. Note that the wider the servo bandwidth, the lower the required Q, hence the easier the realization. These networks therefore find their main use in the compensation of wide-band servos; they ought to be called "wide-band" networks but, paradoxically, they are often referred to as "narrow-band" networks because the low-pass band-pass transformation is a "narrow-band transformation."

The usual *R-L-C* realization of the a-c lead network is shown in Fig. 2. An un-

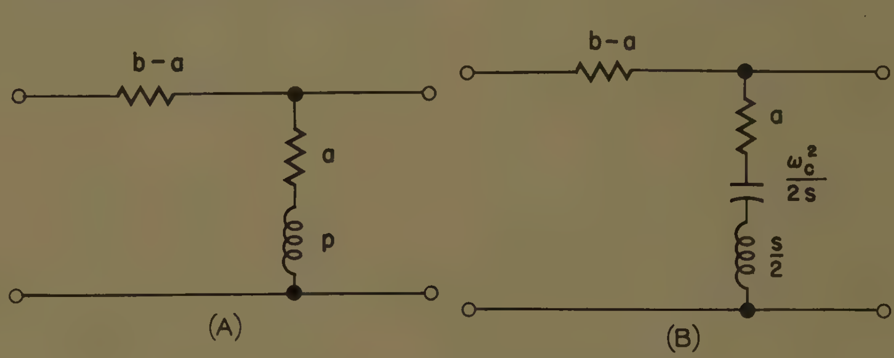

Fig. 2. R-L-C L-network realization

A—Low-pass prototype $G(p)=\frac{p+a}{+bp}$

B—A-c network $G(s)=\frac{s^2+2as+\omega_c^2}{s^2+2bs+\omega_c^2}$

coil $Q=\frac{\omega^2}{2a}$

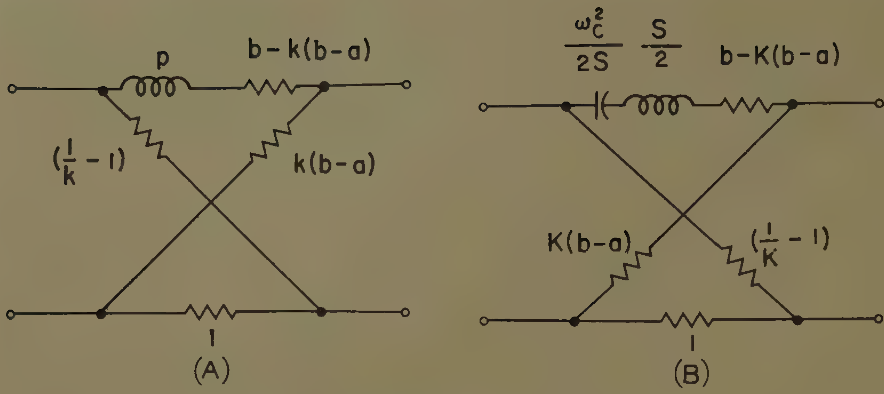

Fig. 3. Ungrounded R-L-C lead network[5]

A—Low-pass prototype

$$G(p)=k\frac{p+a}{p+b}$$

B—A-c network

$$G(s)=k\frac{s^2+2as+\omega_c^2}{s^2+2bs+\omega_c^2}$$

$$\text{coil } Q=\frac{\omega_c}{2[b-k(b-a)]}$$

grounded network with lower coil Q and smaller multiplier k, first described by McDonald,[4] is shown in Fig. 3.

In quantitative terms, a useful measure of the required lead network bandwidth would be the ratio of servo bandwidth to the carrier frequency. The frequency at which the desired phase lead θ_1 is specified is of the same order as the servo half-power frequency. Hence it is plausible to use as a measure of network "relative bandwidth" the ratio ω_1/ω_c. For the optimum lead network (maximum gain) ω_1 is given by $\sqrt{ab}$. The following normalized quantities will be useful in the subsequent analysis:

$$\alpha=\frac{a}{b}=\text{zero-frequency gain} \tag{10}$$

$$\beta=\frac{\sqrt{ab}}{\omega_c}=\text{relative bandwidth} \tag{11}$$

R-C Lead Networks

Function 9 is R-C realizable when the poles are real, i.e., for $b>\omega_c$, which is equivalent to

$$\beta>\sqrt{\alpha} \tag{12}$$

The carrier frequency ω_c must be larger than the lower corner frequency a. Hence the relationship between all the coefficients is

$$a<\omega_c<b \tag{13}$$

This makes the zeros of $G(s)$ complex, so that the function is not realizable as a simple ladder. If the function is minimum phase ($a\geq 0$), the only case considered here, the network design can be carried out by Dasher's procedure[5] and the resulting structure is a 7-element bridged-parallel-T network.

For the simpler structures in common use, the 4-element bridged-T and the 6-element parallel-T, condition 12, is no longer sufficient; larger values of b are required. The determination of the realizability conditions of these various networks forms the subject of this section. In the (α, β) plane, the curve

$$\beta=\sqrt{\alpha} \tag{14}$$

forms the boundary between the R-L-C and R-C regions. The boundaries of the bridged-T and parallel-T regions are defined by other equations in α and β. Finally, each specific structure, e.g., the symmetrical bridged-T, or the parallel-T with three equal capacitors, is characterized by a realizability equation, an equation relating α and β or, alternatively, a, b, and ω_c.

The literature dealing with these simple bridged-T and parallel-T networks is considerable,[6] but apparently only Sobczyk[7] and Benner[8] have considered realizability. The presentation in this paper is based on Sobczyk.

Bridged-T Realizability

The bridged-T networks under con- sideration are shown in Fig. 4. Sobczyk has derived the parameters m and n b comparing the transfer function of thes networks with equation 9, term b term:

$$n=\frac{4a(b-a)-\omega_c^2}{\omega_c^2} \tag{15}$$

$$m=\frac{4(b-a)^2}{4a(b-a)-\omega_c^2} \tag{16}$$

$$T=RC=\frac{1}{2(b-a)} \tag{17}$$

For realizability, both m and n must b positive; hence

$$\omega_c^2<4a(b-a) \tag{18}$$

or

$$\beta>\frac{1}{2\sqrt{1-\alpha}} \tag{19}$$

Equation 19 is plotted in Fig. 5, to gether with equation 14. Any constrain placed on the bridged-T network, i.e., an specific relationship between the networ elements, defines a particular curve in th realizability region. For example, th symmetrical bridged-T is defined by $n=$ leading to

$$\omega_c^2=2a(b-a) \tag{20}$$

or

$$\beta=\frac{1}{\sqrt{2(1-\alpha)}} \tag{21}$$

This equation is also plotted in Fig The symmetrical bridged-T with eleme values is shown in Fig. 6.

Parallel-T Realizability

The transfer function of the parallel- network of Fig. 7 is a bicubic, rather tha a biquadratic. By comparing it term t term to the function

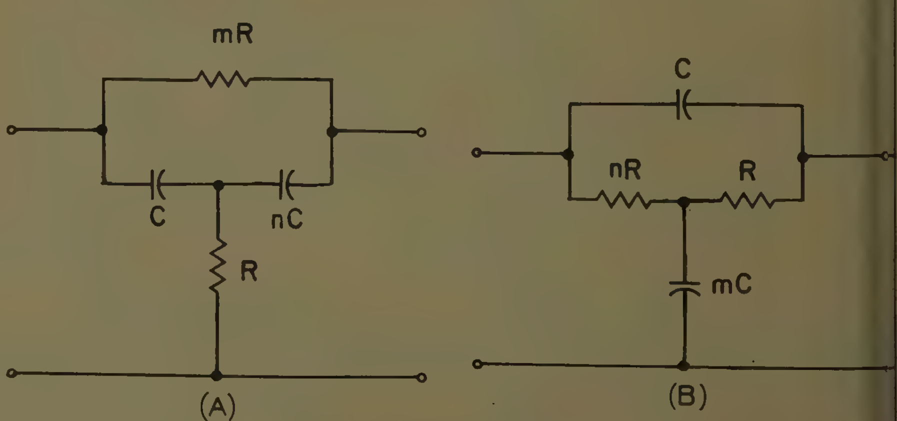

Fig. 4. Bridged-T networks

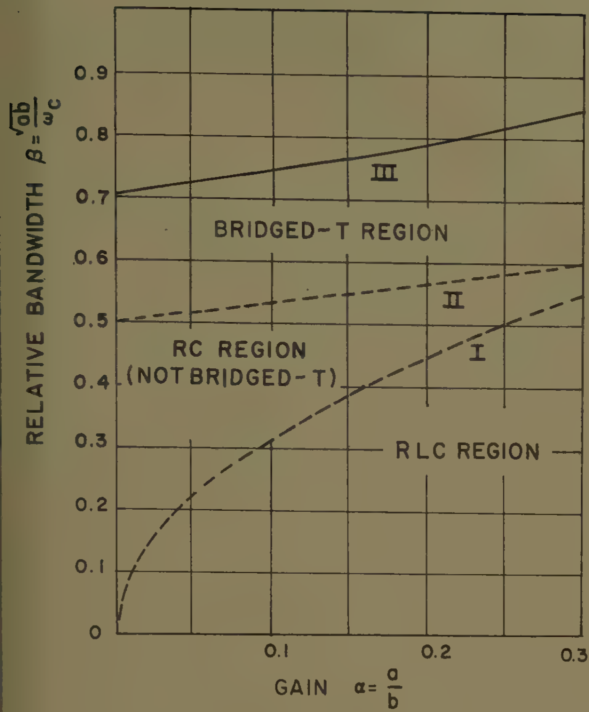

Fig. 5. Bridged-T realizability regions for

$$G(s)=\frac{s^2+2as+\omega_c^2}{s^2+2bs+\omega_c^2}$$

I—*R-L-C/R-C* boundary

$$\beta=\sqrt{\alpha}$$

II—Bridged-T boundary

$$\beta=\frac{1}{2\sqrt{1-\alpha}}$$

III—Symmetrical bridged-T curve

$$\beta=\frac{1}{\sqrt{2(1-\alpha)}}$$

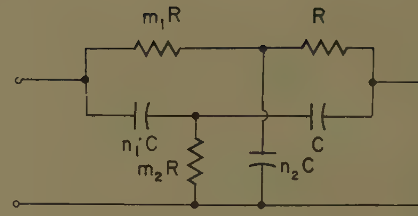

Fig. 7. Parallel-T network

$$G(s)=\frac{(s^2+2as+\omega_c^2)(s+N)}{(s^2+2bs+\omega_c^2)(s+N)} \tag{22}$$

Sobczyk has derived the value of the circuit elements.

$$T=RC=\frac{N}{\omega_c^2} \tag{23}$$

$$n_1=\frac{2(b-a)(2a+N)}{N^2+2aN+\omega_c^2}-1 \tag{24}$$

$$n_2=\frac{\omega_c^2}{N^2}\left[1+\frac{2aN}{\omega_c^2}-\frac{N^2+2aN+\omega_c^2}{2(b-a)N}\right] \tag{25}$$

$$\frac{1}{m_1}=\frac{2(b-a)(2aN+\omega_c^2)N}{(N^2+2aN+\omega_c^2)\omega_c^2}-1 \tag{26}$$

$$\frac{1}{m_2}=\frac{N}{\omega_c^2}\left[(2a+N)-\frac{N^2+2aN+\omega_c^2}{2(b-a)}\right] \tag{27}$$

For realizability all parameters must be positive. This establishes two inequalities:

$$f_1(N)=N^2-2(b-2a)N+[w_c^2-4a(b-a)]<0 \tag{28}$$

$$f_2(N)=[\omega_c^2-4a(b-a)]N^2-2(b-2a)\omega_c^2N+\omega_c^4<0 \tag{29}$$

To meet these inequalities, the parameter N must meet the following conditions

$$(b-2a)-\sqrt{b^2-w_c^2}<N<(b-2a)+\sqrt{b\ -\omega_c} \tag{30}$$

$$\frac{\omega_c^2}{(b-2a)+\sqrt{b^2-\omega_c^2}}<N<\frac{\omega_c^2}{(b-2a)-\sqrt{b^2-\omega_c^2}} \tag{31}$$

The biquadratic transfer function is realizable as a parallel-T if a parameter N can be found which satisfies simultaneously the two inequalities 30 and 31. It can be shown[2] that for

$$\omega_c^2-4a(b-a)<0 \tag{32}$$

a parallel-T realization is always possible. This is not an important case, however, since the simpler bridged-T structure is also realizable; see equation 18.

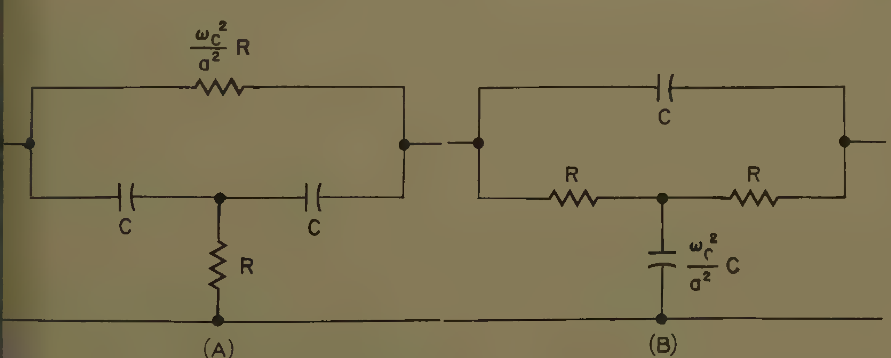

Fig. 6. Symmetrical bridged-T realization

$T=RC=a/\omega_c^2$

For the case of

$$\omega_c^2-4a(b-a)\geq 0 \tag{33}$$

the parallel-T structure is realizable for[2]

$$2\sqrt{a(b-a)}\leq\omega_c\leq\left(\frac{b}{2}-a\right)+\sqrt{\frac{b^2}{4}+ab-a^2} \tag{34}$$

or

$$\frac{\alpha}{(0.5-\alpha)+\sqrt{0.25+\alpha-\alpha^2}}<\beta<\frac{1}{2\sqrt{1-\alpha}} \tag{35}$$

Fig. 8 shows the realizability regions.

Realizability equations have been derived[2] for seven specific parallel-T networks shown in Fig. 9; the first six of these networks are taken from Sobczyk,[7] and the seventh from White.[9] The various equations are shown in Table I and plotted in Fig. 10, where the symmetrical bridged-T is also shown.

Bandwidth Limitations

Two facts emerge from the realizability curves of Fig. 10 and Table I: First, each network must obey a constraint between a, b, and ω_c. This is incompatible with the specifications, where the optimum a and b are determined directly by the specifications θ_1 and ω_1 (equations 6 and 7); the carrier frequency is independent of them.

Second, these specific constraints call for very large values of b and β. Consider the case $\alpha=0.1$, which corresponds to a maximum lead angle of 55 degrees; this is a very common specification. *R-C* realizability alone requires a β of 0.32. Realizability by a symmetrical parallel-T requires a β of 0.61, and a symmetrical bridged-T a β of 0.71. The latter figure would mean a 400-cps servo with crossovers in the vicinity of 300 cps. Such wide-band servos are never encountered in current practice.

It is concluded that *R-C* lead networks are not practically realizable if one insists on minimum zero-frequency attenuation. They can be realized, however, if one starts from a new low-pass prototype:

$$G_1(j\omega)=\frac{j\omega+a_1}{j\omega+b_1} \tag{36}$$

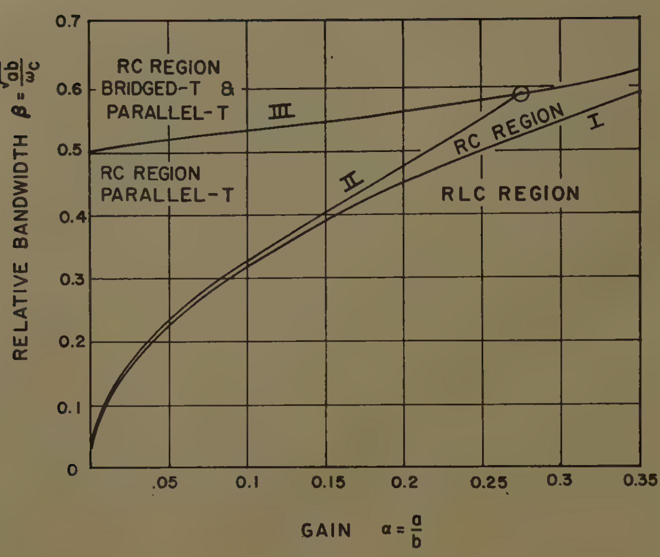

Fig. 8. Parallel-T realizability regions for

$$G(s)=\frac{s^2+2as+\omega_c^2}{s^2+2bs+\omega_c^2}$$

I—*R-L-C/R-C* boundary $\beta=\sqrt{\alpha}$

II—Parallel-T boundary

$$\beta=\frac{\sqrt{\alpha}}{(0.5-\alpha)+\sqrt{0.25+\alpha-\alpha^2}}$$

III—Bridged-T boundary

$$\beta=\frac{1}{2\sqrt{1-\alpha}}$$

as shown in Fig. 1. The value of b_1 can be made sufficiently large so that realizability by the desired network is achieved. The price paid is increased zero-frequency attenuation.

The transfer function of the a-c network is now

$$G(s)=\frac{s^2+2a_1s+\omega_c^2}{s^2+2b_1s+\omega_c^2} \tag{37}$$

New, normalized parameters α_1 and β_1 can be defined by reading equations 10 through 35, the relationships in Table I, the element values in Figs. 6 and 9, and the co-ordinate in Figs. 5, 8, and 10, in terms of a_1, b_1, α_1, and β_1.

Determination of Parameters

The problem now is to derive the values of a_1 and b_1 from the original specifications, the phase lead θ_1 at frequency ω_1. We start with the *two* low-pass prototypes of Fig. 1, the optimum prototype

$$G=\frac{j\omega+a}{j\omega+b} \tag{38}$$

and the modified prototype G_1 of equation 36. For G_1 the point (θ_1, ω_1) is merely *one* point on the curve; thus

$$\tan\theta_1=\frac{\omega_1(b_1-a_1)}{a_1b_1+\omega_1^2} \tag{39}$$

For G the point (θ_1, ω_1) is the point of *maximum* phase lead; thus

$$\tan\theta_1=\frac{b-a}{2\sqrt{ab}}=\frac{1}{2}\left(\sqrt{\frac{b}{a}}-\sqrt{\frac{a}{b}}\right) \tag{40}$$

and

$$\omega_1=\sqrt{ab} \tag{41}$$

Substituting equations 40 and 41 into equation 39 yields

$$\frac{\sqrt{ab}(b_1-a_1)}{a_1b_1-ab}=\frac{b-a}{2\sqrt{ab}} \tag{42}$$

Equation 42 must be solved simultaneously with the realizability equation for the particular structure, and this gives a relationship between the pairs (a, b) and (a_1, b_1). The equation so obtained is a cubic. To sidestep the difficulty of sol-

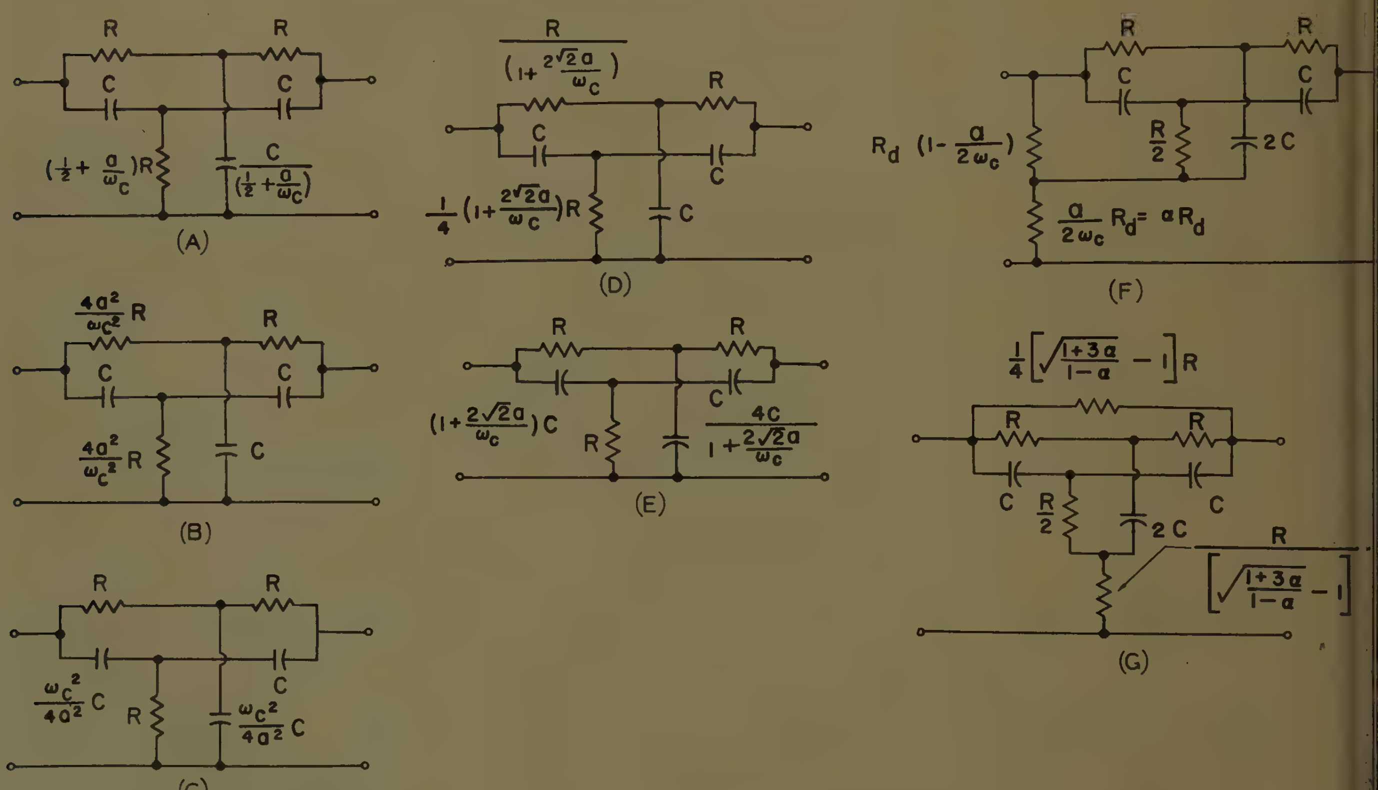

Fig. 9. Various parallel-T networks

A—Symmetrical parallel-T $T=1/\omega_c$

B—Degenerate case, three equal C's, two equal R's $T=1/2a$

C—Degenerate case, three equal R's, two equal C's $T=2a/\omega_c^2$

D—Three equal capacitors $T=\sqrt{2}/\omega_c$

E—Three equal resistors $T=1/\sqrt{2}\omega_c$

F—Full-rejection symmetrical parallel-T, by-passed with input divider $T=1/\omega_c$; $R_d \ll Z_{in}$

G—Full-rejection symmetrical parallel-T, by-passed with bridging resistor[9] $T=1/\omega_c$

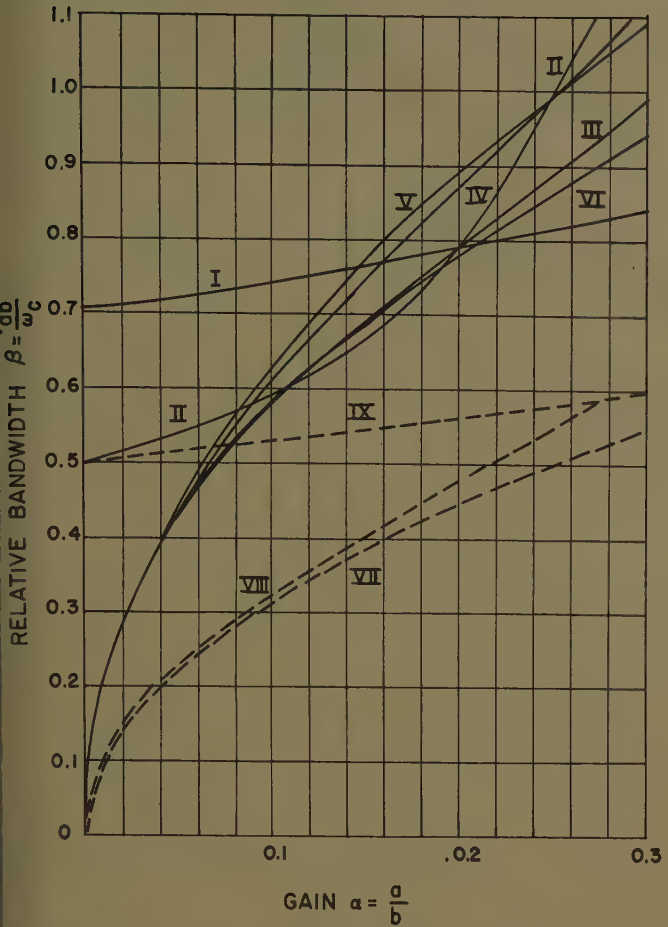

Fig. 10. Realizability curves for various R-C structures

I—Symmetrical bridged-T
II—Degenerate case, three equal C's and two equal R's, or three equal R's and two equal C's
III—Parallel-T, three equal C's or R's
IV—Symmetrical parallel-T
V—Full-rejection circuit with input divider
VI—Full-rejection circuit with bridging resistor[9]
VII—R-L-C/R-C boundary
VIII—Parallel-T boundary
IX—Bridged-T boundary

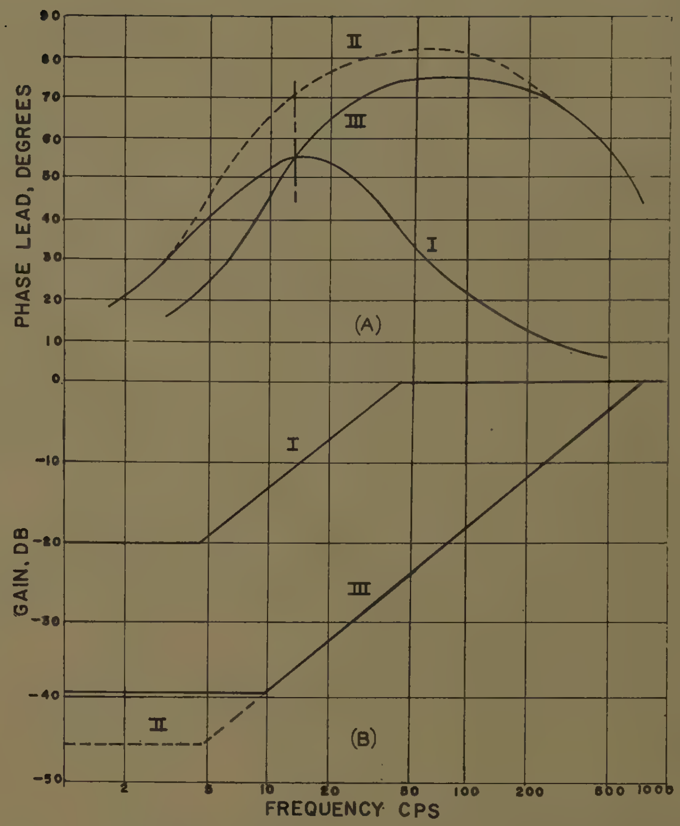

Fig. 11. Gain-phase curves for 55-degree phase lead at 15 cps, with 400-cps carrier
A—Asymptotic gain curves
B—Phase curves

I—R-L-C network
II—Symmetrical parallel-T with unmodified lower corner frequency
III—Symmetrical parallel-T, final design

Table I. Parallel-T Realizability Equations

Network	Condition on Parameters, Fig. 7	Circuit, Fig. 9	Realizability Equation	Realizability Curve, Fig. 10
mmetrical	$m_1=n_1=1$	A	$\beta=\dfrac{4\sqrt{\alpha}}{(1-3\alpha)+\sqrt{1+10\alpha-7\alpha^2}}$	IV
qual C's and 2 equal R's	$n_1=n_2=1$; $m_1=m_2$	B	$\beta=\dfrac{1}{2\sqrt{1-3\alpha}}$	II
qual R's and 2 equal C's	$m_1=m_2=1$; $n_1=n_2$	C	$\beta=\dfrac{1}{2\sqrt{1-3\alpha}}$	II
qual C's	$n_1=n_2=1$	D	$\beta=\dfrac{3\sqrt{2\alpha}}{(1-3\alpha)+\sqrt{1+18\alpha-15\alpha^2}}$	III
qual R's	$m_1=m_2=1$	E	$\beta=\dfrac{3\sqrt{2\alpha}}{(1-3\alpha)+\sqrt{1+18\alpha-15\alpha^2}}$	III
ll-rejection, input divider		F	$\beta=2\sqrt{\alpha}$	V
ll-rejection, bridged[9]		G	$\beta=\dfrac{2\sqrt{\alpha}}{\sqrt{(1-\alpha)(1+3\alpha)}}$	VI

ing the cubic, consider first a simpler equation obtained by assuming $b_1 >> b$, so that

$$G_1=\frac{j\omega+a_1}{b_1} \tag{43}$$

$$\tan\theta_1=\frac{\omega_1}{a_1} \tag{44}$$

The corresponding polar plot is the dashed line of Fig. 1. Substituting equations 40 and 41 into equation 44 yields

$$\frac{b-a}{2\sqrt{ab}}=\frac{\sqrt{ab}}{a_1} \tag{45}$$

or

$$a_1=\frac{2ab}{b-a}=\frac{2a}{1-\dfrac{a}{b}}=\frac{2a}{1-\alpha} \tag{46}$$

for

$$\frac{a}{b}\ll 1 \qquad a_1\approx 2a \tag{47}$$

Equation 47 yields the remarkable result that the lower corner frequency of the optimum low-pass prototype ought to be doubled. The physical significance

is this: With the optimum prototype a set of values a and b can be found for a given maximum phase lead θ_1 at the modulating frequency ω_1. If one now increases the *upper* corner frequency b merely to obtain *R-C* realizability, the new phase lead at the frequency ω_1 will be somewhat larger. This excess of phase lead is not harmful, but it is obtained at the cost of additional attenuation, the zero-frequency gain being a/b. The surplus phase lead is traded in for gain by increasing the *lower* corner frequency a.

As a numerical example, consider a 400-cps carrier-frequency servo to be compensated by 55 degrees of phase lead at 15-cps modulating frequency. The corner frequencies of the optimum low-pass prototype are at $a=4.74$ cps and at $b=47.4$ cps, for a zero-frequency gain α of 0.1. If the value of the upper corner frequency b is now changed to 800 cps for symmetrical parallel-T realizability, the new phase lead at 15 cps will be 71.1 degrees, much larger than required. By increasing the lower corner frequency a to 9.48 cps the phase lead at 15 cps becomes 55.7 degrees, close to the desired value. The corresponding gain and phase-versus-frequency curves are shown in Fig. 11.

The results obtained have been based on a simplified analysis using $b_1 >> b$. A more exact analysis requires simultaneous solution of equation 42 with the appropriate realizability equation. The resulting sets of cubics have been plotted and analyzed.[2] For servo parameters encountered in current practice, say $\alpha<0.25$ and $\beta<0.25$, one again obtains the approximate relationship $a_1=2a$.

It is also to be noted that the phase lead calculations are based on the low-pass prototype, not on the exact envelope transfer function. This approximation yields slightly optimistic results. The true envelope lead is somewhat smaller than the number indicated by the low-pass prototype, but the error is less than 0.5 degree for the modulating frequency ranges used in current servo practice.[2]

Relative Gain

The *R-C* networks are obtained only at the expense of zero-frequency gain. It appears highly desirable to be able to determine the relative gain of various types of network structures in advance of carrying out the detailed network design. This information is obtained from the ratio α_1/α, the ratio of relative gain for a particular *R-C* network to the maximum relative gain obtainable with the *R-L-C* network. The ratio α_1/α can again be obtained in a rigorous way by analysis of the cubics resulting from simultaneous solution equation 42 with the realizability equations.[2] A simpler and equally valid procedure is to solve the realizability equations simultaneously with the use of equation 47.

Bridged-T

From equation 18 the realizability equations for the family of 4-element bridged-T networks is

$$\omega_c^2=ha_1(b_1-a_1) \tag{48}$$

where $h<4$ for bridged-T realizability; for the symmetrical bridged-T h is 2. Rearranging this equation yields

$$\alpha_1=\frac{ha_1^2}{ha_1\ +\omega_c^4} \tag{49}$$

Substituting equation 47 into equation 49 yields

$$\alpha_1=\frac{4ha^2}{4ha\ +\omega_c^2}=\frac{4h\alpha\beta^2}{4h\alpha\beta^2+1}\approx 4h\alpha\beta^2 \tag{50}$$

Hence

$$\frac{\alpha_1}{\alpha}=4h\beta^2 \tag{51}$$

For the symmetrical bridged-T

$$\frac{\alpha_1}{\alpha}=8\beta^2 \tag{52}$$

Parallel-T

In Table I and Fig. 10 all parallel-T's except curve II (which behaves similarly to the bridged-T and is therefore of no practical interest) are characterized by the approximate realizability relationship

$$h\beta_1=\alpha_1 \tag{53}$$

where $h<1$ for parallel-T realizability; for the symmetrical structures h is 1/2 and for the three equal R's and C's, h is $\sqrt{2}/3$. Equation 53 can also be written

$$\omega_c=hb_1 \tag{54}$$

Combining equations 47 and 54 yields

$$\frac{a_1}{b_1}=\frac{2ha}{\omega_c}=2h\sqrt{\alpha\beta} \tag{55}$$

Hence

$$\frac{\alpha_1}{\alpha}=\frac{2h\beta}{\sqrt{\alpha}} \tag{56}$$

and for the symmetrical parallel-T's

$$\frac{\alpha_1}{\alpha}=\frac{\beta}{\sqrt{\alpha}} \tag{57}$$

Comparison

The relative zero-frequency gain of *R-L-C* versus symmetrical parallel-T versus symmetrical bridged-T is obtained from equations 57 and 52:

$$1 \text{ to } \frac{\beta}{\sqrt{\alpha}} \text{ to } 8\beta^2 \tag{58}$$

As a numerical example, take the case of a 400-cps servo, with a 55-degree phase lead required at 40 cps. This is equivalent to $\alpha=\beta=0.1$. The relative gain of the three networks is 12.5 to 4 to 1. The lower the bandwidth, the more unfavorable the ratio for the *R-C* networks but, of course, the larger the Q of the *R-L-C* network. The Q for the conventional resonant damper which is given in Fig. 2, with maximum zero-frequency gain, is

$$Q=\frac{\omega_c}{2a}=\frac{1}{2\sqrt{\alpha\beta}} \tag{59}$$

For the above numerical case, the Q is 16.

Network Design

The network design requires the following steps:

1. Calculate α and β from the specifications.
2. Determine the relative gain of the various types of structures using equation 58. Determine the Q of the *R-L-C* damper using equation 59.
3. Decide on type of structure to be used, decision to be based on results of step 2 plus other factors, such as availability and price of components, structural factors, environmental factors, etc.

For the *R-L-C* network the remaining steps are:

4. Determine a and b from the specifications, using equations 6 and 7.
5. See network element values in Fig. 2 within a constant multiplier.
6. Determine desired impedance level and multiply all element impedance by the appropriate factor.

For the *R-C* networks, the remaining steps are:

4. Determine a_1 from the specification, using equations 7(A) and 47.
5. See appropriate network element values in Fig. 6 and Figs. 9(A), (D), (E), (F), and (G). Element values given within a constant multiplier.
6. Determine desired impedance level and multiply all impedances by appropriate constant. Equations for impedances of *R-C* networks are given by Sobczyk.[7]

Concluding Remarks

Previous design methods are based on frequency response curves,[10] with normalization carried out in terms of "notch ratio" (equivalent to α in this paper) and "notch width." These methods are

ther cumbersome and do not permit lvance determination of the relative gain chievable by the various structures. sing the analytic methods here prented, an equation for relative zeroequency gain is derived, for *R-L-C* ersus parallel-T versus bridged-T. A ecision on which network is to be used an then be based on all the pertinent chnical and economic factors, without e need for extensive tentative designs. nce this decision has been made, the tual network design is almost trivially mple: from the specifications one degns a low-pass prototype as one would r a d-c servo, calculating the *lower* corner equency only. This value is doubled. he upper corner frequency is not needed; is automatically determined by the oice of structure. The accuracy of the sign procedure is well within that reired by the usual phase lead specificaon.

The symmetrical networks considered this paper have realizability curves hich lie well within the interior of the spective realizability regions; see Figs. and 10. It might be argued that asymetrical networks located closer to the undaries are superior. Equations 51 and 56 indicate a possible doubling of relative gain for asymmetrical networks. Unfortunately, however, the input and/or output impedances of the networks become zero or infinite on the realizability boundary.[7] Hence the actual transmission of these asymmetrical networks is likely to be smaller than that of the symmetrical networks. This does not show up in the present analysis where both generator and load impedances have been neglected.

The assumption of zero source impedance and infinite load impedance is not an unreasonable one when the actual load impedance is at least one or two orders of magnitude larger than the source impedance. This condition is not always met in practice; for example, many transistor amplifier and magnetic-amplifier circuits have low input impedance. An exact analysis taking into account both source and load impedance can be expected to show that the zero-frequency transmission is maximized by using an asymmetrical network. However, the optimum is not likely to be very sharp, and the symmetrical structures considered in this paper have at least the merit of simplicity and economy.

References

1. On the Design of A-C Networks for Servo Compensation, Harold Levenstein. *Transactions*, Professional Group on Automatic Control, Institute of Radio Engineers, New York, N. Y., vol. PGAC-2, Feb. 1957, pp. 39–55.
2. Carrier Frequency Networks, Gerald Weiss. *Report R-701-58, PIB-629*, Microwave Research Institute, Polytechnic Institute of Brooklyn, Brooklyn, N. Y., Jan. 1959.
3. Automatic Feedback Control System Synthesis (book), John G. Truxal. McGraw-Hill Book Company, Inc., New York, N. Y., 1955, chap. 6, pp. 401–06.
4. Improvements in the Characteristics of A-C Lead Networks for Servomechanisms, Donald McDonald. *AIEE Transactions*, vol. 69, pt. I, 1950, pp. 293–300.
5. John G. Truxal, *op. cit.*, chap. 3, pp. 203–18.
6. Carrier Compensation for Servomechanisms, H. E. Blanton. *Journal*, Franklin Institute, Philadelphia, Pa., vol. 250, 1950, pp. 391–407; 525–42. (Bibliography gives an extensive listing of papers on bridged-T and parallel-T networks.)
7. Stabilization of Carrier-Frequency Servomechanisms. II. Design Formula for Proportional-Derivative Networks, Andrew Sobczyk. *Ibid.*, vol. 246, 1948, pp. 95–121.
8. Phase Lead for A-C Servo Mechanisms, Arthur H. Benner. *Journal of Applied Physics*, New York, N. Y., vol. 20, 1949, pp. 268–73.
9. Transfer Characteristics of a Bridged Parallel-T Network, Charles F. White. *Report no. R-3167*, Naval Research Laboratory, Washington, D. C., Aug. 1947. (Available from U. S. Department of Commerce as OTS No. PB-106,744.)
10. Basic Feedback Control System Design (book), C. J. Savant, Jr. McGraw-Hill Book Company, Inc., 1958, Appendix IX, pp. 393–405.

Discussion

lph J. Kochenburger (University of onnecticut, Storrs, Conn.): This paper rforms an excellent service, both of mmarizing methods of carrier compensan and of proposing new and practical teria that might be used in design. The agrams shown in the author's Figs. 5, 8, d 10 are of special interest to the designer cause they point out the regimes of operan where certain specific types of carrier mpensation networks will prove to be e most practical.

This discusser wishes to call attention to me additional considerations that should kept in mind by engineers planning to e these techniques:

1. The author refers to the common e of phase lead networks as cancellation tworks. This viewpoint is a common e and has the advantage of providing nple mathematics once an objectionable le has been cancelled and replaced by other pole of lower time constant. Hower, the optimum selection of the comnsating zero (the *b* in the author's notan); i.e. of the low-frequency break point, es not always correspond to exact canlation. Very often, it is found that a ver *b* (i.e. higher low-frequency break nt) than that corresponding to pure ncellation will be desirable.

2. In the author's brief discussion of ase lag compensation he states that such npensation has a minor effect on the root i. Actually, the root loci are modified such networks in a very significant way. The low-gain portion of the loci are swung toward the imaginary axis; a conditional degree of stability is caused; and if the designer fails to take advantage of the gain increase afforded him by the use of such networks, a slow response with very poor damping will result.

3. Again, with reference to phase lag compensation, the difficulties stated by the author are true but are not the only reasons why carrier compensation is impractical for this purpose. A very important consideration is that of carrier-frequency shift. Phase lag networks are especially sensitive to such shifts because of the very small notch widths involved. Notthoff[1] has shown how carrier shifts can cause poor operation when they become an appreciable fraction of the notch width. For example, a typical notch width associated with phase lag compensation rarely would exceed 0.1 cps; 400-cps carrier sources with a frequency regulation better than 0.1 cps are "few and far between."

4. Probably the most significant point that should be added to the author's statements is that operation at high relative bandwidths is undesirable even though, paradoxically, such operation would present the least difficulty from the standpoint of network synthesis—because of the data-sampling effect of carrier data transmission. This effect is somewhat similar to discrete data sampling although it is more difficult to analyze. As in the instance of discrete data sampling, useful control information cannot be transmitted when the signal frequency becomes too high a fraction of the carrier frequency. In practice, a β of 0.3 is a good practical upper limit. For example, if a servo bandwidth of 300 cps were desired, 400-cps carrier would no longer be adequate and at least 1 kc would be recommended. Because of this, the practical regimes of carrier compensation will fall in the region of $\beta<0.3$. From the author's conclusions, this would correspond to the recommended use of *R-L-C* and parallel-T forms of compensating networks.

5. Even phase-lead carrier compensation networks are subject to carrier frequency shift, although not as severely as the phase lag networks. Superposed on this difficulty are the other practical design difficulties mentioned by the author. The necessity of finding very high Q inductive elements when *R-L-C* schemes are employed and of accepting excessive attenuation at zero frequency when parallel-T and other *R-C* networks are employed are important disadvantages. For this reason, I must admit that I have developed a prejudice against carrier compensation in general. Fortunately, in most problems encountered, it has been possible to avoid the issue. Usually some method has been available whereby, without the introduction of excessive new hardware, noncarrier compensation of both phase lag and phase lead types can be introduced in a-c servos. Most often this has been accomplished by feedback methods of compensation.

Reference

1. Phase Lead for A-C Servo Systems with Compensation for Carrier Frequency Changes, Arthur P. Notthoff, Jr. *AIEE Transactions*, vol. 69, pt. I, 1950, pp. 285–92.

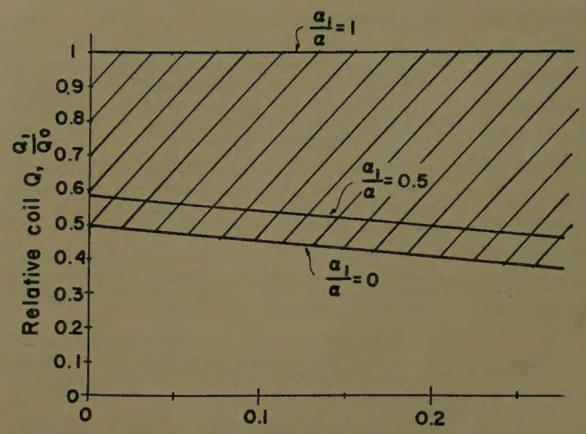

Fig. 12 (left). Realizability region for reduced coil Q

Fig. 13 (right). Relative gain versus relative coil Q for resonant damper

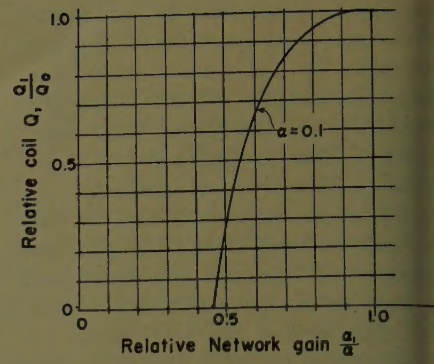

Gerald Weiss: Dr. Kochenburger's compliments are gratefully appreciated, and his additions and corrections are very much to the point.

Inasmuch as the effect of carrier frequency shift on these networks depends on their notch width, a large notch width becomes desirable. In that respect, then, the bridged-T network is the best, the parallel-T network follows, and the *R-L-C* damper is the poorest, that is, the most sensitive to variations in carrier frequency.[1] This surprising result can be rigorously verified by envelope transfer function analysis.[2]

An additional interesting and practical problem is the design of an *R-L-C* damper with a low *Q* coil. Consider the example in the paper, where $\alpha=\beta=0.1$ with a 400-cps carrier; the *Q* required for the optimum network was found to be 16. Now assume that available inductors have a *Q* of only 12. It ought to be possible to design a resonant damper with this coil, and accept some extra attenuation. The alternative would have to be a parallel-T with relative attenuation of 3.2.

Realizability of the lower coil *Q* requires an increase in the *lower* corner frequency *a* [the shunt resistor in Fig. 2(A) of the paper]. This reduces the available phase lead, and the *upper* corner frequency *b* has to be increased by a larger ratio in order to obtain the desired phase lead at the specified frequency. Note that this is the opposite procedure from the *R-C* network design where the upper corner frequency *b* is increased for *R-C* realizability, and then the lower frequency *a* is increased to trade in surplus phase lead for gain.

This problem is solved by starting out with the relationship among the coefficients of the optimum and modified prototypes, equation 42 of the paper,

$$\frac{b_1-a_1}{ab-a_1b_1}=\frac{b-a}{2ab} \qquad (60)$$

One can then define two values of coil *Q*, the value Q_0 for the optimum network (maximum gain), and the value Q_1 of the available coil:

$$Q_0=\frac{1}{2\sqrt{\alpha\beta}} \qquad (61)$$

$$Q_1=\frac{\omega_c}{2a_1} \qquad (62)$$

$$\frac{Q_1}{Q_0}=\frac{a}{a_1}\le 1 \qquad (63)$$

Substituting a_1 and β from equations 61 and 62 into equation 60, one can determine the relative gain α_1/α and also the relative value of the series resistor [see Fig. 2(A) of this paper], $(b_1-a_1)/(b-a)$.

$$\frac{\alpha_1}{\alpha}=\frac{1-\dfrac{1-\alpha}{2}\dfrac{Q_0}{Q_1}}{\alpha+\dfrac{1-\alpha}{2}\dfrac{Q_1}{Q_0}} \qquad (64)$$

$$\frac{b_1-a_1}{b-a}=\frac{1+\alpha\left(\dfrac{Q_0}{Q_1}\right)^2}{1-\dfrac{1-\alpha}{2}\dfrac{Q_0}{Q_1}} \qquad (65)$$

These quantities must always be positive hence one obtains the realizability conditio

$$\frac{1-\alpha}{2}<\frac{Q_1}{Q_0}\le 1 \qquad (66$$

which is plotted in Fig. 12, where th relative coil *Q* for half-gain is also shown Equation 64 is also shown in Fig. 13 fo $\alpha=0.1$. The diagrams indicate that a reduction in coil *Q* up to 50% can b achieved.

I concur emphatically with Dr. Kochenburger's strictures against carrier lea compensation. In my opinion it is the lea compensation per se, rather than the carrie compensation, which is the main villain Lead networks increase the system band width, require high amplifier gain, an render the system more vulnerable to noise The resulting bandwidth is often far i excess of that required by the application This weakness of the lead compensatio scheme is accentuated in carrier-frequenc systems because of the presence of addi tional high-frequency noise in the form c carrier frequency and harmonics. In addi tion to this, the *R-C* carrier lead network require a further increase in amplifier gai with concurrent reduction in signal-to noise ratio.

References

1. Effects of Variation in Carrier Frequenc on the Performance of Carrier Contro Systems Utilizing Two-Phase Servo Motor E. W. Mehelich, G. J. Murphy. *Proceeding* National Electronics Conference, Chicago, Il vol. 14, 1958, pp. 506–11.

2. Analysis of Notch Network Performanc for A.C. Servomechanism Carrier Frequenc Drift, C. A. Casazza. *M.E.E. Thesis*, Polytechn Institute of Brooklyn, Brooklyn, N. Y., June 196

Power Apparatus and Systems—June 1961

Conference Papers Open for Discussion

Conference papers listed below have been accepted for AIEE Transactions and are now open for written discussion until August 28. Duplicate double-spaced typewritten copies for each discussion should be sent to Edward C. Day, Assistant Secretary for Technical Papers, American Institute of Electrical Engineers, 33 West 39th Street, New York 18, N. Y., on or before August 28.

Preprints may be purchased at 50¢ each to members; $1.00 each to nonmembers if accompanied by remittance or coupons. Please order by number and send remittance to:

AIEE Order Department
33 West 39th Street
New York 18, N. Y.

56-83* Analysis of the Shading Coil Magnet...................Kubiak
60-1028 The Effect of Variable Plasma Conductivity on MHD Energy Converter Performance...........................Coe, Eisen
60-1033 Magneto-Thermionic Power Generation.................Schock
60-1066 Thermoelectricity Application Considerations.........Sorensen
61-31 Aluminum Conduit Use in the Hydrocarbon and Chemical Process Industries.................................Esch, Brown
61-186 Accuracy in Process Computer Instrumentation Systems.........
....Gaines, Patterson
61-646 Computer Solutions to Nuclear Ice-Breaker Propulsion Problems
....Rodgers
61-650 Characteristics of a Synchronous Inductor Motor.............
....Snowdon, Madsen

* Preprints of this paper are no longer available.

AIEE PUBLICATIONS

	Member Prices	Nonmember Prices: Basic Prices*†	Nonmember Prices: Extra Postag for Foreign Subscription
Electrical Engineering			
Official monthly publication containing articles of broad interest, technical papers, digests, and news sections: Institute Activities, Current Interest, New Products, Industrial Notes, and Trade Literature. Automatically sent to all members and enrolled students in consideration of payment of dues. (Members may not reduce the amount of their dues payment by reason of nonsubscription.) Additional subscriptions are available at the nonmember rates.		annually $12* Single copies $1.50*	$1.00
Bimonthly Publications			
Containing all officially approved technical papers collated with discussion (if any) in three broad fields of subject matter as follows:	annually	annually	
Communication and Electronics	$5.00	$8.00*	$0.75
Applications and Industry	$5.00	$8.00*	$0.75
Power Apparatus and Systems	$5.00	$8.00*	$0.75
Each member may subscribe to any one, two, or all three bimonthly publications at the rate of $5.00 each per year. A second subscription to any or all of the bimonthly publications may be obtained at the nonmember rate of $8.00 each per year.			
Single copies may be obtained when available.	$1.50 each	$1.50* each	
AIEE Transactions			
An annual volume in three parts containing all officially approved technical papers with discussions corresponding to six issues of the bimonthly publication of the same name bound in cloth with a stiff cover.	annually	annually	
Part I Communication and Electronics	$4.00	$8.00*	$0.75
Part II Applications and Industry	$4.00	$8.00*	$0.75
Part III Power Apparatus and Systems	$4.00	$8.00*	$0.75
Annual subscription to all three parts (beginning with vol. 77 for 1958).	$10.00	$20.00*	$2.25
Annual subscription to any two parts.		$15.00*	$1.50

AIEE Standards

Listing of Standards, test codes, and reports with prices furnished on request.

Special Publications

Committee reports on special subjects, bibliographies, surveys, and papers and discussions of some specialized technical conferences, as announced in ELECTRICAL ENGINEERING.

---

*Discount 25% of basic nonmember prices to college and public libraries. Publishers and subscription agencies 15% of basic nonmember prices. For available discounts on Standards and special publications, obtain price lists from Order Department at Headquarters.

†Foreign prices payable New York exchange

Send all orders to:

Order Department
American Institute of Electrical Engineers
33 West 39th Street, New York 18, N. Y.